

UC Santa Cruz

UC Santa Cruz Electronic Theses and Dissertations

Title

The Role of the VC1080 Operon in Vibrio Cholerae Biofilm Formation

Permalink

<https://escholarship.org/uc/item/2v15p5n9>

Author

Mouw, Megan

Publication Date

2021

Peer reviewed|Thesis/dissertation

UNIVERSITY OF CALIFORNIA

SANTA CRUZ

**THE ROLE OF THE VC1080 OPERON IN *Vibrio cholerae* BIOFILM
FORMATION**

A thesis submitted in partial satisfaction of the requirements for the degree of

MASTER OF SCIENCE

in

MICROBIOLOGY AND ENVIRONMENTAL TOXICOLOGY

by

Megan M. Mouw

March 2021

The thesis of Megan Mouw is Approved:

Professor Fitnat H. Yildiz, Ph.D., Chair

Professor Karen M. Ottemann, Ph.D.

Professor Chad W Saltikov, Ph.D.

Quentin Williams
Acting Vice Provost and Dean of Graduate Studies

Copyright © by
Megan Mouw
2020

TABLE OF CONTENTS

LIST OF FIGURES -----	4
ABSTRACT -----	5
ACKNOWLEDGEMENTS -----	6
CHAPTER 1: Introduction -----	7
CHAPTER 2: The role of the VC1080 operon on <i>Vibrio cholerae</i> biofilm formation-- ---	26
References -----	107
Appendices -----	127

LIST OF TABLES/FIGURES

Figure/Table number	Figure title	Page
Table 2.1	Domains, localization, and size of VC1080	37
Table 2.2	Top 5 homologs for VC1080	37
Figure 2.1	Sequence alignment of top 5 homologs for VC1080	38
Table 2.3	Domains, localization, and size of VC1081	39
Table 2.4	Top 5 homologs for VC1081	39
Figure 2.2	Sequence alignment of top 5 homologs for VC1081	40
Table 2.5	Domains, localization, and size of VC1082	41
Table 2.6	Top 5 homologs for VC1082	41
Figure 2.3	Sequence alignment of top 5 homologs for VC1082	42
Table 2.7	Domains, localization, and size of VC1083	43
Table 2.8	Top 5 homologs for VC1083	43
Figure 2.2	Sequence alignment of top 5 homologs for VC1083	44
Table 2.9	Domains, localization, and size of VC1084	45
Table 3.0	Top 5 homologs for VC1084	45
Figure 2.5	Sequence alignment of top 5 homologs for VC1084	46
Table 3.1	Domains, localization, and size of VC1085	47
Table 3.2	Top 5 homologs for VC1085	47
Figure 2.8	Sequence alignment of top 5 homologs for VC1085	48
Table 3.3	Domains, localization, and size of VC1086	49
Table 3.4	Top 5 homologs for VC1086	49
Figure 3.1	Sequence alignment of top 5 homologs for VC1086	50
Table 3.5	Domains, localization, and size of VC1087	51
Table 3.6	Top 5 homologs for VC1087	51
Figure 3.2	Sequence alignment of top 5 homologs for VC1087	52
Figure 3.3	<i>vpsL</i> expression in operon deletion strains	54
Figure 3.4	Spot biofilm morphologies of VC1080 operon deletion mutants.	57
Figure 3.5	Spot biofilm morphologies of VC1080 operon overexpression strains	60

Figure 3.6	Genetic dependency of VC1086 and VC1084	63
Figure 3.7	Overexpression phenotype of the VC1080 operon and dependency on VC1086 and VC1084	66
Figure 3.8	Pellicle biofilms of each VC1080 operon overexpression strain	67
Figure 3.9	c-di-GMP quantification from spot biofilms	73
Figure 4.0	Analysis of motility phenotypes of VC1080 operon members	76
Figure 4.1	Homology of VC1080 operon with <i>Shewanella oneidensis</i> MR-1	80
Figure 4.2	Expression of the V1080 operon in response to nitric oxide	81
Figure 4.3	Genetic dependency of VCA0719 and VC1086	85
Figure 4.4	Model for NO signaling through VC1080 genes in <i>V. cholerae</i>	89
Table 3.7	Bacterial Strains	94
Table 3.8	Plasmids	97
Table 3.9	Primers	99

The Role of the VC1080 Operon in *Vibrio cholerae* Biofilm Formation

By

Megan Mouw

ABSTRACT

Vibrio cholerae is an environmental pathogen that relies on biofilm formation for its infectivity. Here we investigate a genomic region that we suspect is involved in regulation of *V. cholerae* biofilm formation in response to environmental signals. The genomic region is particularly enriched in two component system proteins with domains that are able to degrade c-di-GMP. The genomic region spans from VC1080 to VC1087 in the *V. cholerae* genome and will be referred to as the VC1080 operon. This study provides information on the VC1080 to VC1087 gene products obtained by various bioinformatic analysis and presents results from the initial studies investigating the influence of each gene on *V. cholerae* biofilm formation and motility.

ACKNOWLEDGEMENTS

Thank you for my parents for all of their support. Despite living half-way across the world, my Dad has been by my side throughout this entire process. I appreciate his words of wisdom, and emotional and financial support. Thank you to my Mom for making me believe that I'm capable of anything. None of this would have been possible without my parents. Thank you to my sister Michelle for her emotional support. She always knew the right thing to say to keep me pushing forward. Thank you to my advisor Fitnat for the opportunity to conduct this research. Your belief in me and what I'm capable of, drove me to push harder, learn more, and achieve greater. I'm leaving here with an expanded vision of what I'm capable of as a scientist, and that is directly thanks to you. To the rest METX faculty, I'm honored that I had the opportunity to study and learn under your guidance. I'll take the lessons that were taught by each of you forward into my next career steps. To the members of the Yildiz lab old and new. Everything that I learned during my time here was the result of someone taking the time to teach me. Working with each of you made the hard days bearable, and the great days greater. You all taught me that one of the most important determinants of success in science is collaboration, teamwork, and paying it forward. I promise that everything you all generously taught me, will get passed down to the next person who needs it. To all the friends that I've made along the way. You've enriched my time here in the way that only friends can. Thank you for the laughs and the listening ears. I'm excited for the relationships that I've developed during my time at UCSC to continue to blossom for a lifetime.

CHAPTER 1: Introduction

Megan M. Mouw & Fitnat H. Yildiz

Biofilms are prevalent and significant

While planktonic growth of bacteria in pure culture has been the mainstay of microbiological technique for decades, bacteria found naturally in natural environments have a marked tendency to interact with surfaces. Bacteria on surfaces are typically found as biofilms, which are defined as “aggregates of microorganisms in which cells are embedded in a self- produced matrix of extracellular polymeric substances that are adherent to each other and/or a surface” (H. C. Flemming et al. 2016). Biofilm matrix is composed of polysaccharides, proteins, lipids and extracellular DNA (eDNA) (H. C. Flemming and Wingender 2010).

Biofilms are one of the most widely distributed and successful modes of life on Earth as they drive biogeochemical cycling in the environment (H. C. Flemming and Wurtz 2019), have applications in biotechnology, and are associated with persistent infections in plants and animals (H. C. Flemming et al. 2016) (De Vos 2015). Furthermore, biofilms can contaminate medical devices and implants (Khatoon et al. 2018) and contribute to biofouling and contamination of drinking water (H.-C. Flemming 2008).

Biofilms exhibit emergent properties that distinguish them from planktonic bacteria. These properties comprise “novel structures, activities, patterns and properties that arise during the process, and as a consequence, of self-organization in complex

systems.” (H. C. Flemming et al. 2016). Fundamental to emergent properties is the ability of biofilm-forming bacteria to produce biofilm matrix, which encases the cells of a biofilm. Although the precise molecular interactions of biofilm matrix components have not been fully defined, several functions of matrix have been determined, including but not limited to: adhesion, aggregation, cohesion, water retention, protection, enzymatic activity, nutrition, and genetic exchange (H. C. Flemming and Wingender 2010). The matrix enables the biofilm to capture nutrient resources - an essential process for all organisms. Nutrients are captured by the sponge-like EPS matrix, becoming ‘sorbed substances’ which influence the exchange of nutrient, gases, and other molecules in the biofilm. When cells decay and lyse, their debris can be used as nutrients by surviving cells; a process that has been investigated in detail in *Bacillus subtilis* biofilms, which uses DNA from lysed cells as a source of phosphorus, carbon and energy (López et al. 2009). *P. aeruginosa* has also been shown to specifically produce extracellular DNases in biofilms to exploit DNA from lysed cells as a nutrient resource (Mulcahy, Charron-Mazenod, and Lewenza 2010).

Bacterial biofilms tend to bring organisms into close proximity, which enables the exchange of metabolites, signaling molecules, genetic material and defensive compounds. Cells with different metabolic capacities or physiological gradients provide opportunities for cooperation, and biofilms can produce steep gradients of pH, redox conditions, as well as electron acceptors and donors. The availability of

oxygen as an electron acceptor is one of the most important external triggers of the establishment of gradients in the biofilm. In aquatic habitats, in which oxygen is present in the water phase, the upper layer of the biofilm is aerobic, while deep layers of the biofilm become anaerobic (Chang et al. 2015)(H. C. Flemming et al. 2016).

Given the high cell densities and species diversity of many biofilms, it is not surprising that biofilms are the primary sites for the exchange of metabolic byproducts between species (West et al. 2006). For example, exchange of amino acids and sugars is a common mutualistic interaction in biofilm subcommunities (Zelezniak et al. 2015). An interesting example of metabolic interactions between different species in biofilms is the process of nitrification, in which ammonia-oxidizing bacteria convert ammonium into nitrite, which is then oxidized by nitrite-oxidizing bacteria. As a preceding step, the nitrite-oxidizing bacterium *Nitrospira moscoviensis* uses urease to produce ammonia for oxidation by ammonia-oxidizing bacteria that lack this enzyme (Koch et al. 2015).

Studies of models of mixed-species biofilms clearly demonstrate the occurrence of cooperative behavior in biofilms (K. W. K. Lee et al. 2014). For example, a study of a biofilm formed by *P. aeruginosa*, *Pseudomonas protegens* and *Klebsiella pneumoniae* found that stress tolerance was present to an equal extent in all three community members. Furthermore, a biofilm community with three species was shown to tolerate exposure to the phenylurea herbicide linuron by synergistic

degradation of the toxin, which none of the cognate mono-species biofilms was able to degrade (Breugelmans et al. 2008). However, cooperation does not necessarily occur in all biofilms, and many species-species interactions in biofilms competitive in nature. Competition within biofilms is mediated by antibiotics, bacteriocins, extracellular membrane vesicles, and type VI secretion systems. These weapons of competition drive strategies that include the inhibition of initial adhesion to the biofilm, or the production of biosurfactants with antimicrobial properties (Rendueles and Ghigo 2015). It has been shown that *Salmonella Typhimurium* responds to the presence of competing strains in biofilms by driving up the expression of genes associated with biofilm matrix production, epithelial invasion, and antibiotic tolerance. Furthermore, inactivation of the type VI secretion system of competing strains annuls these genetic responses, suggesting that type VI secretion-derived cell damage may activate these changes (Lories et al. 2020).

Another emergent property of biofilms is their enhanced resistance or tolerance to antibiotics and other antimicrobial agents. Resistance refers to genetic or heritable characteristics, whereas tolerance denotes a characteristic that is specific to biofilms and that is lost following dispersal to free-living bacterial cells. Tolerance in biofilms can be a product of the biofilm matrix itself, or a property of the slow growth of cells within the biofilm. EPS components of the biofilm matrix can substantially quench the activity of antimicrobial substances that diffuse through the biofilm in a form on inhibition known as diffusion-reaction inhibition (Daddi Oubekka et al. 2012). This is

a process that can involve chelation of antimicrobial substances, enzymatic degradation, or reaction of EPS with oxidizing disinfectants. In *Pseudomonas aeruginosa*, the pel polysaccharide, which is one of three main polysaccharides required for biofilm development, plays a role in enhancing resistance to aminoglycoside antibiotics (Colvin et al. 2011). In *V. cholerae*, antibiotics that inhibit protein synthesis results in changes in cell size, shape, and biofilm architecture. Antibiotic-induced changes also affect biofilm population dynamics and community assembly by enabling invasion of biofilms by bacteriophages and intruder cells of different species. (Díaz-Pascual et al. 2019). High cell density increased genetic competence, and accumulation of mobile genetic elements that occur in biofilms contribute to enhance uptake of resistance genes by horizontal gene transfer. It has been suggested that the environment within the biofilm is ideal for the uptake of resistance genes, especially considering the increased cell-to-cell contact that occurs within in the biofilm; a property that is required for some mechanisms of gene transfer. Conjugation has been shown to be up 700-fold more efficient in biofilms compared with free-living bacterial cells (Król et al. 2013). A study of *Staphylococcus aureus* showed that conjugal plasmid transfer occurred in biofilms but not in cultures of free-living bacterial cells, providing another example of a behavior that occurs in a biofilms but that is not possible for planktonic cells (Savage, Chopra, and O'Neill 2013).

In general, biofilm formation occurs in four main stages: (1) bacterial attachment to a surface, (2) microcolony formation, (3) biofilm maturation and (4) detachment (also termed dispersal) of bacteria which may then colonize new areas (C. Liu et al. 2020). Each step of this process must be highly regulated in biofilm-forming bacteria. While biofilm formation is a complex process regulated by several different factors in various bacteria, some regulators of biofilm formation, such as second messengers, are common to nearly all bacteria (Jenal, Reinders, and Lori 2017). The second messenger c-di-GMP is universally recognized as a “switch molecule” that controls the bacterial transition between a planktonic lifestyle and biofilm formation (Dahlstrom and O’Toole 2017) and will be the main form of biofilm regulation discussed in this thesis.

***Vibrio cholerae* is a model organism for studying the biofilm lifecycle**

V. cholerae is a gram-negative facultative anaerobe that spends much of its life cycle inhabiting brackish or saltwater (Teschler et al. 2015). Infection of the human host can lead to the disease cholera, which is characterized by diffuse watery diarrhea, and typically occurs through the ingestion of contaminated food or water. Thus, cholera primarily impacts regions that lack adequate sanitation and clean drinking water. In

such regions, three to five million people are affected by cholera annually, resulting in 100,000-120,000 deaths (Charles and Ryan 2011)(Harris et al. 2012)(Sack et al. 2004). Biofilm formation contributes to *V. cholera*'s persistence in the aquatic environment and evidence has shown that *V. cholerae* can form biofilm-like aggregates during infection, which could play a critical role in pathogenesis and disease transmission (Teschler et al. 2015). Furthermore, there have been reports that previously biofilm-associated cells are hyper-infectious (Tamayo, Patimalla, and Camilli 2010). Estimation of the relative infectivity of different forms of *V. cholerae* cells suggest that the enhanced infectivity of *V. cholerae* shed in human stools is largely due to the presence of clumps of cells that disperse in vivo, providing a high dose of the pathogen. This supports a model of cholera transmission in which in vivo-formed biofilms contribute to enhanced infectivity and environmental persistence of pathogenic *V. cholerae* (Faruque et al. 2006). Recent studies have shown that biofilm-grown *V. cholerae* cells upregulate virulence factors compared to planktonic-grown cells, priming biofilm-grown cells for infection and driving a hyper-infectious phenotype (Gallego-Hernandez et al. 2020). Thus, there is great public health interest in better understanding the role that biofilms play in *V. cholerae* pathogenesis.

Regulation of *V. cholerae* biofilm formation

Biofilm formation enhances environmental survival and infectivity of *V. cholerae*; therefore, regulation of biofilm formation in *V. cholerae* has been extensively studied.

Vibrio polysaccharide (VPS) is the major component of the *V. cholerae* biofilm, and the *vps* genes are clustered in two regions, the *vps*-I cluster (*vpsU*, *vpsA-K*, VC0916-27) and the *vps*-II cluster (*vpsL-Q*, VC0934-39), separated by an intergenic region containing the *rbm* gene cluster that encodes biofilm matrix proteins (J. C. N. Fong et al. 2010). In-frame deletions of the *vps* clusters and genes encoding matrix proteins drastically altered biofilm formation phenotypes. A group of transcriptional activators have been identified to control *V. cholerae* biofilm formation and *vps* gene expression, with VpsR considered to be the master regulator (Teschler et al. 2015). VpsR is a response regulator and part of a two-component signal transduction system; it binds directly to *vps* promoter regions that control the production of vibrio polysaccharide (*vps*), the major component of the biofilm matrix (Zamorano-Sánchez et al. 2015). Disruption of *vpsR* prevents the expression of Vibrio polysaccharide and matrix proteins, abolishing the formation of biofilms. VpsT is a second positive regulator of *V. cholerae* biofilm formation and is also a response regulator (Casper-Lindley and Yildiz 2004). *vpsT* is positively regulated by VpsR, and disruption of *vpsT* reduces the expression of *vps* and matrix protein genes and biofilm forming capacity. VpsR and VpsT, bind to nonoverlapping target sequences in the regulatory region of *vpsL* *in vitro*. VpsR binds to a proximal site (the R1 box) as well as a distal site (the R2 box) with respect to the transcriptional start site identified upstream of *vpsL*. The VpsT binding site (the T box) is located between the R1 and R2 boxes. Similar to VpsR (Zamorano-Sánchez et al. 2015). VpsT binds to the *vps* promoter region to directly control the expression of *vps* genes. VpsT also binds directly to Bis-

(3'-5')-cyclic dimeric guanosine monophosphate (c-di-GMP), an association that is required for DNA association and transcriptional regulation. c-di-GMP is a central regulator of biofilm formation in *V. cholerae* and will be discussed further in later sections. It has been shown that VpsR can bind to c-di-GMP, resulting in the transcription of the *pvpsL* promoter of biosynthesis genes. Though this mechanism of activation is still unclear, it is speculated that VpsR's mechanism of activation is dependent on both the concentration of VpsR and the level of c-di-GMP to increase transcription, resulting in finely tuned regulation (Hsieh, Waters, and Hinton 2020) (Hsieh, Hinton, and Waters 2018).

c-di-GMP is a central regulator of the biofilm lifecycle

The nucleotide based signaling molecule Bis-(3'-5')-cyclic dimeric guanosine monophosphate (c-di-GMP) controls the transition from planktonic to biofilm lifestyles in many bacteria. Intracellular c-di-GMP levels can change dynamically through the activity of two enzymes called diguanylate cyclases and phosphodiesterases, which produce and degrade c-di-GMP respectively (Hengge 2009) (Hengge et al. 2016). Diguanylate cyclases (DGCs), which are proteins with a conserved GGDF domains, produce c-di-GMP from two molecules of GTP, while phosphodiesterases (PDEs), which are proteins with a conserved EAL and/or HD-GYP domains domains that degrade c-di-GMP. Degradation of c-di-GMP occurs by a two-step process in which one set of

phosphodiesterases (PDE-As) linearize the molecule into 5'-phosphoguanilyl-(3',5')-guanosine (pGpG), followed by hydrolysis by phosphodiesterases (PDE-Bs) called into two GMPs. Orn is the primary PBE-B in *Pseudomonas aeruginosa* (Orr et al. 2015).

c-di-GMP modifying proteins are frequently paired with sensory domains such that the presence or absence of an environmental signal can alter intracellular levels of the second messenger (Römling, Galperin, and Gomelsky 2013). An active DGC is a dimer of two subunits with GGDEF domains, each of which bind one molecule of GTP (Paul et al. 2004)(Chan et al. 2004)(Wassmann et al. 2007). PDE activity is associated with two amino acid sequence motifs: EAL and HD-GYP domains. HD-GYP proteins form a subfamily of the HD superfamily of metal-dependent phosphohydrolases and are unrelated to the EAL proteins (Galperin et al. 1999). Although GGDEF, EAL, and HD-GYP domains can occur separately, composite proteins in which a GGDEF domain is covalently linked to either EAL or HD-GYP domains do exist (Hengge 2009).

Many species possess GGDEF and EAL domain proteins in which the amino acids essential for enzymatic function are not conserved (Tschowri, Busse, and Hengge 2009). Despite being enzymatically degenerate, some GGDEF and EAL domain proteins do still bind GTP or c-di-GMP to allosterically control the activity of a partner protein or domain; acting as c-di-GMP receptors (Tschowri, Busse, and

Hengge 2009). Most degenerate GGDEF and EAL domain proteins are still involved in c-di-GMP regulated processes such as biofilm formation and motility, but through direct macromolecular interactions rather than by synthesizing and degrading c-di-GMP directly (Wang et al. 2005). An example of a degenerate GGDEF-containing protein is PelD from *P. aeruginosa* (Merighi et al. 2007) and the PleD paralogue PopA (Duerig et al. 2009), and CdgG from *V. cholerae* (Beyhan, Odell, and Yildiz 2008).

Several other c-di-GMP receptors have been identified, including the PilZ-containing proteins. The PilZ domain is often associated with regulatory, catalytic (including GGDEF, EAL and HD-GYP) or transport domains and has a phylogenetic distribution that is similar to that of GGDEF and EAL domains (Amikam and Galperin 2006). The PilZ domain has two consensus motifs, RxxxR and D/NxSxxG, required for c-di-GMP and it is found in several proteins affecting flagellar motility (Amikam and Galperin 2006). The *V. cholerae* genome encodes five proteins with predicted PilZ domains: PlzA (VC0697), PlzB (VC1885), PlzC (VC2344), PlzD (VCA0042), and PlzE (VCA0735). All of these Plz proteins except PlzB have the two consensus motifs involved in PilZ c-di-GMP binding. PlzC, PlzD, and PlzE were demonstrated to bind c-di-GMP in vitro (Roelofs et al. 2015) (Jason T. Pratt et al. 2007).

C-di-GMP can also bind to other proteins. In *V. cholerae* VpsT, VpsR, and FlrA and MshE all act as c-di-GMP receptors. At the transcriptional level, c-di-GMP represses transcription of flagellar genes. A large set of proteins is required for a functional flagellum, and their expression is regulated by a well- characterized four level transcriptional hierarchy (Prouty, Correa, and Klose 2001). Transcriptional activation begins with the alternative sigma factor σ^{54} -dependent regulator FlrA (VC2137). C-di-GMP binds to FlrA and alters its activity, impairing FlrA's ability to activate the expression of the *flrBC* operon, which is as two component system that is essential for flagellar biosynthesis and motility (Srivastava et al. 2013). FlrA is an orthologue of FleQ, the master regulator of flagellar gene expression in *Pseudomonas aeruginosa*. Structural studies showed that FleQ binds to an intercalated dimer of c-di-GMP and binding of c-di-GMP to FleQ imposes a change in its oligomeric, inhibiting its ATPase activity (Arora et al. 1997). Recently, there has been a characterized interaction between c-di-GMP and the ATPase MshE, which promotes pilus polymerization. low levels of c-di-GMP correlate with enhanced retraction and loss of retraction is facilitated by the ATPase PilT, which increases near-surface roaming motility, and impairs initial surface attachment (Jones et al. 2015). This suggests that c-di-GMP directly controls MshE activity, thus regulating MSHA pilus extension and retraction dynamics, and modulating *V. cholerae* surface attachment and colonization (Floyd et al. 2020).

***V. cholerae* biofilm formation**

Attachment

A critical step in the formation of a biofilm is the process of cell attachment.

In *V. cholerae*, attachment is aided by the type IV mannose-sensitive hemagglutinin (MSHA) pilus. During early stages of biofilm formation, flagellar function and production is repressed to stabilize *V. cholerae* surface attachment. *V. cholerae* biofilm formation is a multistep process that begins with bacteria mechanically scanning the surface using roaming or orbiting movements. This process is facilitated by a cell surface structure MSHA pili and polar flagellum driven by a Na⁺ motor. Roaming and orbiting motility are ablated in strains lacking mannose sensitive hemagglutinin pili (MSHA) type IV pili, and strains lacking MSHA are also defective in initial surface attachment (Utada et al. 2014)(Watnick and Kolter 1999). It is notable that only orbiting cells attach to surfaces and after attachment *V. cholerae* does not exhibit surface motility (Utada et al. 2014). Thus, MSHA pili-surface binding is crucial to arrest cell motion near the surface and transition to surface attachment and microcolony formation. Recent studies have shown that the MSHA pilus is a dynamic extendable and retractable system that is directly controlled by c-di-GMP (Floyd et al.2020.) (Jones et al. 2015). Specifically, c-di-GMP interacts together with MshE, to promote pilus extension, while low levels of c-di-GMP promote retraction. Loss of retraction impairs initial surface attachment in *V. cholerae*. Overall, these studies indicate that c-di-GMP directly controls MshE

activity, thus modulating *V. cholerae* surface attachment and colonization (Floyd et al. 2020.). *V. cholerae* motility and biofilm formation are inversely regulated by the second messenger signaling molecule c-di-GMP. Elimination of the flagellum results in a flagellum-dependent biofilm regulatory (FDBR) response, which elevates c-di-GMP levels, increases biofilm gene expression, and enhances biofilm formation (Wu et al. 2020). Furthermore, the diguanylate cyclase CdhH has been found to impact intracellular c-di-GMP levels and influence swim speed directions. CdgD has also been identified as the dominant DGC involved in post attachment c-di-GMP production in biofilms (Zamorano-Sánchez et al. 2019). Thus, flagella apparently play an important role in attachment in the early stages of bacterial attachment. c-di-GMP also regulates reversible cell attachment in *V. cholerae*. Specifically, a conserved c-di-GMP receptor, LapD, and its associated periplasmic protease, LapG, together control the stability of two c-di-GMP-regulated adhesins, FrhA and CraA (Kitts et al. 2019). In this system, LapG is a calcium-dependent protease that processes both FrhA and CraA, thus controlling cell adhesion and biofilm formation (Kitts et al. 2019).

Matrix production

Following the initial stages of cellular attachment, cells produce the extracellular matrix, which is essential for the development of three-dimensional mature biofilms. The *V. cholerae* biofilm matrix is composed primarily of polysaccharides,

phospholipids, proteins, and small amounts of nucleic acids. *Vibrio* polysaccharide (VPS) makes up 50% of the biofilm matrix mass. Two types of VPS are produced during biofilm formation: the repeating unit of the major variant of the polysaccharide portion of VPS is $[\rightarrow 4)\text{-}\alpha\text{-L-GalpNAcAGly3OAc-(1}\rightarrow 4)\text{-}\beta\text{-D-Glcp-(1}\rightarrow 4)\text{-}\alpha\text{-D-Glcp-(1}\rightarrow 4)\text{-}\alpha\text{-D-Galp-(1}\rightarrow]_n$, whereas the minor variant partially replaces $\alpha\text{-D-Glc}$ with $\alpha\text{-D-GlcNAc35}$ (Yildiz et al. 2014). Genes involved in VPS production are organized into two *vps* clusters. In frame deletion of 15 out of 18 *vps* genes resulted in strains with reduced colony corrugation compared to wildtype, highlighting the importance of *vps* for biofilm architecture (Yildiz et al. 2014).

Matrix proteins are also an important component of the biofilm matrix, and three are produced and secreted by *V. cholerae* at various times during biofilm formation. *rbmA* (rugosity and biofilm structure modulator A), is required for rugose colony formation and biofilm structure integrity in *V. cholerae* (J. C. N. Fong et al. 2006). Transcription of *rbmA* is positively regulated by the response regulator VpsR but not VpsT. RbmA participates in the early cell-cell adhesion events and is found throughout the biofilm where it localizes to cell-cell contact sites (J. C. N. Fong et al. 2006). Crystal structures of RbmA show that the protein folds into tandem fibronectin type III (FnIII) folds. RbmA is thought to serve as a tether by maintaining flexible linkages between cells and the extracellular matrix (Giglio et al. 2013). It has also been shown that RbmA binds VPS directly, and uses a binary structural switch within

its first fibronectin type III domain to control RbmA structural dynamics and the formation of VPS-dependent higher-order structures (J. C. Fong et al. 2017)

Bap1 and its homolog RbmC also play non-redundant roles in biofilm formation (J. C. N. Fong and Yildiz 2007)(Absalon, Van Dellen, and Watnick 2011). Bap1 plays an important role in surface adhesion and is likely to be primarily produced by the founder cell (Berk et al. 2012.). Bap1 is secreted at the cell-surface interface and gradually radially accumulates on nearby surfaces, while remaining highest near the founder cell. In rugose pellicles, Bap1 is uniquely required for maintaining pellicle strength over time, as loss of Bap1 leads to a morphologically distinct pellicle structure. Bap1 also contributes to pellicle hydrophobicity, enabling it to spread and remain at an air-water interface (Hollenbeck et al. 2014). RbmC is larger than Bap1 and is secreted at discrete sites on the cell surface as biofilms develop. RbmC and Bap1 form flexible envelopes surrounding the cell that can grow as cells divide (Berk et al. 2012). During biofilm formation on a solid-water interface, RbmA, RbmC and Bap1 were unable to accumulate on the surface of cells that did not produce VPS, and RbmC was shown to be critical for incorporating VPS throughout the biofilm. Thus, the mature biofilm is a composite of organized clusters composed of cells, VPS, RbmA, Bap1 and RbmC (Berk et al. 2012).

Biofilm dispersal in *V. cholerae*

While the transition from planktonic growth to biofilm growth has been relatively well studied in *V. cholerae*, understanding of the environmental triggers and molecular mechanisms that trigger biofilm dispersal is still in its early stages (Singh et al. 2017). However, studies have identified some clues concerning the regulation of *V. cholerae* biofilm dispersal: quorum sensing, bile salts, and starvation signals all appear to promote dispersal in *V. cholerae* (Hay and Zhu 2015)(Singh et al. 2017) (Z. Liu, Stirling, and Zhu 2007)(Bridges, Fei, and Bassler 2020). (Christopher M. Waters et al. 2008a)(Z. Liu, Stirling, and Zhu 2007)(Hammer and Bassler 2003a). High-content image screens have facilitated the identification of components required for *V. cholerae* biofilm dispersal. These components have been categorized into three classes: signal transduction, matrix disassembly, and cell motility. It is proposed that the three functional categories represent the chronological steps required for the disassembly of a biofilm. First, the stimuli that activate dispersal must accumulate. Subsequently, the gene expression pattern established by detection of these stimuli must repress biofilm matrix production and activate production of enzymes required to digest the biofilm matrix. Finally, cells must escape through the partially digested, porous matrix, which requires changes in the direction of movement. It has also been shown that the DbfS-DbfR two-component system controls matrix production. While not yet tested explicitly, it is possible that DbfS-DbfR also orchestrates the initiation of matrix digestion and the launch of motility. Together, these steps ensure that when environmental conditions are appropriate, *V. cholerae* cells can exit the sessile

lifestyle and disseminate to new terrain that is ripe for biofilm formation or, alternatively during disease, to a new host (Bridges, Fei, and Bassler 2020).

It is known that quorum sensing plays a significant role in promoting *V. cholerae* biofilm dispersal, as HapR, the master regulator of quorum sensing, is the main negative regulator of biofilm formation in *V. cholerae* (Christopher M. Waters et al. 2008b) (Hammer and Bassler 2003b). Quorum sensing is a cell-cell communication process involving the production, secretion, and detection of chemical signal molecules known as autoinducers (AIs) that allow bacteria to synchronize the behavior of the population (Papenfort and Bassler 2016). In the low- cell density state (i.e., when AI levels are low), the AI receptors function as kinases, and funnel phosphate to the response regulator, LuxO. LuxO-P activates four genes encoding the Qrr small regulatory RNAs (sRNAs). The Qrr sRNAs destabilize the mRNA encoding a major regulator of QS, HapR (Lenz et al. 2004). This relay culminates in the expression of low-cell density specific genes, including genes required for biofilm formation and virulence factor production (Zhu and Mekalanos 2003). When the cell density increases, the AIs accumulate, bind their cognate receptors, and switch the receptors to phosphatases. Phosphatase activity leads to dephosphorylation of LuxO and termination of qrr expression. The mRNA encoding HapR is stabilized, and HapR protein is produced (Lenz et al. 2004). HapR is a DNA-binding transcription factor that initiates a program of gene expression that switches the cells from the individual, low-cell-density state to the high-cell-density state. Quorum sensing

deficient mutants form thicker biofilms and do not detach as easily from biofilm when compared to wildtype, highlighting the importance of this process for biofilm dispersal. Quorum sensing has been shown to play a role in biofilm dispersal in a number of species, including *V. cholerae* (Hammer and Bassler 2003a) (Zhu and Mekalanos 2003) (Beyhan et al. 2007a). In *V. cholerae*, HapR, the master regulator of quorum sensing, is the main negative regulator of biofilm formation in *V. cholerae* (Hammer and Bassler 2003a). Disruption of *hapR* enhances biofilm formation, and HapR binds directly to the regulatory regions of *vpsL*, the first gene in an operon encoding genes responsible for the production of Vibrio polysaccharide (C. M. Waters et al. 2008). HapR level increase when cell density and quorum sensing autoinducers levels are high (Z. Liu, Stirling, and Zhu 2007). It has been shown that HapR production at high cell density in *V. cholerae* alters the expression of 14 genes encoding proteins with GGDEF and/or EAL domains, which modulate intracellular levels of c-di-GMP (C. M. Waters et al. 2008). QS control of these genes results in increased intracellular levels of c-di-GMP at low cell density and decreased c-di-GMP at high cell density (C. M. Waters et al. 2008). HapR has also been shown to bind directly to VpsT, repressing its expression and contributing to the reduction in biofilm formation that occurs at high cell density (Beyhan et al. 2007b) .

Beyond quorum sensing, it has also been shown that *V. cholerae*'s general stress response is important for fine tuning biofilm dispersal. Singh et al. showed that *Vibrio cholerae* combines information from individual stress response and collective quorum

sensing avenues of sensory input, to make decisions on whether to disperse from the biofilm (Singh et al. 2017). They find that dispersal is promoted in large biofilms under distress and prevented when biofilm populations are small (Singh et al. 2017). Authors grew biofilms in microfluidic devices with a flow rate of 0.1 mL/min. Biofilms were grown in M9 minimal medium, supplemented with 2mM SO₄, 100mM CaCl₂, MEM vitamins, 0.5% glucose, and 15mM triethanolamine (pH 7.1). It was initially observed that halting flow over a mature biofilm causes biofilm dispersal and authors hypothesized that this effect could be due to altered solute concentrations once flow is stopped. When the carbon source (glucose) was removed from the flow while leaving the flow rate unchanged, a biofilm dispersal response was observed. Removal of oxygen resulted in a weak but significant response, while the addition of NO had no measurable effect compared with controls in which the flow rate and medium composition were left unchanged (Singh et al. 2017).

It has been shown that RpoS, which regulates the generalized stress response during nutrient depletion, is elevated when flow of medium is stopped, or glucose is removed during flow cell biofilm experiments. Analysis of HapR accumulation using translational fusion of sfGFP to HapR also showed that HapR levels substantially increase during biofilm development, even when flow and nutrient supply are not interrupted, though a statistically significant increase of HapR upon flow stoppage was apparent. Overexpression of *rpoS*, *hapR* and both genes together by induction under an IPTG inducible promoter triggered biofilm dispersal, with *rpoS* causing a

larger response than *hapR* (Singh et al. 2017).

HapR and RpoS act synergistically to regulate dispersal and HapR induction alone cannot promote dispersal in the complete absence of RpoS. When *hapR* is under the control of an inducible promoter and inserted into the *rpoS* deletion background, it is unable to disperse.

The following model has been described for biofilm dispersal decisions in *V. cholerae*: when biofilms are small, autoinducer retention in the biofilm is slow, yielding low HapR levels. Under low HapR levels, dispersal will not occur in either the presence or absence of nutritious flow, which yielding low and high RpoS levels respectively. On the other hand, biofilms naturally accumulate autoinducers as they increase in size, leading to induction of *hapR* which "primes" the group for dispersal in the event of nutrient depletion. In such biofilms with high HapR levels, dispersal can be induced either by a change in flow conditions or by the removal of a nutrient source, which both lead to RpoS induction (Singh et al. 2017).

In conclusion, biofilm formation is a process that beneficial for bacteria in many ways. Biofilms offer protection from environmental stresses and antibiotics and allow for cooperation and competition among members of the biofilm. c-di-GMP is a main switch molecule controlling the transition from planktonic to biofilm lifestyles. While biofilm formation is highly beneficial, it can also be a costly lifestyle for many

bacteria. In the case of *V. cholerae* - a model organism for studying biofilm formation - the process is highly regulated in response to environmental conditions. *V. cholerae* biofilm regulators affect and are in turn effected by levels of intracellular c-di-GMP and control the production of matrix components such as *vps* in order to regulate the switch between biofilm and planktonic lifestyles. While the transition from planktonic phase to biofilm phase has been reasonably well studied on the molecular level, our understanding of signals that lead to a degradation of c-di-GMP and transition back into the planktonic lifestyle are still in their early stages. This thesis aims to investigate an operon may affect *V. cholerae* biofilm formation by encoding gene products that can degrade c-di-GMP. We suspect that a consequence genetic activation of genes in our region of interest may lead to changes in c-di-GMP regulated phenotypes such as motility and biofilm formation.

CHAPTER 2: Characterizing the role of a genomic region in *Vibrio cholerae* that is enriched in two-component systems with c-di-GMP degrading capability

Introduction:

Two component systems

Two-component systems constitute a prevalent form of regulatory control in response to environmental changes in bacteria. This protein family is critical for the adaptation of microorganisms to a variety of stress conditions, in pathogenic and symbiotic interaction with eukaryotic hosts and in essential cellular pathways. The prototypical two-component system responds to a change in an environmental condition by modifying gene expression, and/or by modifying the biochemical activities of target proteins (Groisman, 2016).

Classical two-component systems consist of a sensor protein and a regulator. Sensor proteins respond to a physical or chemical signal by modifying the phosphorylated state of a cognate regulatory protein by using ATP to autophosphorylate at a conserved histidine residue. The phosphorylated sensor serves as a phosphodonor to its partner regulator, which is phosphorylated at a conserved aspartic acid residue. The vast majority of sensors also display phosphatase activity toward their respective phosphorylated regulators. Regulators are often DNA-binding transcriptional repressors and/or activators. The consequence of two component system induction is typically a change in the transcriptional profile of an organism, as phosphorylation usually increases the affinity of a regulator for its DNA target (Groisman, 2016). Certain regulators lack DNA-binding domains and exert their regulatory effects by

establishing direct interactions with protein or RNA targets. The signals acting on sensors, and the genes regulated by the regulators, typically differ among two component systems. Differences in input signals and regulated genes/proteins have been reported even for homologous systems of closely related bacterial species (Pontes et al. 2011)(Chen and Groisman 2013).

Not all two-component system are composed of a single histidine kinase and response regulator pair. The modularity of the TCS separates signal input, phosphotransfer, and output response; allowing bacteria to dramatically expand and diversify their signaling capabilities (Capra and Laub 2012). For example, hybrid two-component systems constitute a protein family that harbors the sensor and regulator domains of a classical two-component system fused in a single protein. Phosphorelays are a more complex version of the TCS in which a sensor kinase first transfers the phosphoryl group to a RR possessing a domain with the conserved aspartate but no output domain. The RR then transfers the phosphoryl group to a histidine-containing phosphotransfer protein, which serves as the phosphodonor to the terminal RR, which possesses and output domain mediating a cellular response (Capra and Laub 2012).

While the majority of two-component systems have a sensor that only affects the phosphorylated state of its cognate regulator, some regulators phosphorylate more than one regulator, with several distinct sensors converging on a given regulator. In other cases, a given sensor may serve as a phosphodonor for multiple regulators.

These are examples of one-to-many (divergent), and many-to-one (convergent) TCS. In a convergent signaling pathway, distinct signals activate different sensors that modify the phosphorylation state of a single regulator to generate an output. In a divergent signaling pathway, a sensor responds to a signal by modifying the phosphorylation state of two regulators, thereby generating two different outputs (Groisman 2016).

Two component systems in *Vibrio cholerae*

The genome of *V. cholerae* is predicted to encode 43 histidine kinases (HKs) and 53 response regulators (RRs), according to the reference genome of O1 EL Tor strain N16961

(http://www.ncbi.nlm.nih.gov/Complete_Genomes/RRcensus.html and <http://www.p2cs.org>) and data published by Teschler *et al.* (Teschler, Cheng, and Yildiz 2017). It is currently unknown how many of these two component systems are involved in convergent, divergent, or phosphorelay signaling. These two-component signal transduction systems (TCSs) allow *V. cholerae* to sense and respond to a variety of environmental stimuli, such as nutrient availability, pH, oxygen, osmolarity, quorum sensing signals and numerous host factors. Biofilm formation is an important strategy used by *V. cholerae* to respond to changing environmental conditions.

Several response regulators in *V. cholerae* have been reported to lead to increased biofilm formation, including VpsR and VpsT, which are positive regulators of biofilm formation (Casper-Lindley and Yildiz 2004) (Beyhan et al. 2007b). LuxO positively regulates biofilm formation through regulation of small regulatory RNAs responsible for repressing translation of *hapR*, which in turn represses biofilm gene expression (Vance, Zhu, and Mekalanos 2003). VxrAB (VCA0565-66) is a TCS that positively regulates biofilm formation in *V. cholerae* (Teschler, Cheng, and Yildiz 2017).

Two component systems can also repress biofilm formation. NtrC negatively regulates the expression of core regulators of biofilm formation (*vpsR*, *vpsT*, and *hapR*) and mutants lacking NtrC had increased biofilm formation and *vpsL* expression (Cheng et al. 2018). PhoB acts as a repressor of biofilm formation under phosphate-limited conditions, and CarSR, which is involved in antimicrobial peptide resistance, and VieA both negatively regulate biofilm formation (J. T. Pratt, McDonough, and Camilli 2009)(Bilecen et al. 2015)(Tischler, Lee, and Camilli 2002)(Martinez-Wilson et al. 2008). The *carRS* system also regulates the expression of the *vps* genes responsible for biofilm formation through an extracellular matrix consisting of *Vibrio* exopolysaccharide (Samanta et al. 2020). VarSA represses biofilm formation by interfering with the LuxO-mediated activation of Qrr sRNAs. This is achieved through its activation of the inhibitory regulatory small RNAs CsrBCD and their subsequent inhibition of the global regulator CsrA. Repression of CsrA reduces Qrr sRNA levels, leads to increased HapR levels and decreased *vps*

gene expression (Jang et al. 2011)(Tsou et al. 2011). VarA of the VarS/VarA system is involved in the regulation of virulence proteins in the classical *V. cholerae* O395 strain, and VarS is involved in the expression of the virulence proteins CT and TCP from the *V. cholerae* classical and El Tor strains. This expression is through regulation of ToxT expression in response to environmental changes due to different toxin-inducing conditions (Tsou et al. 2011).

TCS systems harboring c-di-GMP signaling modules

The genome of *V. cholerae* contains numerous genes encoding confirmed or putative c-di-GMP metabolic enzymes: 31 genes encoding GGDEF domains, 12 genes encoding EAL domains, 10 genes encoding tandem GGDEF-EAL genes, and 9 genes encoding HD-GYP domains. A handful of diguanylate cyclases and EAL domain phosphodiesterase enzymes have been shown to impact motility, biofilm formation and virulence in animal models (McKee et al. 2014b)(Beyhan, Odell, and Yildiz 2008).

While many of the two component systems described thus far exert their affects by altering gene expression, other two component system response regulators can exert their affects by altering levels of intracellular signaling molecules such as c-di-GMP. In *V. cholerae*, a well-characterized example of a two-component system that affects

levels of c-di-GMP is the VieASB regulatory system which will be discussed in detail in the following section.

The *vieSAB* operon is a three-protein phosphorelay that regulates *V. cholerae* virulence gene expression and biofilm formation in classical strains of *V. cholerae* (Tischler, Lee, and Camilli 2002). The operon was first identified in a screen for genes induced during colonization of the infant mouse small intestine (Camilli and Mekalanos 1995). The VieSAB system differs from conventional two-component systems as it encodes three components; the two response regulators, VieA and VieB, as well as the sensor histidine kinase VieS (S. H. Lee et al. 1998).

VieA is a response regulator that contains an EAL domain (Tamayo, Tischler, and Camilli 2005). This EAL domain confers c-di-GMP phosphodiesterase (PDE) activity to the VieA protein. This PDE activity is supported by the ability of VieA to hydrolyze an enzymatically synthesized c-di-GMP substrate (Tamayo, Tischler, and Camilli 2005). VieA also contains a putative helix-turn-helix DNA binding domain. Deletion of either the DNA binding domain or the EAL domain of VieA leads to increased levels of c-di-GMP in vivo (Tamayo, Tischler, and Camilli 2005).

Phosphotransfer assays have revealed VieS as the cognate sensor histidine kinase of the response regulator VieA (Martinez-Wilson et al. 2008). The rapid phosphotransfer that occurs between VieS and VieA is consistent with a cognate interaction and is abolished when the D52A phosphorylation site of VieA is mutated (Martinez-Wilson

et al. 2008). Deletion of both *vieA* and *vieS* leads to increased c-di-GMP activity, motility defects, and increased biofilm formation (Tischler and Camilli 2004).

VieB is the second response regulator in the VieSAB three-component system, and has been shown experimentally to inhibit the VieS-VieA phosphotransfer (Mitchell et al. 2015). Phosphotransfer assays between the cytoplasmic portion of VieS and VieA are inhibited in the presence of VieB. VieB does not become phosphorylated in this reaction, indicating that VieB is not a phosphate sink nor does it compete with VieA for phosphorylation (Mitchell et al. 2015). However, it cannot be ruled out that VieB acts as a phosphatase against itself. By using a point-mutation approach to mimic either the phosphorylated or unphosphorylated state of VieB, it has been shown that unphosphorylated VieB is an active inhibitor of VieS-VieA phosphotransfer, while phosphorylated VieB is less active against this phosphotransfer (Mitchell et al. 2015). Overall, the VieSAB system plays a role in the upregulation of virulence genes in host-cell adhered *V. cholerae* in a manner that is dependent on a reduction in c-di-GMP levels. Some additional studies of HD-GYP, EAL, and GGDEF domain proteins in *V. cholerae* and other bacteria are needed to gain a full understanding their roles in c-di-GMP signaling.

V. cholerae is an environmental pathogen that relies on biofilm formation as a critical component of its infection cycle. Here we investigate a genomic region that spans from VC1080 to VC1087 in the *V. cholerae* genome and will be referred to as the

VC1080 operon (Figure 2.9). The VC1080 operon is particularly enriched in two component system proteins (tables 2.1-3.4). Bioinformatic analysis of the region revealed that the region encodes a c-di-GMP phosphodiesterase that is predicted to actively degrade ci-di-GMP. Based on the presence of two-component signaling genes and genes that code of c-di-GMP degrading enzymes, we hypothesize that the region is involved in regulating biofilm formation in response to environmental signals through a modulation of intracellular c-di-GMP levels. This chapter provides information on VC1080 to VC1087 gene products obtained by various bioinformatic analysis and presents results from studies investigating the influence of each gene on *V. cholerae* biofilm formation and motility, two c-di-GMP regulated phenotypes.


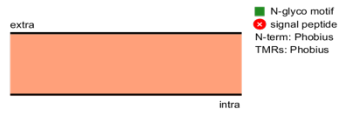
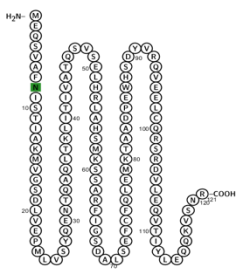
Results

Bioinformatic analysis of VC1080 operon gene products

The following section details an analysis of each gene product encoded in the VC1080 operon presented in the genomic context order. These analyses include domain analysis, cellular localization, size and structural homologs.

VC1080

Table 2.1

Predicted function	Histidine phosphotransfer protein
Domains	Histidine containing phosphotransfer domain 
Localization	Cytoplasmic  
Size (amino acids)	121

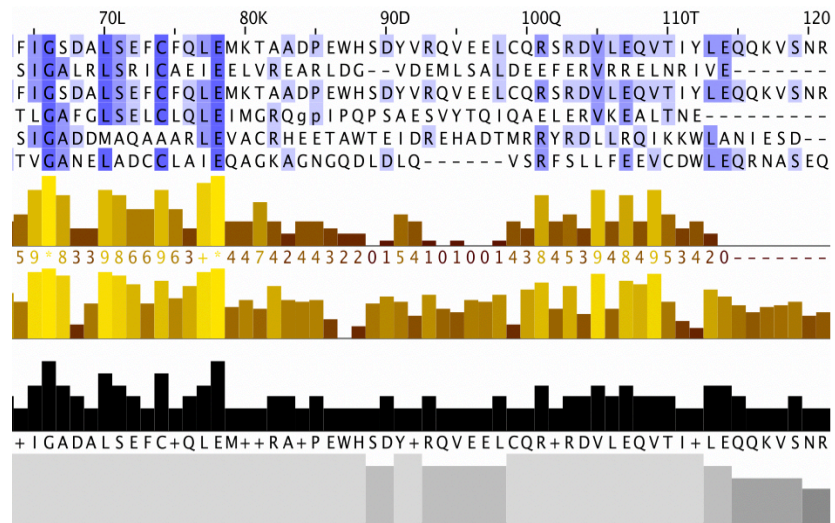
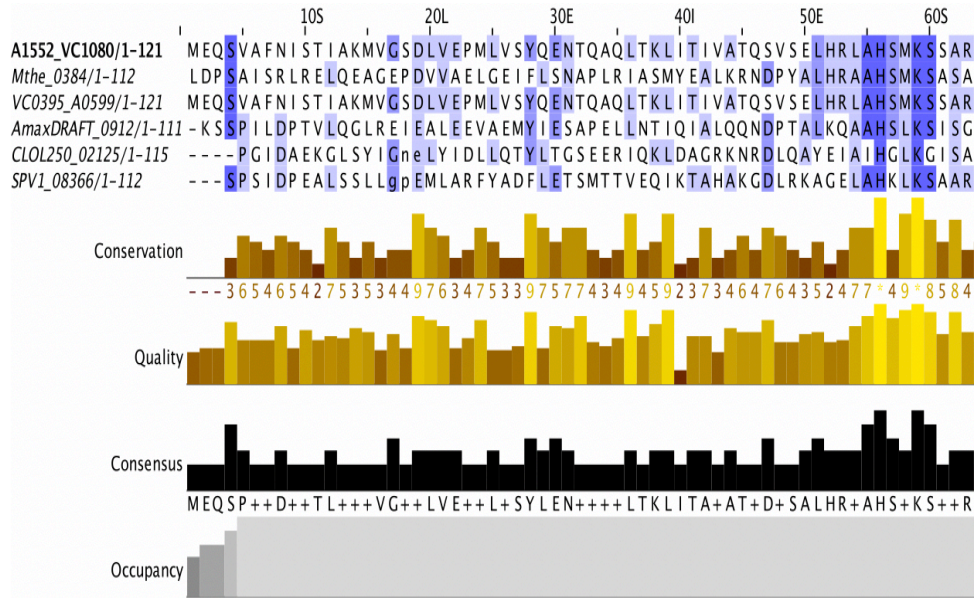
Top 5 homologs for VC1080

Table 2.2

Gene name	Protein name	Organism
Mthe_0384	Multi-sensor hybrid histidine kinase (EC 2.7.13.3)	<i>Methanotherix thermoacetophila</i> (strain DSM 6194 / JCM 14653 / NBRC 101360 / PT) (<i>Methanosaeta thermophila</i>)
VC0395_A0599	Phosphorelay protein LuxU	<i>Vibrio cholerae</i> serotype O1 (strain ATCC 39541 / Classical Ogawa 395 / O395)
AmaxDRAFT_0912	Histidine kinase (EC 2.7.13.3)	<i>Arthrospira maxima</i> CS-328
CLOL250_02125	Stage 0 sporulation protein A homolog (EC 2.7.13.3)	<i>Clostridium</i> sp. L2-50
SPV1_08366	Histidine kinase (EC 2.7.13.3)	<i>Mariprofundus ferrooxydans</i> PV-1

Top 5 sequence alignment for VC1080


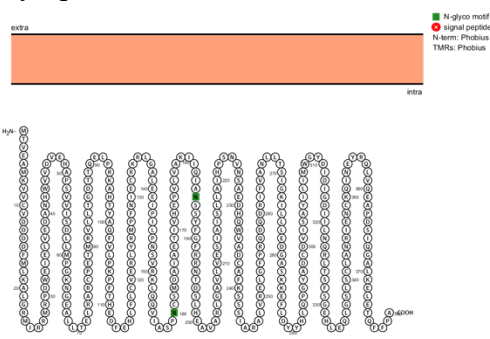
Figure 2.1



Bioinformatic analysis of VC1080 : Protein domains for VC1080 were obtained using Interpro (<https://www.ebi.ac.uk/interpro/>). Localization of proteins were obtained using protter (<https://wlab.ethz.ch/protter/start/>) (Table 2.1) Homologs and alignments were generated using data from Phyre2 (Table 2.2 and Figure2.1) (<http://www.sbg.bio.ic.ac.uk/~phyre2/html/page.cgi?id=index>). Based on bioinformatic analysis, VC1080 is likely a histidine phosphotransfer protein. Most revealing is the sequence alignment with LuxU, the phosphorelay protein from *Vibrio cholerae* serotype *O1*. Presence of a HPT protein suggests that genes encoded in the VC1080 operon may be involved in a phosphorelay type signaling cascade.

VC1081

Table 2.3

Predicted function	Response regulator
Domains	CheY-like receiver (REC) domain 
Localization	Cytoplasmic 
Size (amino acids)	380

Top 5 homologs for VC1081

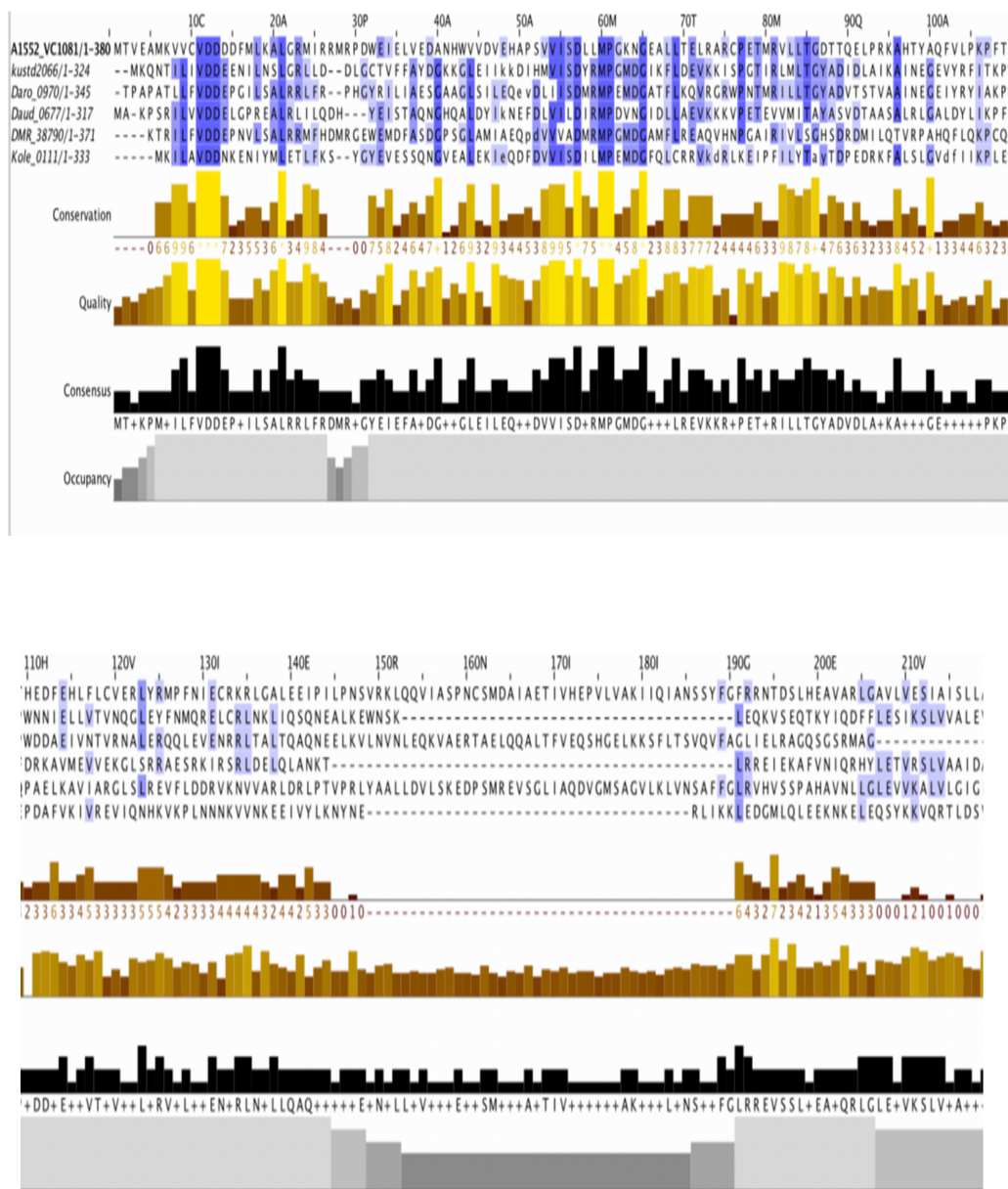
Table 2.4

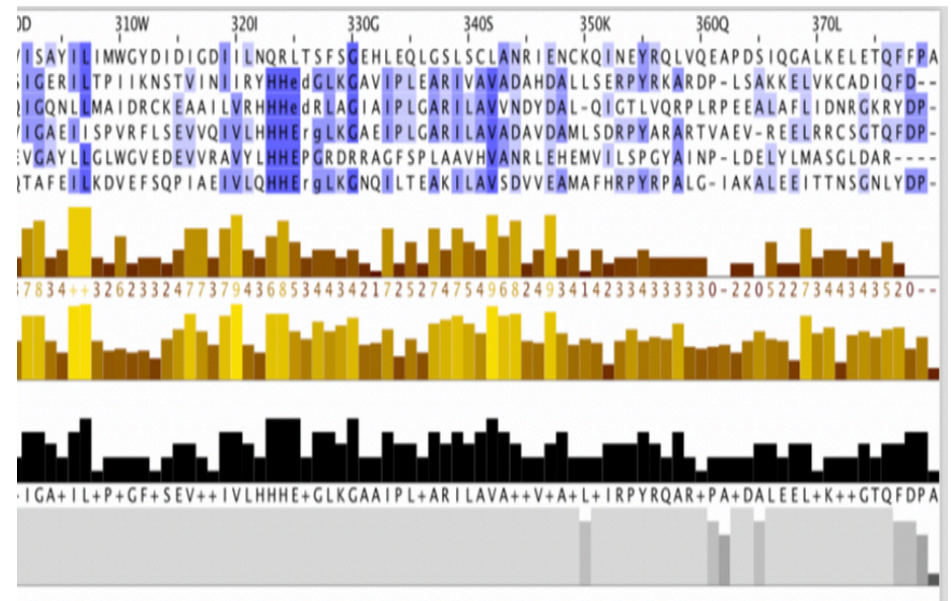
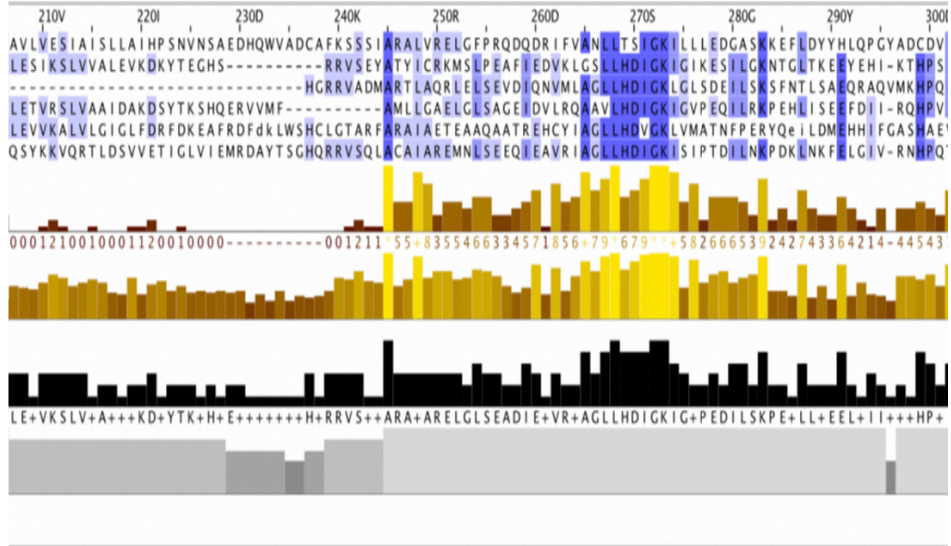
Gene name	Protein name	Organism
atoC kustd2066	Similar to sigma 54 response regulatory protein	<i>Kuenenia stuttgartiensis</i>
Daro_0970	Response regulator receiver: Metal-dependent phosphohydrolase, HD subdomain	<i>Dechloromonas aromatica</i> (strain RCB)
Daud_0677	Stage 0 sporulation protein A homolog	<i>Desulforudis audaxviator</i> (strain MP104C)
DMR_38790	Response regulator receiver protein	<i>Desulfovibrio magneticus</i> (strain ATCC 700980 /

		DSM 13731 / RS-1)
Kole_0111	Response regulator receiver modulated metal dependent phosphohydrolase	<i>Kosmotoga olearia</i> (strain ATCC BAA-1733 / DSM 21960 / TBF 19.5.1)

Sequence alignment for top 5 homologs for VC1081

Figure 2.2



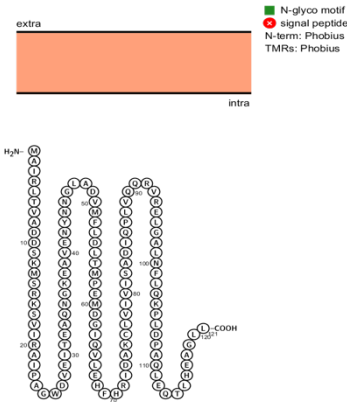


Bioinformatic analysis of VC1081: Protein domains for VC1081 (Table 2.3) were obtained using Interpro (<https://www.ebi.ac.uk/interpro/>). Localization of proteins were obtained using protter (<https://wlab.ethz.ch/protter/start/>) (Table 2.3). Homologs and alignments were generated using data from Phyre2 (Figure 2.2) (<http://www.sbg.bio.ic.ac.uk/~phyre2/html/page.cgi?id=index>).

Based on bioinformatic analysis, VC1081 likely encodes a response regulator protein. The protein may have metal-metal-dependent phosphohydrolase activity based on homology with proteins with similar function in *Kosmotoga olearia* and *Dechloromonas aromatica*, however this is yet to be confirmed.

VC1082

Table 2.5

Predicted function	Histidine Kinase
Domains	Unknown
Localization	Cytoplasmic 
Size (amino acids)	121

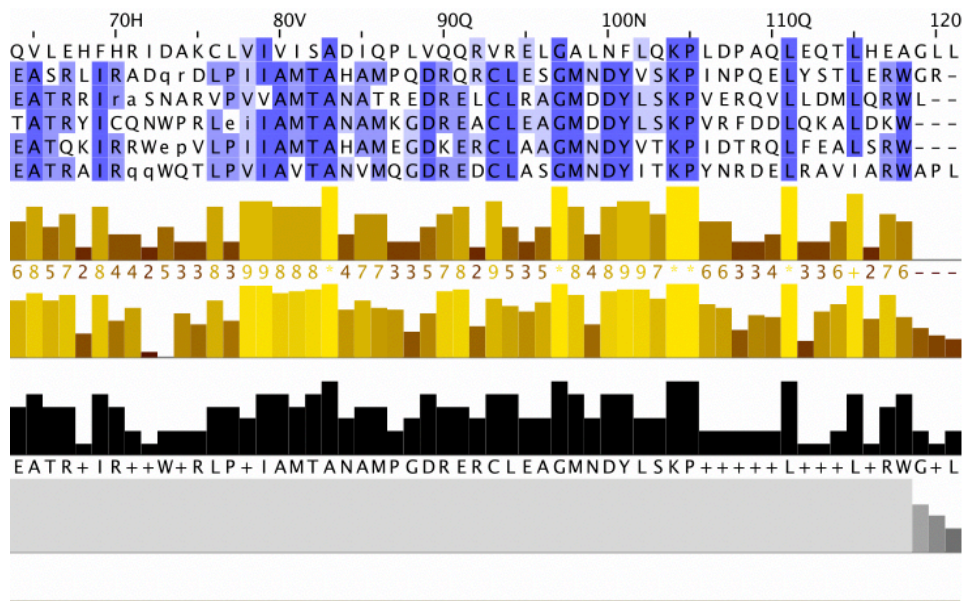
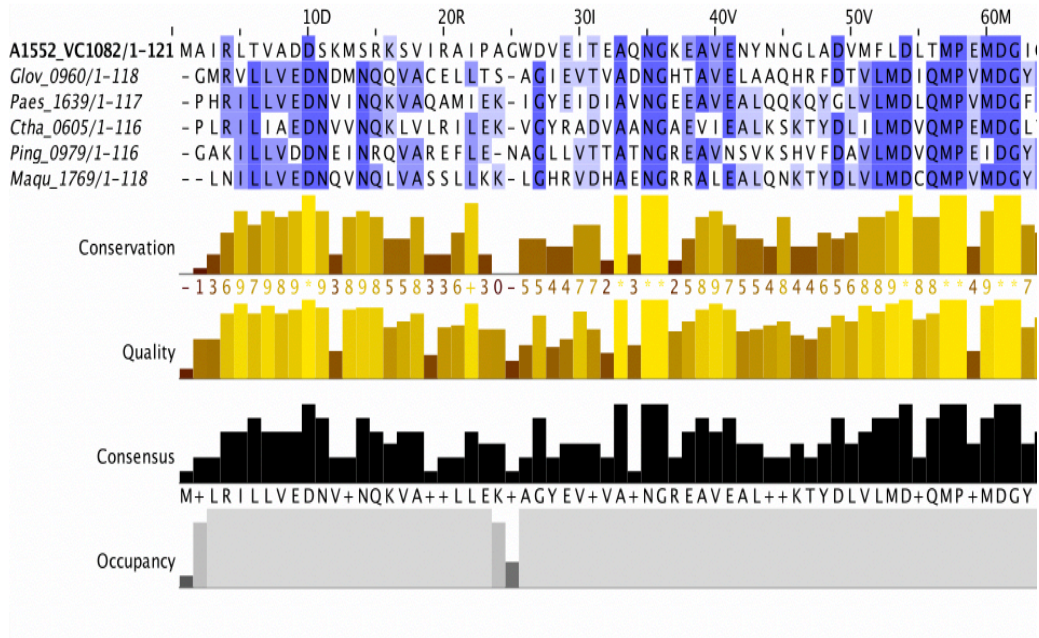
Top 5 homologs for VC1082

Table 2.6

Gene name	Protein name	Organism
Glov_0960	Histidine kinase (EC 2.7.13.3)	<i>Geobacter lovleyi</i> (strain ATCC BAA-1151 / DSM 17278 / SZ)
Paes_1639	Histidine kinase	<i>Prosthecochloris aestuarii</i> (strain DSM 271 / SK 413)
Ctha_0605	Multi-sensor hybrid histidine kinase (EC 2.7.13.3)	<i>Chloroherpeton thalassium</i> (strain ATCC 35110 / GB-78)
Ping_0979	Histidine kinase (EC 2.7.13.3)	<i>Psychromonas ingrahamii</i> (strain 37)
Maqu_1769	Histidine kinase (EC 2.7.13.3)	<i>Marinobacter hydrocarbonoclasticus</i> (strain ATCC 700491 / DSM 11845 / VT8)

Sequence alignment of top 5 homologs for VC1082

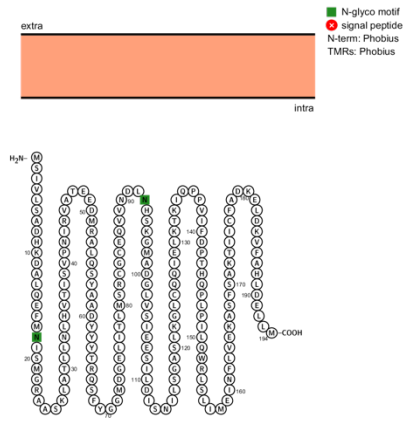
Figure 2.3



Bioinformatic analysis of VC1082: Protein domains for VC1082 (Table 2.5) were obtained using Interpro (<https://www.ebi.ac.uk/interpro/>). Localization of proteins were obtained using protter (<https://wlab.ethz.ch/protter/start/>) (Table 2.5). Homologs and alignments were generated using data from Phyre2 (Table 2.5 and Figure 2.3) (<http://www.sbg.bio.ic.ac.uk/~phyre2/html/page.cgi?id=index>). Based on homology to other species, VC1082 is likely a histidine kinase protein that is responsible for sensing a yet uncharacterized environmental signal. It is also unclear which gene encodes the cognate response regulator of VC1082.

VC1083

Table 2.7

Predicted function	Methyl-accepting chemotaxis protein
Domains	Unknown
Localization	Cytoplasmic 
Size (amino acids)	585

Top 5 homologs

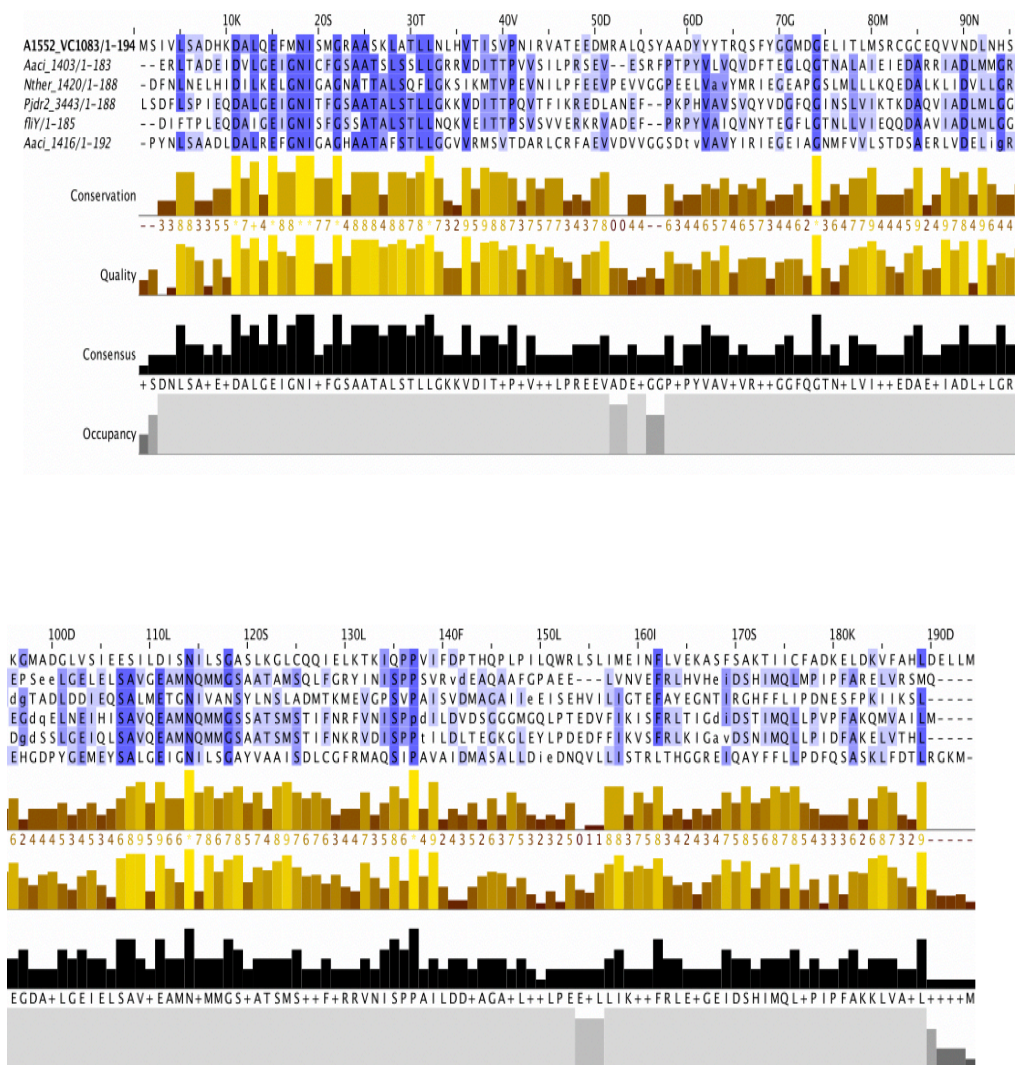
Table 2.8

Gene name	Protein name	Organism
Aaci_1403	CheC, inhibitor of MCP methylation	<i>Alicyclobacillus acidocaldarius</i> subsp. <i>acidocaldarius</i> (strain ATCC 27009 / DSM 446 / JCM 5260 / NBRC 15652 / NCIMB 11725 / NRRL B-14509 / 104-1A) (<i>Bacillus acidocaldarius</i>)
Nther_1420	CheC, inhibitor of MCP methylation	<i>Natranaerobius thermophilus</i> (strain ATCC BAA-1301 / DSM 18059 / JW/NM-WN-LF)
Pjdr2_3443	CheC, inhibitor of MCP methylation	<i>Paenibacillus</i> sp. (strain JDR-2)
fliY GTNG_1084	Flagellar motor switch protein	<i>Geobacillus thermodenitrificans</i> (strain NG80-2)

Aaci_1416	CheC, inhibitor of MCP methylation	<i>Alicyclobacillus acidocaldarius</i> subsp. <i>acidocaldarius</i> (strain ATCC 27009 / DSM 446 / JCM 5260 / NBRC 15652 / NCIMB 11725 / NRRL B-14509 / 104-1A) (<i>Bacillus acidocaldarius</i>)
-----------	------------------------------------	--

Sequence alignment of top 5 homologs for VC1083

Figure 2.4


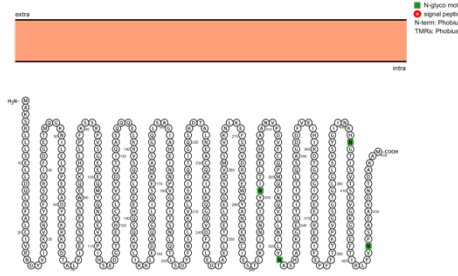


Bioinformatic analysis of VC1083: Protein domains for VC1083 (Table 2.7) were obtained using Interpro (<https://www.ebi.ac.uk/interpro/>). Localization of proteins were obtained using protter (<https://wlab.ethz.ch/protter/start/>) (Table 2.7). Homologs and alignments were generated using data from Phyre2 (Table 2.8 and Figure 2.4) (<http://www.sbg.bio.ic.ac.uk/~phyre2/html/page.cgi?id=index>).

Based on bioinformatic analysis and homology, VC1083 is likely a methyl-accepting chemotaxis protein. Biofilm formation and motility are typically inversely regulated processes, and both are influenced by c-di-GMP, so we hypothesize that genes in the region may influence *V. cholerae* motility when overexpressed or deleted. These hypotheses are further explored in this chapter.

VC1084

Table 2.9

Predicted function	Histidine Kinase
Domains	transferase 
Localization	Cytoplasmic 
Size (amino acids)	439

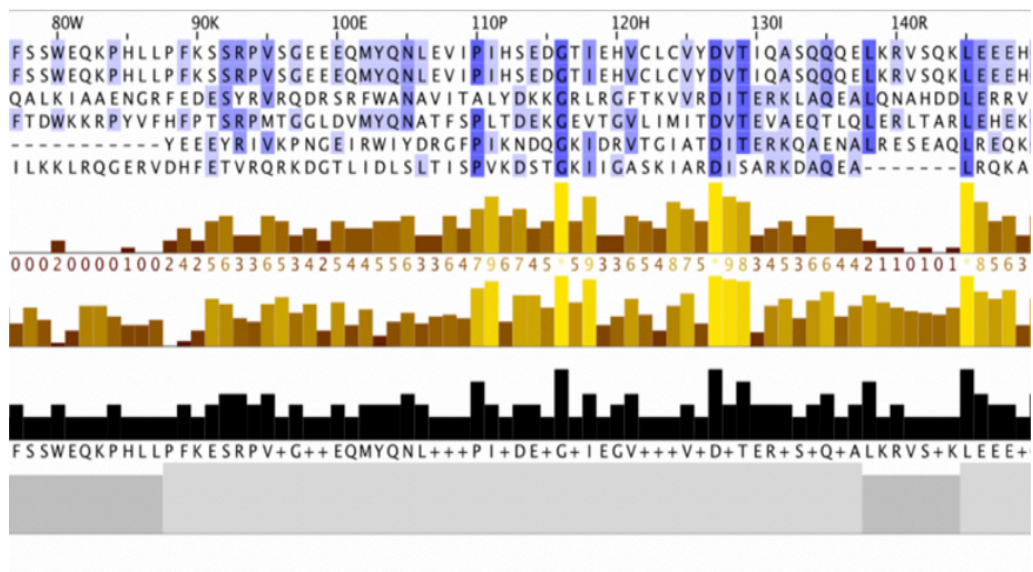
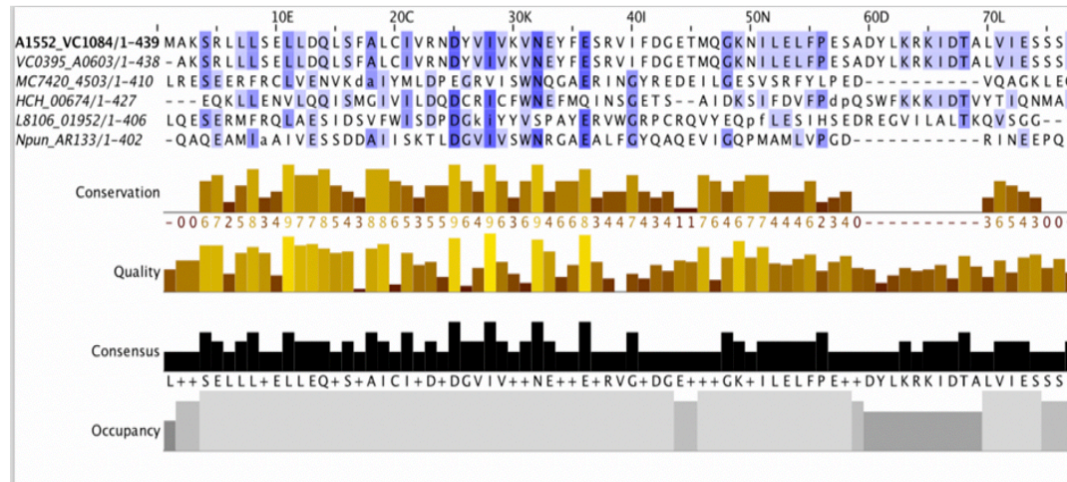
Top 5 homologs for VC1084

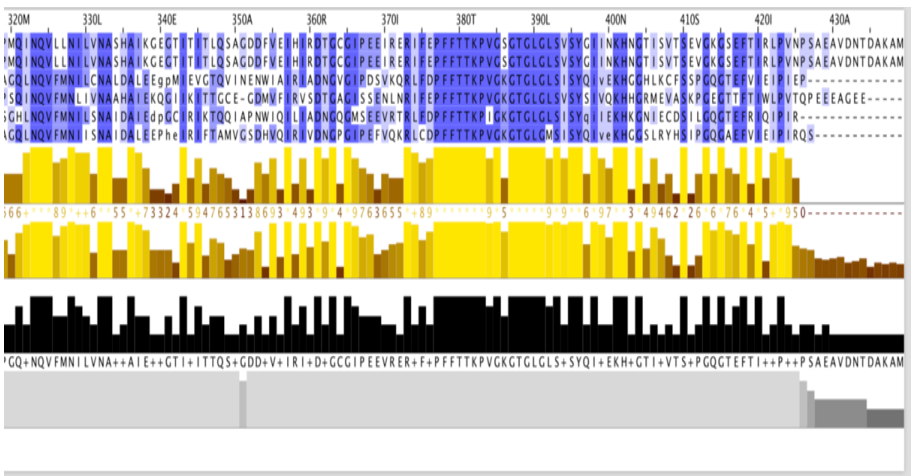
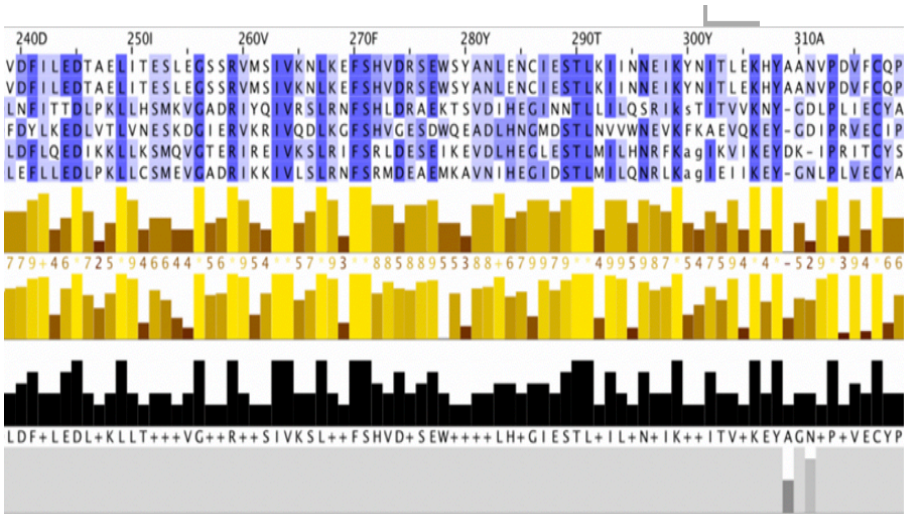
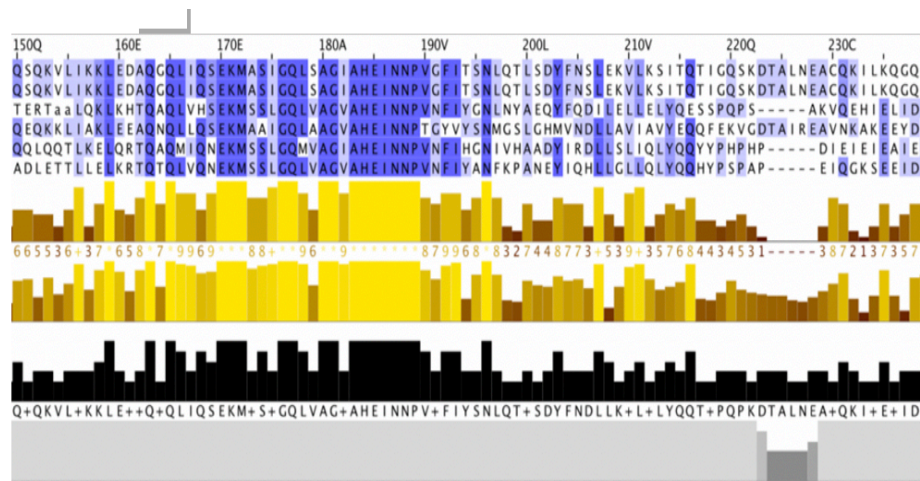
Table 3.0

Gene name	Protein name	Organism
VC0395 A0603	Histidine kinase (EC 2.7.13.3)	<i>Vibrio cholerae</i> serotype O1 (strain ATCC 39541 / Classical Ogawa 395 / O395)
MC7420 4503	PAS fold family	<i>Coleofasciculus chthonoplastes</i> PCC 7420
HCH_00674	Histidine kinase (EC 2.7.13.3)	<i>Hahella chejuensis</i> (strain KCTC 2396)
L8106_01952	PAS/PAC Sensor Signal Transduction Histidine Kinase	<i>Lyngbya sp.</i> (strain PCC 8106) (<i>Lyngbya aestuarii</i> (strain CCY9616))
Npun_AR133	PAS/PAC sensor signal transduction histidine kinase	<i>Nostoc punctiforme</i> (strain ATCC 29133 / PCC 73102)

Sequence alignment for top 5 VC1084 homologs

Figure 2.5




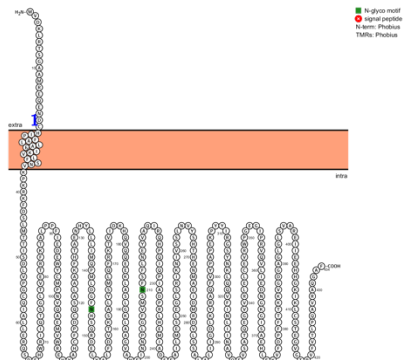


Bioinformatic analysis of VC1084: Protein domains for VC1084 (Table 2.9) were obtained using Interpro (<https://www.ebi.ac.uk/interpro/>). Localization of proteins were obtained using protter (<https://wlab.ethz.ch/protter/start/>) (Table 2.9). Homologs and alignments were generated using data from Phyre2 (Table 3.0 and Figure 2.5) (<http://www.sbg.bio.ic.ac.uk/~phyre2/html/page.cgi?id=index>).

Based on bioinformatic analysis and homology, VC1084 is likely a sensor histidine kinase. Considering that the protein does not have a periplasmic domain, it is likely that the signal being sensed by this protein is freely diffusible, or that the protein may rely on other specialized sensing protein to relay a signal.

VC1085

Table 3.1

Predicted function	Sensor histidine kinase
Domains	Dimerization and histidine phosphotransfer domain, catalytic ATP-binding domain 
Localization	Cytoplasm 
Size (amino acids)	434

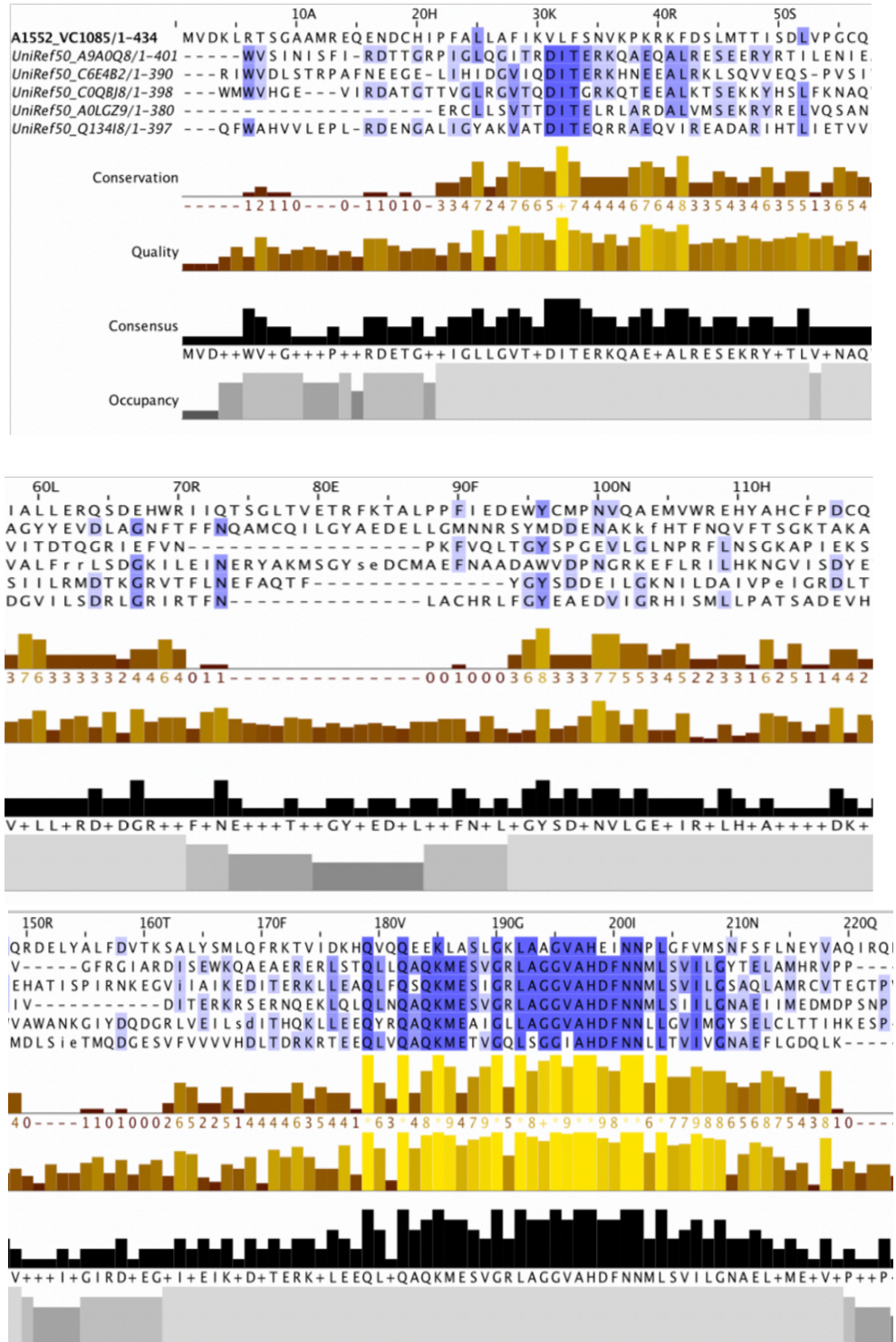
Top 5 homologs for VC1085

Table 3.2

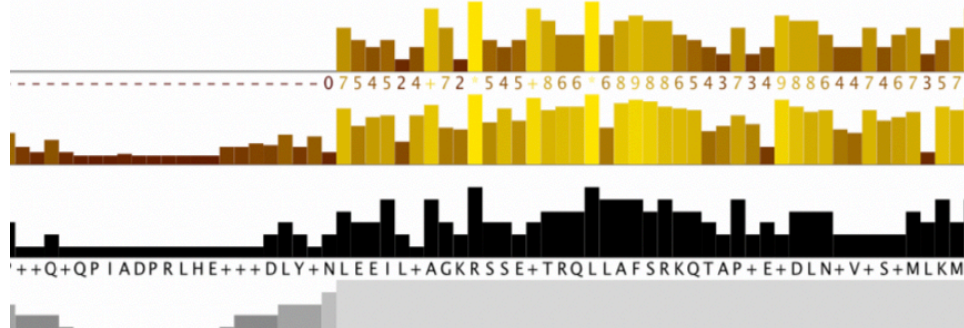
Gene name	Protein name	Organism
Dole_3272	Histidine kinase (EC 2.7.13.3)	<i>Desulfococcus oleovorans</i> (strain DSM 6200 / Hxd3)
GM21_1351	Histidine kinase (EC 2.7.13.3)	<i>Geobacter</i> sp. (strain M21)
HRM2_39420	Histidine kinase (EC 2.7.13.3)	<i>Desulfobacterium autotrophicum</i> (strain ATCC 43914 / DSM 3382 / HRM2)
Sfum_1007	Histidine kinase (EC 2.7.13.3)	<i>Syntrophobacter fumaroxidans</i> (strain DSM 10017 / MPOB)
RPD_3277	Histidine kinase (EC 2.7.13.3)	<i>Rhodopseudomonas palustris</i> (strain BisB5)

Sequence alignment for top 5 VC1085 homologs

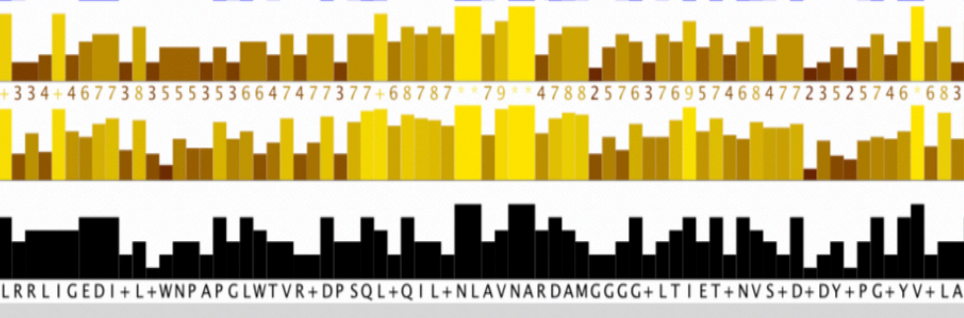
Figure 2.6



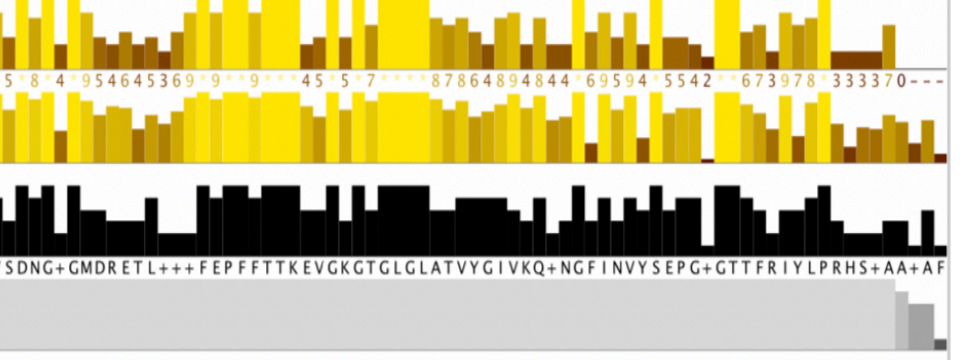
230I 240A 250L 260V 270H 280D
 HHPQIQPIADPRLHEMIADSEAILMESLEGLSRIKNIVSSUNVYSHTHENMAEIDMRDVLSSALAL
 -----HDP LYEDLREILSAAKRSSEITRQLLAFARKQTspKVIDLSDTVENMLKMK
 VWQD-----LEQIVQAGKRSSQITRQLLAFSRKEiaPREVNLNEHFTEMQKT
 IVT-----NLEEYKAAERSSSLTRQLLAFARKQTaPKILNLNHVLADMLKM
 -----LYDNI EHKNAGLRAATLVRQLLAFSRKQidPRVVDLNTI I I SET EKM
 -----ARQDLRSLARDISRAGQRGAELTQRLLAFSRRQkVELDCNELVDMSMHKL



290I 300V 310I 320V 330Q 340V 350P 36
 IIGDLKYRAQFVYPAPAEKPYIRGSYKLLQQVFINLIINAVQSVSATQEGVVRLELCEVRWPGEGIPRVQVL
 LRRLLIGEDI DLAWNPGGLWTVNMDPAQISQILANLLVNARDAIGGVGKVTIETGNVSFDQDYIPGDYVVLAL
 LGRLLIGEDIRMFNPAPGLWTIDADTTQLDQILVNLAVNARDAMNGGVLTIETANVRVDRSYsqEYVQLA
 LMRLLIGEDI DLTWNPAPNLWSVKIDPSSQIDQILANLCVNARDSIKSVGKVTIETGNISFDEAYnPGSYVMMAL
 LRRLLIGEDI QLESTLEPDLWPVRI DPSSQLEQVILNLAVNARDAMPDGGRLTIRTANVTLDdeAVAGPYVLE
 LRPTLR EDIVIDTDLDPGLRTAYADRSQLESAILNLALNAQDAMLGGRLSITTSNVSLDa dVRPGDYVVLVS




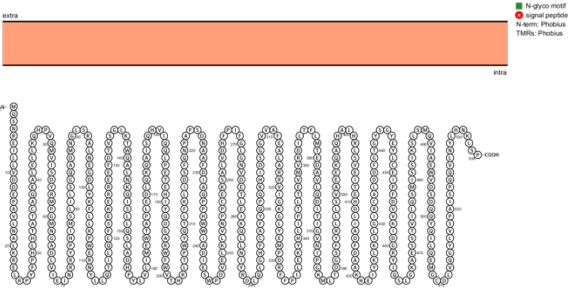
30L 370A 380F 390A 400I 410L 420V 430A
 IEDNGKGISAEHL EKVFDPFFFTTKVGDGAGLGLSVAREIIEEHHGKIKLCSLEGVTRVFVTLPAQAVRAQGF
 VSDGCGMDRKTDRLL FEPFFFTTKEVGKGTGLGLATVYGVISQNGGFINVYSEPGQTTFR IYLP RHGGA----
 VSDGCGMDRET LAQIFEPFFFTTKEVGKGTGLGLATVYGVIRQHNGGFINVYSEPGHGTTFQINFRFSGAA---
 VSDNGSGMDKKILDKLFEPFFFTTKSIGQGTGLGLATVYGVVKQNHGFINVYSEPGETTFR IYLPVHSETAVA-
 VTDNGAGIDKDTLRRIFEPFFFTTKEKGRGTGLGLATVYGV I KQSSGHISVRSRPRCCTTFSIYLPVVEVEAE-
 VTDNGSGMPREVL EHVFEFPHYTTKEVGKGSGLGLSMVYGFVKQSNGHVSVYSEPLGTTVRLYLPAIATGQPA-



Bioinformatic analysis of VC1085: Protein domains for VC1085 (Table 3.1) were obtained using Interpro (<https://www.ebi.ac.uk/interpro/>). Localization of proteins were obtained using protter (<https://wlab.ethz.ch/protter/start/>) (Table 3.1). Homologs and alignments were generated using data from Phyre2 (Table 3.2 and Figure 2.6) (<http://www.sbg.bio.ic.ac.uk/~phyre2/html/page.cgi?id=index>). Based on bioinformatic analysis and homology, VC1085 is likely a sensor histidine kinase. Considering that the protein does not have a periplasmic sensing domain, it is likely that the signal being sensed by this protein is freely diffusible, or that the protein relies on other specialized sensing proteins to relay the signal.

VC1086

Table 3.3

Predicted function	Response regulator
Domains	EAL domain (active) 
Localization	Cytoplasmic 
Size (amino acids)	536

Top 5 homologs for VC1085


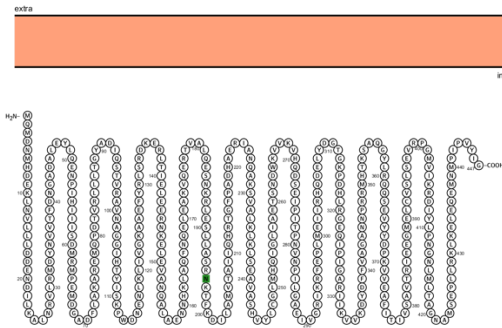
Table 3.4

Gene name	Protein name	Organism
Msip34_1854	Diguanylate cyclase/phosphodiesterase with PAS/PAC sensor(S)	<i>Methylovorus glucosetrophus</i> (strain SIP3-4)
CAP2UW1_3428	Diguanylate cyclase/phosphodiesterase with PAS/PAC and GAF sensor(S)	<i>Accumulibacter phosphatis</i> (strain UW-1)
Tcr_1150	Diguanylate cyclase/phosphodiesterase with PAS/PAC and GAF sensor(S)	<i>Hydrogenovibrio crunogenus</i> (strain XCL-2) (<i>Thiomicrospira crunogena</i>)
LHK_02557	Diguanylate cyclase/phosphodiesterase with PAS/PAC sensor	<i>Laribacter hongkongensis</i> (strain HLHK9)
amb1214	Predicted signal transduction protein	<i>Magnetospirillum magneticum</i> (strain AMB-1 / ATCC 700264)

Bioinformatic analysis of VC1086: Protein domains for VC1086 (Table 3.3) were obtained using Interpro (<https://www.ebi.ac.uk/interpro/>). Localization of proteins were obtained using protter (<https://wlab.ethz.ch/protter/start/>) (Table 3.3). Homologs and alignments were generated using data from Phyre2 (Table 3.4 and Figure 2.7) (<http://www.sbg.bio.ic.ac.uk/~phyre2/html/page.cgi?id=index>). Based on bioinformatic analysis and homology, VC1086 is likely a response regulator with a EAL domain. The presence of an EAL domain indicates that the protein has phosphodiesterase activity and can degrade c-di-GMP.

VC1087

Table 3.5

Predicted function	Response Regulator
Domains	Signal receiver domain; HD-GYP domain (inactive) 
Localization	Cytoplasmic 
Size (amino acids)	447

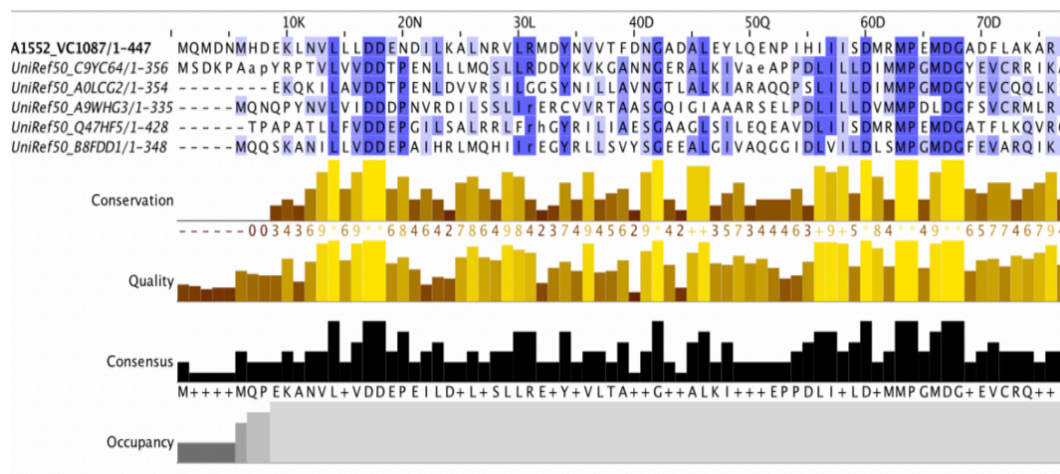
Top 5 homologs for VC1087

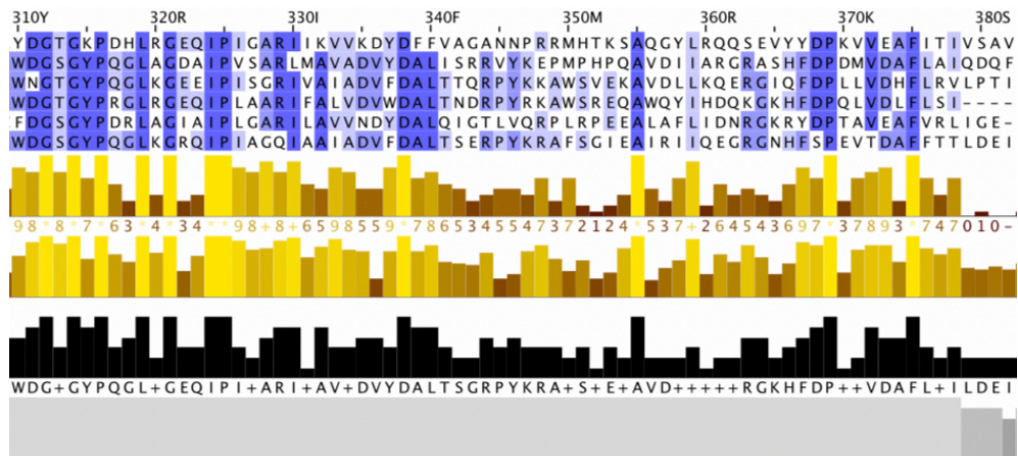
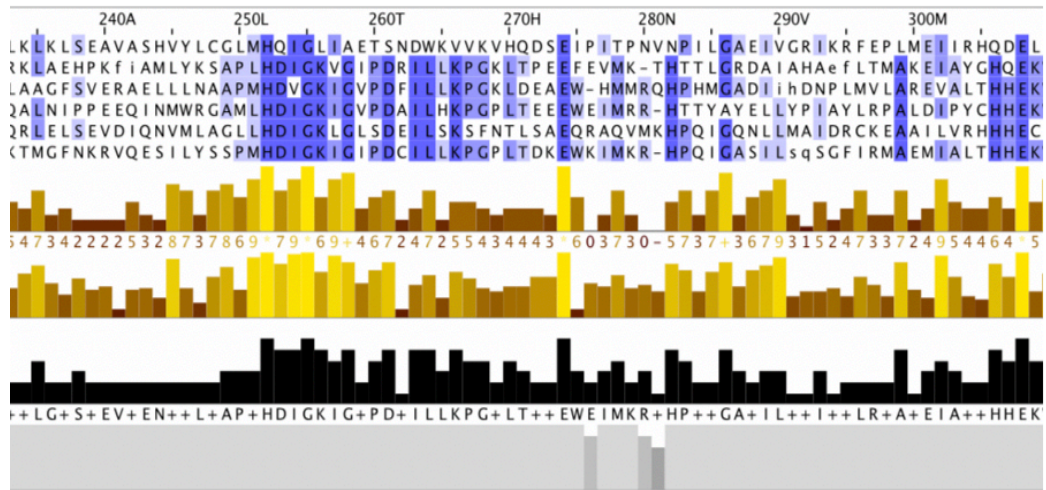
Table 3.6

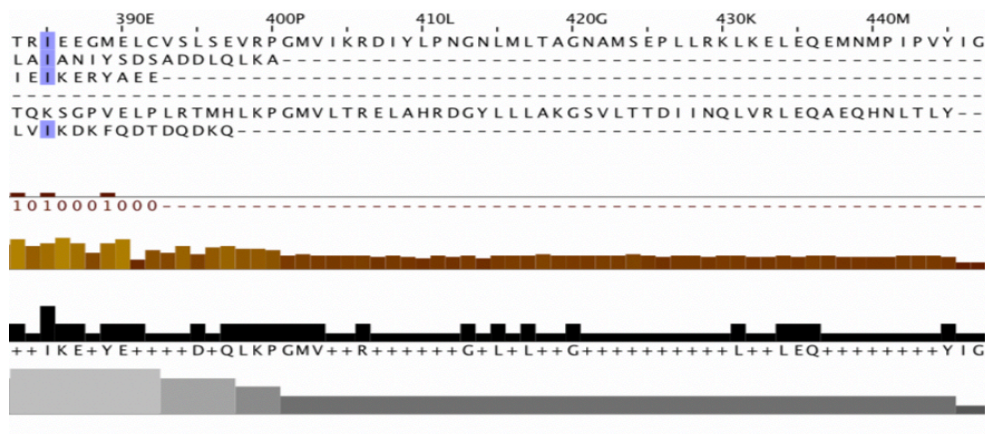
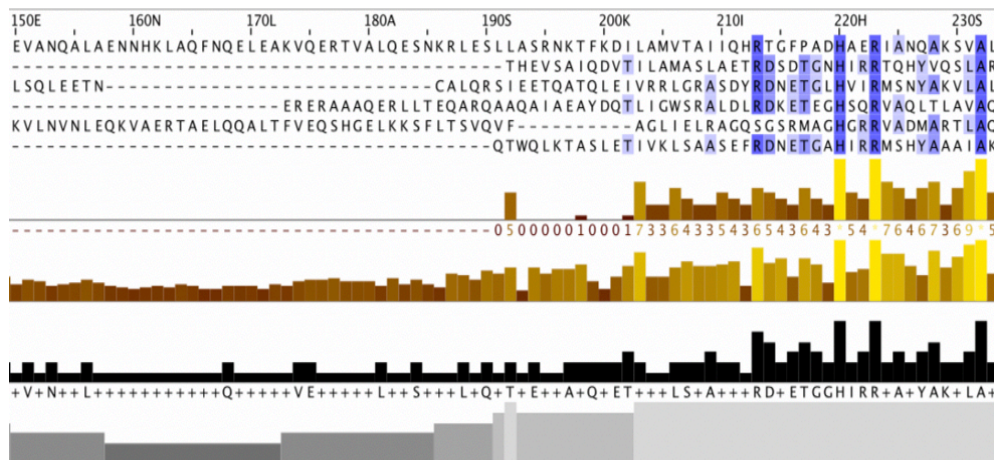
Gene name	Protein name	Organism
Mmc1_3165	Response regulator receiver modulated metal dependent phosphohydrolase	<i>Magnetococcus marinus</i> (strain ATCC BAA-1437 / JCM 17883 / MC-1)
Caur_3090	Metal dependent phosphohydrolase	<i>Chloroflexus aurantiacus</i> (strain ATCC 29366 / DSM 635 / J-10-fl)
Daro_0970	Response regulator receiver: Metal-dependent phosphohydrolase, HD subdomain	<i>Dechloromonas aromatica</i> (strain RCB)
Dalk_4886	Response regulator receiver modulated metal dependent phosphohydrolase	<i>Desulfatibacillum aliphaticivorans</i>
ACP_1051	Response regulator	<i>Acidobacterium capsulatum</i> (strain ATCC 51196 / DSM 11244 / JCM 7670 / NBRC 15755 / NCIMB 13165 / 161)

Sequence alignment for top 5 homologs of VC1087

Figure 2.8







Bioinformatic analysis of VC1087: Protein domains for VC1087 (Table 3.5) were obtained using Interpro (<https://www.ebi.ac.uk/interpro/>). Localization of proteins were obtained using protter (<https://wlab.ethz.ch/protter/start/>) (Table 3.5). Homologs and alignments were generated using data from Phyre2 (Table 3.6 and Figure 2.8) (<http://www.sbg.bio.ic.ac.uk/~phyre2/html/page.cgi?id=index>). Based on bioinformatic analysis and homology, VC1087 is likely a response regulator with an HD-GYP domain. The presence of an HD-GYP domain suggests that the protein has phosphodiesterase activity, however, studies have shown that this protein is enzymatically inactive (McKee et al. 2014).

Tables 2.1-3.6 and Figures 2.1-2.8: Domains and predicted function of each gene in the VC1080 operon obtained from Protter and Microbes online. Top 5 homologs of VC1080 calculated by a PSI-BLAST (Position-Specific Iterated Basic Local Alignment Search Tool) scan of the amino acid sequence against a large sequence database (Uniref50) via Phyre2. Images were generated with JalView.

Bioinformatic analysis of the VC1080 operon gene products

The gene products of the VC1080 operon are not well understood, though VC1086 is the best studied. VC1086 is an EAL-domain containing response regulator (Table 3.3, 3.4, Figure 2.7). This protein is predicted to be localized to the cytoplasm, and possesses the residues characteristic of EAL enzymatic activity (Schmidt, Ryjenkov, and Gomelsky 2005). As a response regulator, the activity of VC1086 is modulated by a cognate histidine kinase. Two histidine kinases have been demonstrated to phosphorylate VC1086 in vitro; VC1084 (Tables 2.9, 3.0, Figure 2.5) , which is encoded in the same operon as VC1086, and VCA0719, a nitric oxide responsive histidine kinase (Plate and Marletta 2012). Interestingly, these two histidine kinases also rapidly transfer their phosphoryl group to VC1087 (Tables 3.5, 3.6, Figure 2.8) another gene product encoded in the VC1080 region (Plate and Marletta 2012). VC1087 is a response regulator with a predicted HD-GYP domain, which is typically associated with phosphodiesterase activity, though it lacks an intact HD motif rendering it enzymatically inactive (McKee et al. 2014b). Based on the lack of an HD motif, it is expected that c-di-GMP hydrolysis by the VC1080 operon gene products is achieved solely through the activity of VC1086. Furthermore, analysis of *vpsL* expression in the VC1080 (Tables 2.1,2.2, Figure 2.1) deletion strain have revealed that VC1080 does not exhibit differences in *vpsL* expression compared to wildtype, suggesting that VC1080 is not involved in the regulation of *vpsL* expression (Shikuma et al. 2009). Overall, bioinformatic analysis and prior studies of the VC1080 operon gene products support the hypothesis that the region may be involved

in modulating levels of c-di-GMP and c-di-GMP regulated phenotypes such as motility and biofilm formation.

Furthermore, a recent study found that VC1087 binds to glucose-specific enzyme IIA (EIIA^{gluc}), when cells are grown in biofilm (Pickering, Smith, and Watnick 2012).

This interaction was not observed in cells grown planktonically. EIIA^{gluc} is a central regulator of bacterial metabolism and an intermediate in the phosphoenolpyruvate phosphotransferase system (PTS), a conserved phosphotransfer cascade that controls carbohydrate transport. This finding raises the intriguing possibility that carbohydrate abundance may also influence expression or activity of genes encoded in the VC1080 region.

Bioinformatic analysis and investigations into VC1080 operon homologs in other bacterial species can give further insight into the potential role of genes encoded in the operon in *V. cholerae*. The amino acid sequence of each gene encoded in the VC1080 operon was scanned against a large sequence database Phyre2. This analysis revealed the top 5 homologous proteins for each gene. From this analysis, it is clear that the region is highly enriched in two component system genes, some of which harbor c-di-GMP degrading domains (tables 2.1-3.4). We interpret the presence of multiple two component system coding genes, including a histidine phosphotransferase protein, to indicate that the proteins encoded in this region may be involved in a phosphorelay signaling cascade. The presence of multiple response

regulators and histidine kinases, all of which are cytoplasmic with the exception of VC1085, suggests that the region may be responsible for integrating multiple environmental signals into a cellular response. The cytoplasmic localization of the proteins suggests that some of these signals may be freely diffusible, or perhaps rely on other specialized sensing proteins to relay signals to their cognate sensor histidine kinases. The presence of EAL and HD-GYP domains suggests this region's proteins reduce intracellular c-di-GMP, which would subsequently affect c-di-GMP responsive phenotypes such as biofilm formation and motility. The following results display the organization and predicted function of each gene in the VC1080 operon.

Analysis of biofilm gene expression in the absence of VC1080 operon members

Given the results of the bioinformatic analysis, we predicted that the role of VC1080 operon members was to regulate c-di-GMP levels and c-di-GMP responsive phenotypes. Based on the presence of two-component system proteins, we suspected that these c-di-GMP-mediated changes may be responsive to an environmental signal. To assess this hypothesis, we first examined whether these gene products influence biofilm formation, which is a characteristic c-di-GMP modulated phenotype. Production of Vibrio polysaccharide, the main component of the *V. cholerae* biofilm matrix, is required for *V. cholerae* biofilm formation and is modulated by c-di-GMP. We asked if deletion of any of the genes in the VC1080 operon would lead to changes in levels of *vpsL*, the first gene in the *vps-II* cluster, which along with the *vps-I* cluster genes, encodes components that are required for VPS production and biofilm formation. We used a transcriptional fusion of the regulatory region of *vpsL* and the luciferase transcriptional reporter *luxCADBE* (*PvpsL-lux*). Deletion of both VC1087 and VC1081 significantly increased *vpsL* expression, while other operon members had no effect (Fig. 3.3). These changes in *vpsL* levels in the absence of some VC1080 operon members lent support to our hypothesis that the VC1080 operon was involved in biofilm formation through modulation of c-di-GMP.

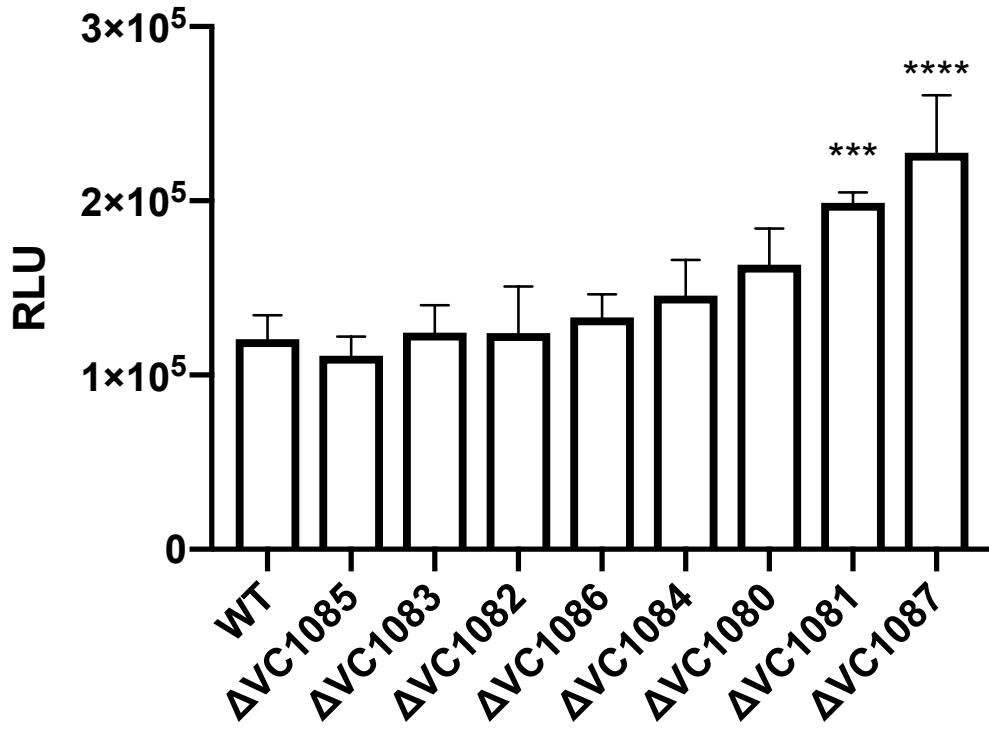


Figure 3.3: *vpsL* expression in operon deletion strains. Cultures of VC1080 deletion strains harboring the *PvpsL-lux* construct were grown overnight in LB containing chloramphenicol (5 $\mu\text{g}/\text{mL}$). These cultures were diluted 1:200 and 200 μL added to a white, flat-bottom 96-well plate. Luminescence and optical density (600 nm) were measured using a Perkin Elmer Victor3 multilabel counter. Relative luminescence units (RLU) are expressed as luminescent counts $\cdot \text{min}^{-1} \cdot \text{mL}^{-1} \cdot \text{OD}_{600}^{-1}$. Assays were performed in three independent biological replicates. Statistical analysis was performed using GraphPad Prism 7. *** $p \leq 0.001$ **** $p \leq 0.0001$. WT (smooth wildtype).

Analysis of biofilm spot morphology phenotypes in strains lacking VC1080 operon members

To examine the effect that genes encoded in the VC1080 operon have on *V. cholerae* biofilm formation directly, we individually deleted each gene and conducted spot biofilm morphology assays to determine if changes in *vpsL* expression might be reflected in changes in biofilm spot morphology. This experiment was performed in the Rugose variant of *V. cholerae* A1552, which harbors a single point mutation in the *vprC* gene, which is a diguanylate cyclase. This allows the rugose variant to form robust biofilms under laboratory conditions, allowing us to visually evaluate biofilm corrugation patterns (Beyhan and Yildiz 2007). This is due to an increase in c-di-GMP, which leads to an increase in biofilm matrix production. Any changes to colony corrugation can be interpreted as due to changes in c-di-GMP and biofilm matrix production.

Strains lacking each gene were cultured overnight, diluted 1:200, and 3 μ L were spotted onto LB agar. After 48 hours, we did not observe any marked changes in *V. cholerae* spot biofilm corrugation in the absence of any gene encoded in the VC1080 region (Fig. 3.4). One possibility to explain these results is that, under the conditions tested, the genes encoded in this region are not expressed at high enough levels to observe phenotypes.

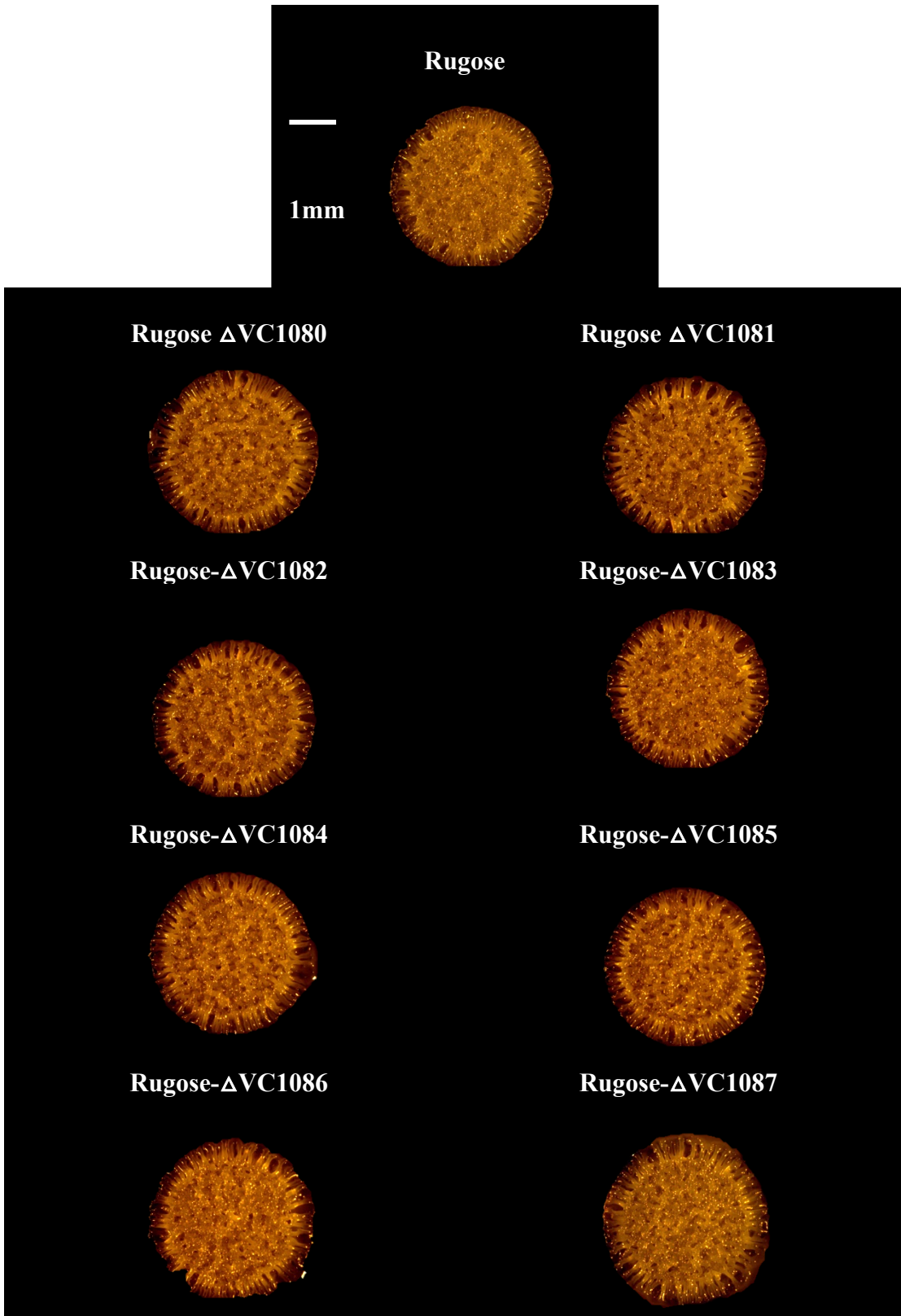


Figure 3.4: Spot biofilm morphologies of VC1080 operon deletion mutants.

Overnight cultures of each deletion mutant were spotted onto standard LB agar plates and incubated at 30 °C for 48 hours. The experiment was repeated in two biological replicates, images presented are representative of isolated trials.

Analysis of biofilm spot morphology phenotypes of strains overexpressing VC1080 operon members

To further evaluate the effect of the VC1080 operon on *V. cholerae* biofilm formation, and to evaluate the hypothesis that genes may not be expressed under the conditions tested, we examined the effect of overexpression of VC1080 operon genes. Each gene encoded in the VC1080 operon was individually overexpressed on pMMB67EH, which controls gene expression through an IPTG inducible promoter. Strains were cultured overnight, diluted 1:200, and 3 μ L were spotted onto LB agar containing 0.1 mM IPTG. After 48 hours, we observed a reduction in *V. cholerae* spot biofilm corrugation when VC1086 was overexpressed, as well as a noticeable reduction in the corrugation of VC1084 (Figure 3.5). Colony corrugation pattern of the other strains remained similar to the rugose parent strain. Considering that VC1086 is an active PDE, we suspect that the reduction in corrugation is due to a reduction in levels of c-di-GMP, and a subsequent reduction in the production of biofilm matrix components. VC1084 is a histidine kinase, and we hypothesize that the VC1086 (RR) and VC1084 (HK) may function as a cognate histidine kinase response regulator pair to control levels c-di-GMP in response to environmental stimuli.

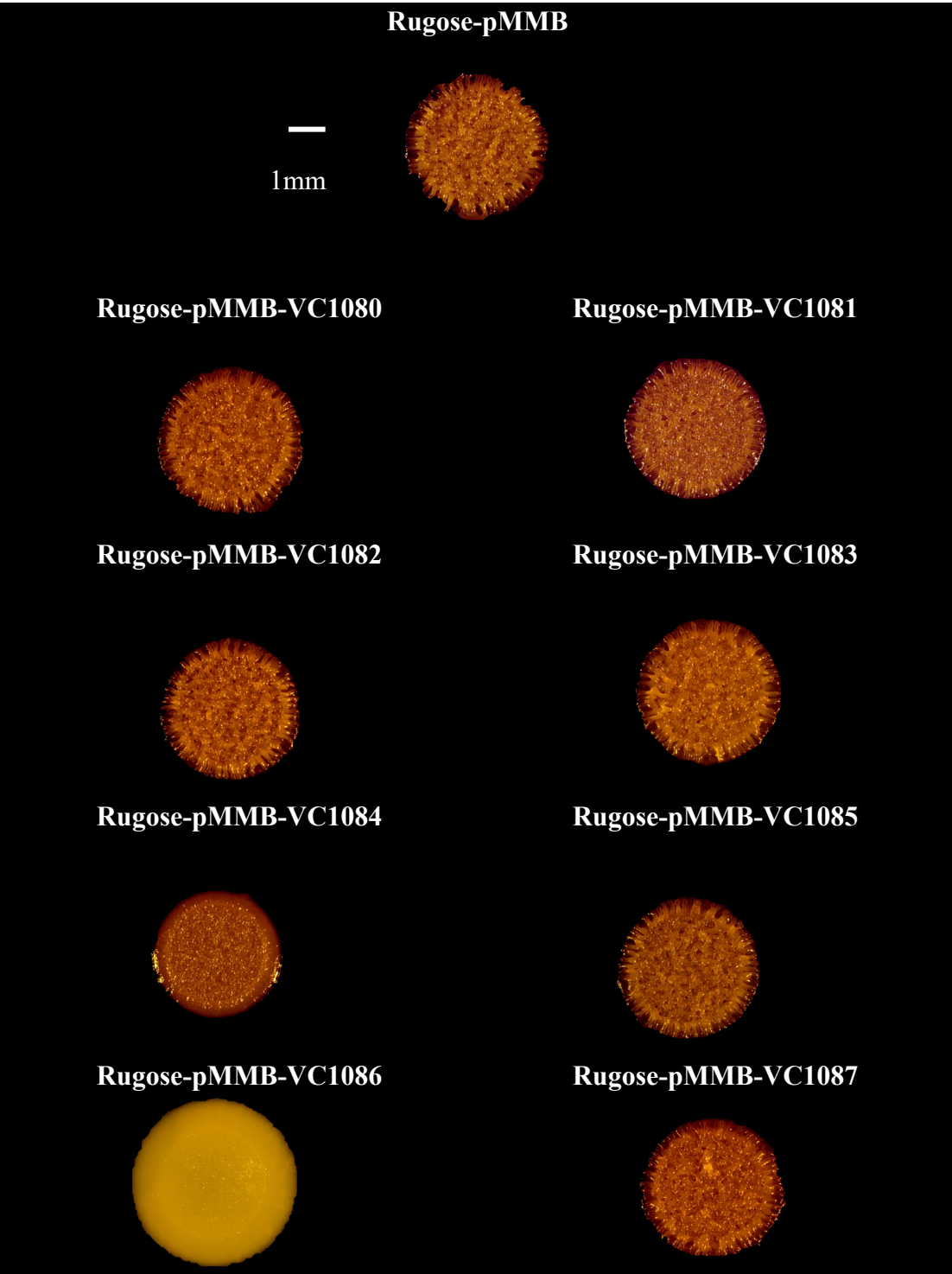


Figure 3.5: Spot biofilm morphologies of VC1080 operon overexpression strains. Overnight cultures of each overexpression strain were diluted 1:200. 3 μ L were spotted onto standard LB agar plates containing 0.1 mM IPTG + ampicillin 100 μ g/ μ l and incubated at 30 °C for 48 hours. The experiment was repeated in two biological replicates, images presented are representative of isolated trials.

We aimed to further evaluate the relationship between two two-component system gene products encoded in the VC1080 operon. Specifically, we were interested in the relationship between the RR VC1086 and the HK VC1084. VC1084 has been shown to phosphorylate VC1086 in vitro, and we aimed to evaluate this relationship in vivo using spot morphologies (Plate and Marletta 2012). The HK VC1084 was overexpressed on pMMB67EH in the deletion background of VC1086. Colony corrugation of this strain was compared to that of the otherwise WT overexpressing VC1084, allowing us to evaluate the dependency of VC1084 mediated phenotypes on the presence of VC1086. Compared to overexpression of VC1084, which displays less corrugation compared to the parent strain, overexpression of VC1084 in the absence of VC1086 appeared similar to the rugose parent strain, suggesting that the activity of VC1084 is dependent on the presence of VC1086 (Figure 3.6). Activation of VC1086 by VC1084 would lead to a reduction in levels of intracellular c-di-GMP, and thus a reduction in the production of biofilm matrix components and reduced biofilm corrugation.

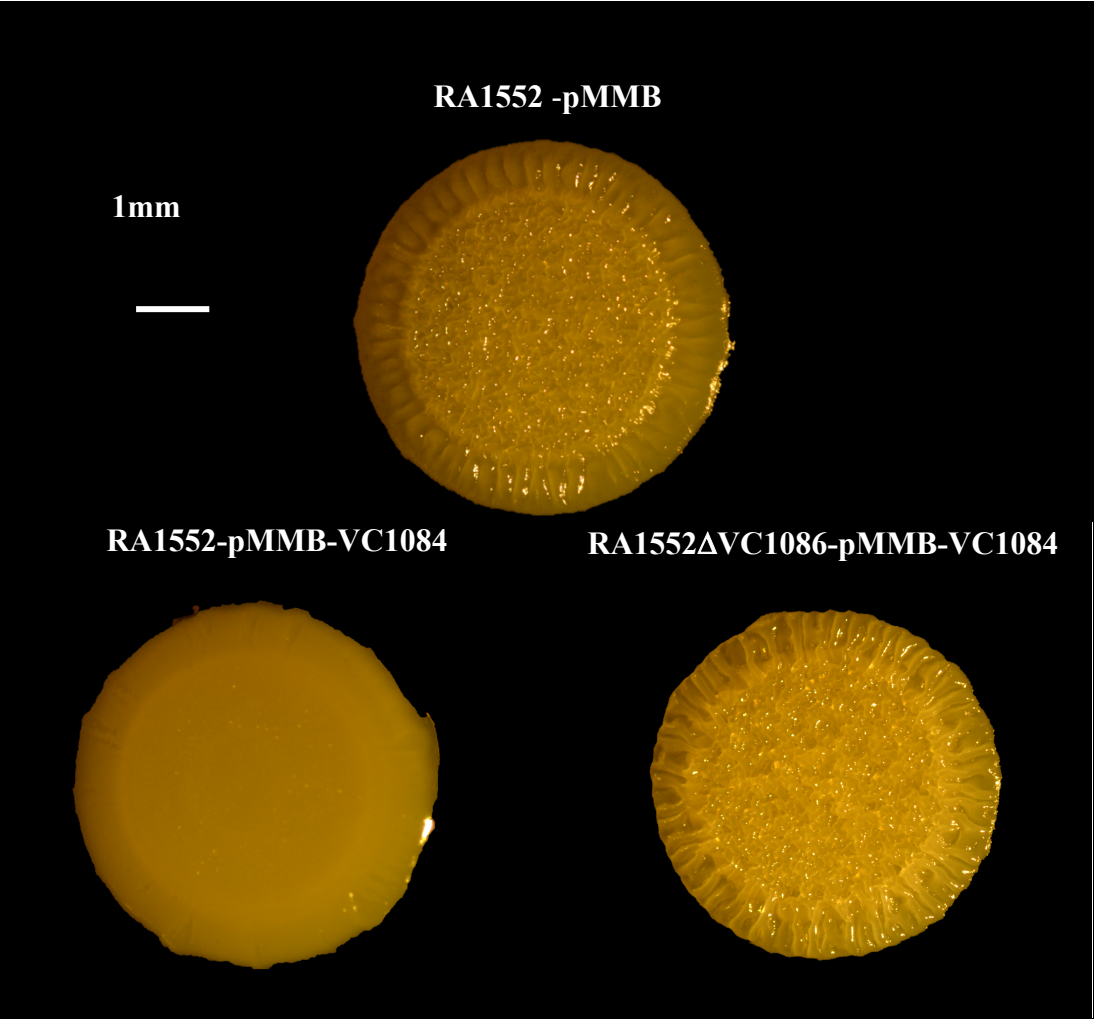


Figure 3.6: Genetic dependency of VC1086 and VC1084. Overnight cultures of each overexpression strain were spotted onto standard LB agar plates containing IPTG and ampicillin and incubated at 30 °C for 48 hours. Overexpression was achieved using the pMMB67EH plasmid. The experiment was repeated in three biological replicates, images presented are representative of one isolated trial.

Analysis of overexpression of VC1080 operon and dependency of biofilm formation on VC1080 operon members

We evaluated changes in biofilm corrugation when the entire VC1080 operon was overexpressed by creating a construct that replaced the native VC1080 promoter region with an IPTG-inducible promoter (pTAC). We observed spot biofilm morphologies of this strain and found that the loss in corrugation was comparable to that of the Δ VC1086 strain. To evaluate the dependency of the VC1080-87 overexpression phenotype on the presence of VC1084 and VC1086, we overexpressed the entire operon in the deletion background of these two genes. Overexpression of the entire operon in the absence of VC1086 yielded a phenotype that was almost identical to the rugose parent strain, demonstrating the importance of VC1086 for generating the overexpression phenotype of the VC1080 operon (Fig. 3.7). The biofilm spot morphology when the entire operon is overexpressed in the absence of VC1084 is very similar to the phenotype when the entire operon overexpressed on its own, however, the spots are smaller and slightly more compact, implying slightly more biofilm matrix production. This supports a role for VC1084 in mediating the VC1080 operon overexpression phenotype, but to a far less extent than VC1086.

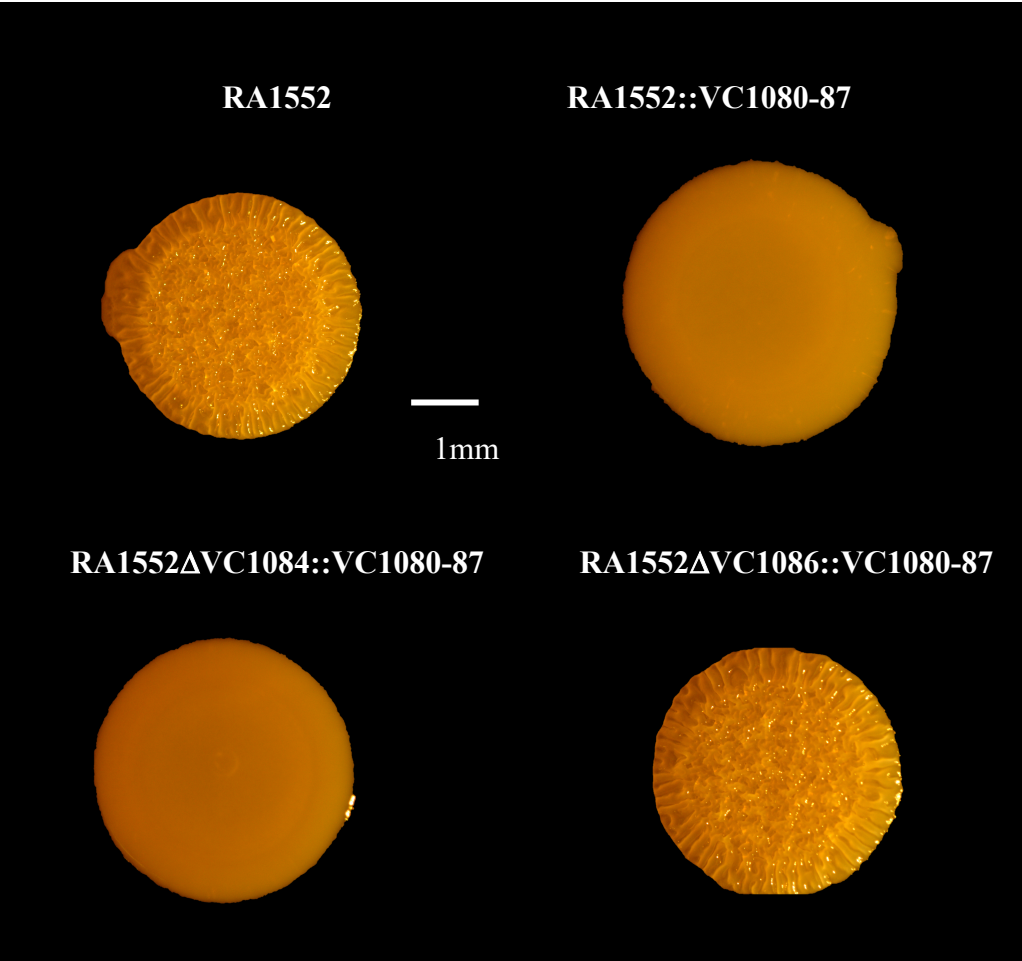


Figure 3.7: Overexpression phenotype of the VC1080 operon and dependency on VC1086 and VC1084. The VC1080 operon was overexpressed by replacing the native promoter with an IPTG inducible promoter. Overnight cultures of each strain (RA1552, RA1552::VC1080-87, R Δ VC1086:: VC1080-87 , R Δ VC1084:: VC1080-87) were diluted 1:200. 3 μ L were spotted onto standard LB agar plates containing 0.1 mM IPTG and 100 μ g/ μ l ampicillin and incubated at 30 °C for 48 hours. The experiment was repeated in two biological replicates, images presented are representative of isolated trials.

Overexpression VC1086, VC1084, and VC1081 affects *V. cholerae* pellicle biofilm morphology

Previous work has established that the *V. cholerae* A1552 rugose variant forms a stable hydrophobic pellicle, which is a biofilm formed at a liquid-air interface (J. C. N. Fong et al. 2006a). When cultures are grown statically, the parent rugose strain forms an evenly corrugated biofilm, a few millimeters tall (Figure 3.8). Having established that overexpression of specific genes in the VC1080 operon leads to changes in spot biofilm morphology, we sought to determine if changes could also be observed in pellicle biofilms. As expected, overexpression of VC1086 lead to a vast reduction pellicle corrugation, while VC1084 lead to a less noticeable, but nevertheless significant reduction in corrugation (Figure 3.8). Interestingly, pellicle biofilms of VC1081 also displayed a reduction in corrugation, albeit to a lesser extent when compared to VC1084 and VC1086. As a poorly studied response regulator with an unknown output domain, this VC1081 pellicle morphology represents a novel phenotype that has not been described to date. Considering that VC1081 does not have a characterized c-di-GMP hydrolyzing domain or a growth defect, it likely that the effect this gene has on biofilm formation is occurring through a yet to be determined regulatory interactions. Overall, these results support the finding that overexpression of genes in the VC1080 operon lead to changes in biofilm formation, and that these changes are not limited to biofilms formed on solid agar surfaces, but also those formed at the water-air interface.

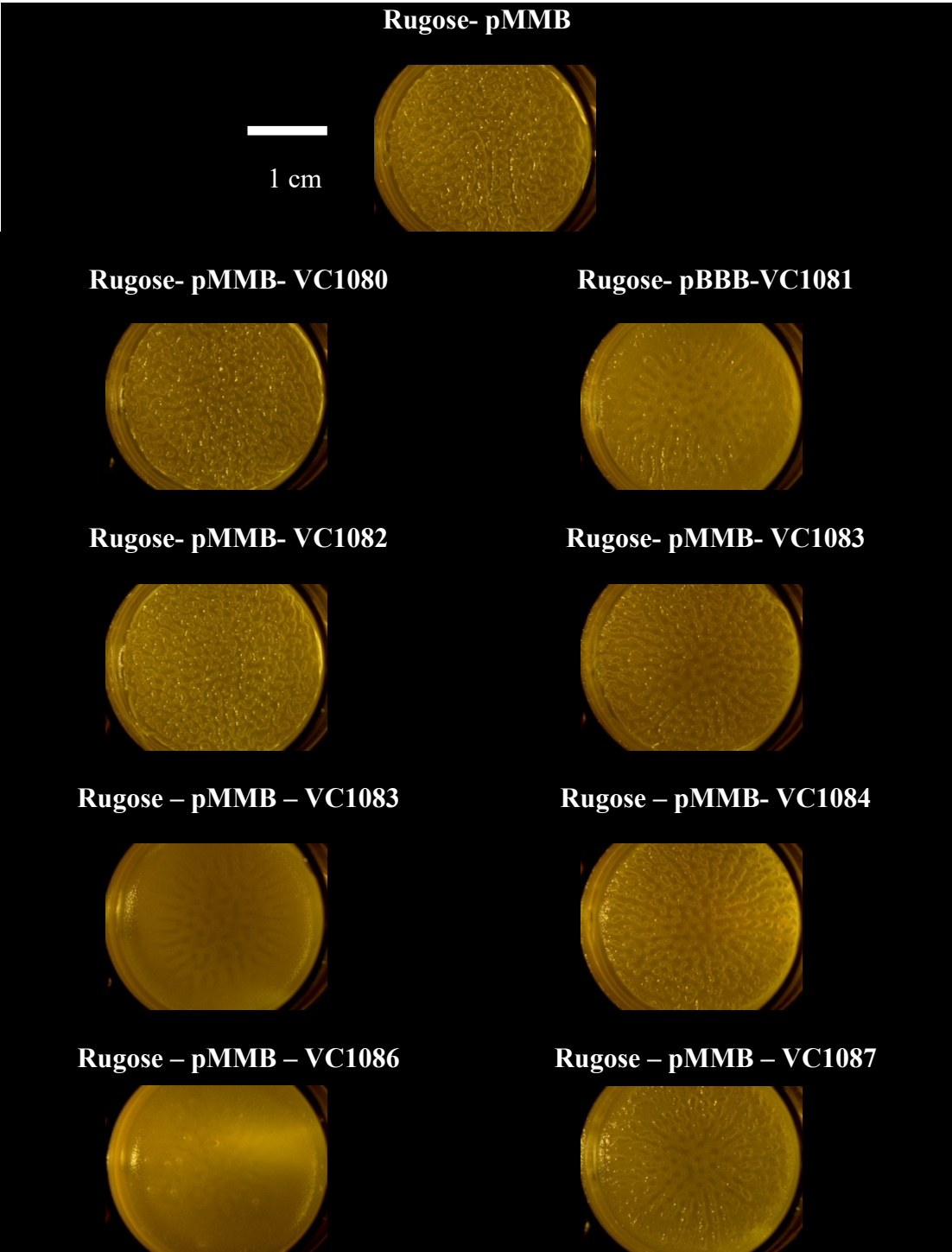


Figure 3.8: Pellicle biofilms of each VC1080 operon overexpression strain. Each gene in the VC1080 operon was overexpressed on pMMB67EH, under the control of an IPTG inducible promoter. Strains were grown overnight and diluted 1:200 into fresh LB amp 24-well plates containing 0.1mM IPTG + 100 µg/µl ampicillin. Pellicles were incubated at 30 °C and imaged after 48 hours. The experiment was repeated with two biological replicates, images presented are representative of isolated trials.

Analysis of c-di-GMP production in strains overproducing VC1080 operon members

Studies discussed above show that overexpression of VC1080 operon members, specifically VC1084 and VC1086 lead to a decrease in colony corrugation. As VC1086 harbors an EAL domain, we reasoned that this decrease in biofilm formation could be due to altered c-di-GMP production. To directly evaluate the effect of overexpression of genes in the VC1080 region on c-di-GMP levels, we quantified c-di-GMP directly in spot biofilms using mass spectrometry. Spot colony biofilms were grown under the same conditions as for the biofilm spot morphology assays, total nucleotide pool was extracted, and cellular c-di-GMP levels were determined by mass-spec analysis. As expected, overexpression of VC1086 showed the greatest reduction in c-di-GMP, reducing c-di-GMP levels by three-fold, while overexpression of VC1084 lead to a two-fold reduction in c-di-GMP levels compared to that of the rugose strain (Figure 3.9). This result lends support to our hypothesis that the colony biofilm phenotype changes observed when VC1086 and VC1084 are overexpressed, are likely due to a reduction in levels of c-di-GMP. Interestingly, VC1081 overexpression also led to a decrease in c-di-GMP compared to wildtype, though the change was not statistically significant. This result is in line with the prior observation that VC1081 overexpression leads to a reduction in pellicle biofilm corrugation. While VC1081 likely does not directly affect c-di-GMP levels through degradation as it does not have a c-di-GMP hydrolyzing domain, and it may instead affect or

modulate other genes that are able to influence c-di-GMP. In summary, the spot biofilm and pellicle biofilm phenotypes observed when VC1086, VC1084, and are over-expressed, are likely the result of a reduction in c-di-GMP.

c-di-GMP from Spot Biofilms

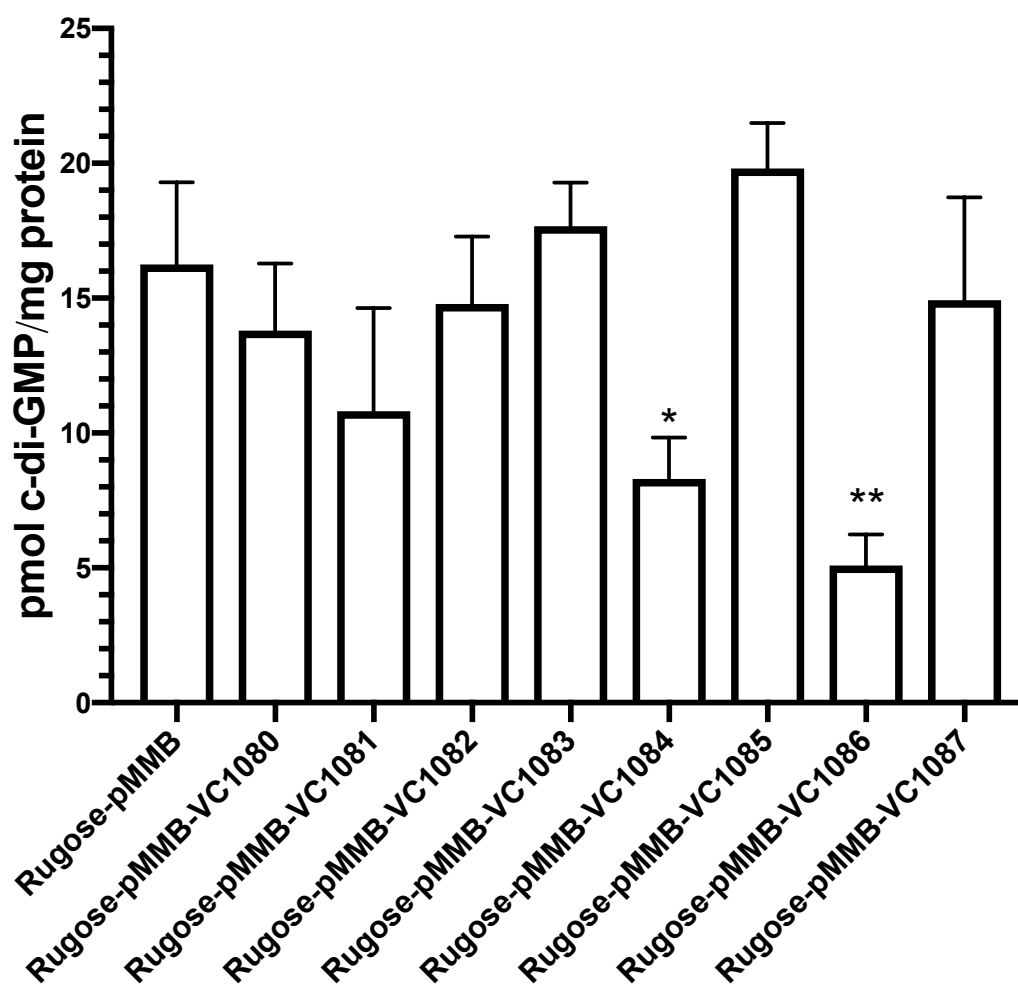


Figure 3.9: c-di-GMP quantification from biofilm spots. Colony biofilms of *V. cholerae* strains were grown for 48 hours at 30°C on LB agar plates containing 0.1mM IPTG and 100 µg/µl ampicillin. Intracellular c-di-GMP quantification via mass spectrometry was done for a given strain from 20 spot biofilms. The experiment was completed in two biological replicates. Each data point represents the average of three technical replicates. Statistical analysis performed by Graphpad Prism 7. One way ANOVA * $p \leq 0.05$, ** $p \leq 0.01$.

Analysis of motility phenotypes associated with VC1080 operon products

From the results presented thus far, overexpression of the VC1080 operon leads to biofilm changes that are modulated by changes in c-di-GMP. There is a characteristic inverse relationship between biofilm formation and motility in *V. cholerae*, where a decrease in production biofilm matrix components is generally seen together with an increase in motility (X. Liu et al. 2010). As a c-di-GMP regulated phenotype, we wondered if overexpression of the VC1080 operon genes in the rugose background may also affect *V. cholerae* motility. We found that overexpression of VC1086 lead to a zone of motility that is 1 cm larger than the rugose parent strain, while overexpression of VC1081 leads to a zone of motility that is 0.5 cm smaller than that of the parent strain (Figure 4.0). It appears that the decrease in c-di-GMP induced by overexpression of VC1086 not only decrease biofilm formation, but also increase motility, another c-di-GMP regulated process. The decrease in motility when VC1081 is more puzzling, though it may represent a novel example of how motility and biofilm production are not always perfectly inversely related in *V. cholerae*, and points to an interesting uncharacterized regulatory role for VC1081 that needs to be further explored.

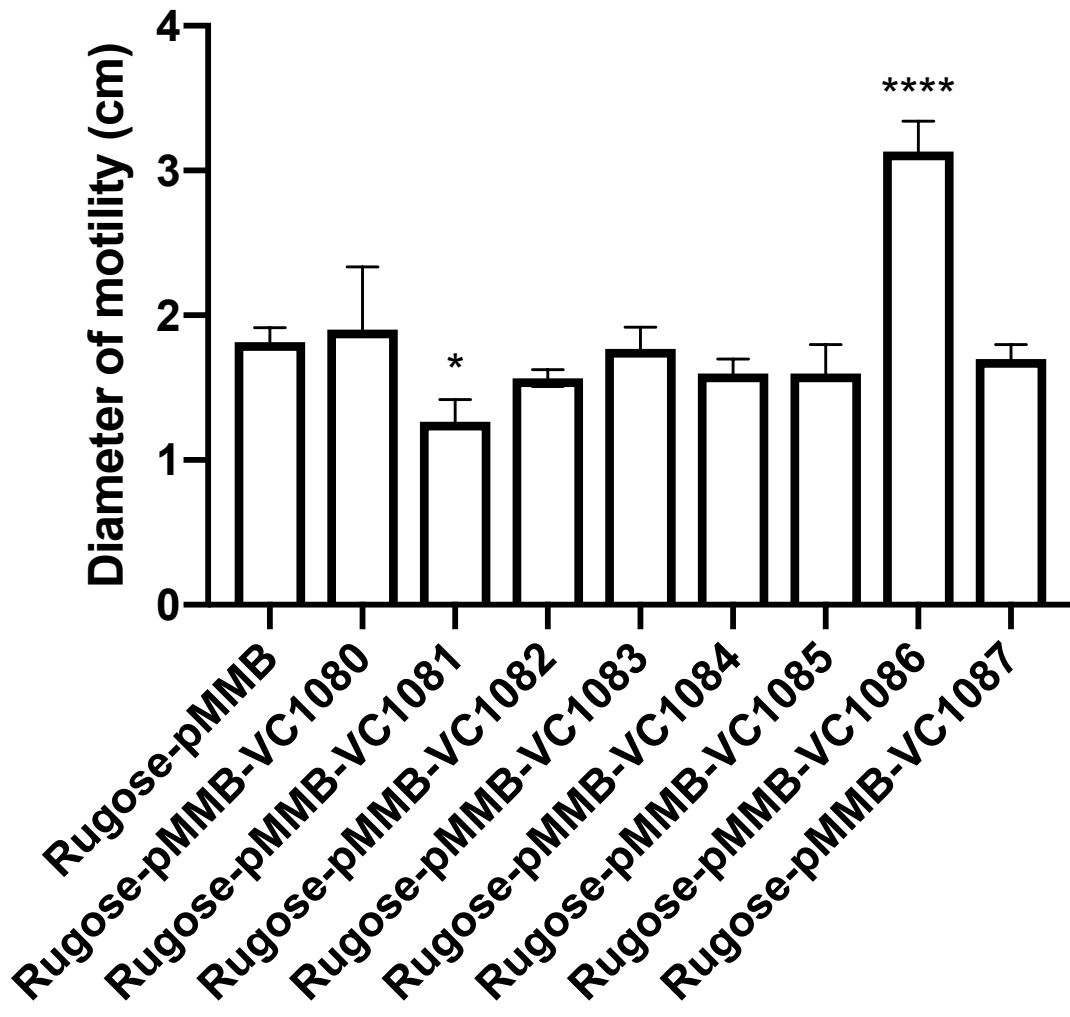


Figure 4.0: Analysis of motility phenotypes of VC1080 operon members: Single colonies of VC1080 strains were inoculated into LB motility plates containing IPTG and ampicillin and incubated at 30°C for 22 hours. The zone of motility for each mutant was measured and compared to that of the parent strain. Experiment was completed in three biological replicates. Each data points represents the average of two technical replicates. Statistical analysis performed with GraphPad Prism 7. *** $P \leq 0.0001$, * $p \leq 0.05$.

Nitric Oxide reduces expression of the VC1080 operon

We next sought to determine signals that affected expression of the VC1080 operon. To identify signals, we looked to operons containing similar genes in other bacterial species. Conservation of gene organization suggests that the proteins are functionally related members of the same signaling network. Of particular interest was *Shewanella oneidensis*, which also encodes several genes with homology to those found in the VC1080 region (Figure 4.1). In particular, HnoD, a VC1087 homolog in *Shewanella oneidensis*, has been shown to control the activity of a VC1086 homolog, HnoB (Plate and Marletta 2012). HnoD was found to significantly inhibit the PDE activity of HnoB in a manner that was dependent on the phosphorylation state of HnoD in *Shewanella oneidensis*. Phosphorylated HnoD was no longer inhibitory, and this loss of inhibition was independent of HnoB phosphorylation (Plate and Marletta 2013). Thus, HnoD and HnoB form a coherent feed-forward loop to control c-di-GMP levels (Mangan and Alon, 2003). Based on the experiments above, we hypothesize that nitric oxide may be a signal for the VC1080 operon. To evaluate this hypothesis we evaluated VC1080 operon expression by fusing the promoter region upstream of VC1080 to *luxCDABE* reporter genes. A region 245 base pairs upstream of VC1080, which is predicted to be the VC1080 operon promoter, was cloned into pBBR-*lux*, such that expression of the operon could be monitored by monitoring fluorescence. This experiment was performed in the wildtype *V. cholerae* A1552 strain, under anaerobic conditions to facilitate the activity of the nitric oxide donor. We found that addition of a nitric oxide donor, DETANONOate, at a concentration of

500 μ M, led to a three-fold reduction in expression of the VC1080 operon (Figure 4.2). This finding fits well with a previously described model in *Shewanella onedensis* whereby nitric oxide represses the activity of VC1086, increasing levels of c-di-GMP, thereby increasing biofilm formation (Plate and Marletta 2012). We speculate that a similar signaling cascade may be occurring in *V. cholerae*.

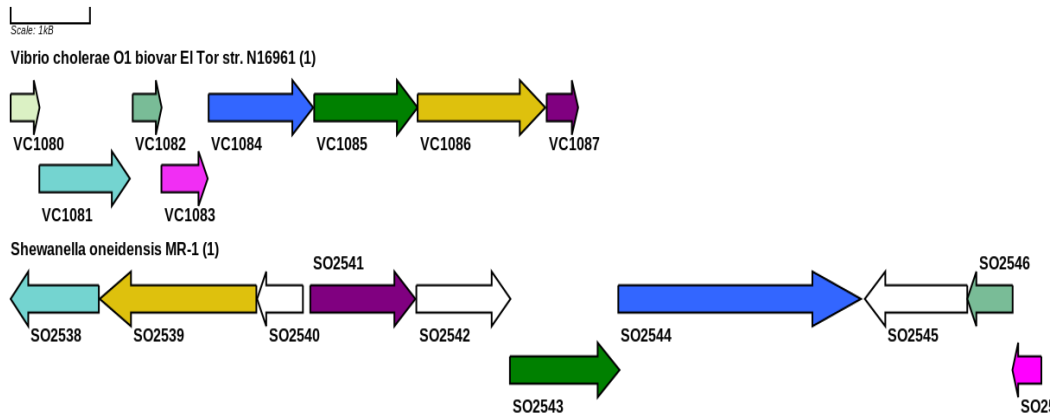


Figure 4.1: Homology of VC1080 operon with *Shewanella oneidensis* MR-1: Matching colors represent homologous genes. *Shewanella* encodes a homolog for each gene in the VC1080 operon except VC1080. Scales are consistent for both *V. cholerae* and *S. oneidensis*. Image generated with GeneViewer.

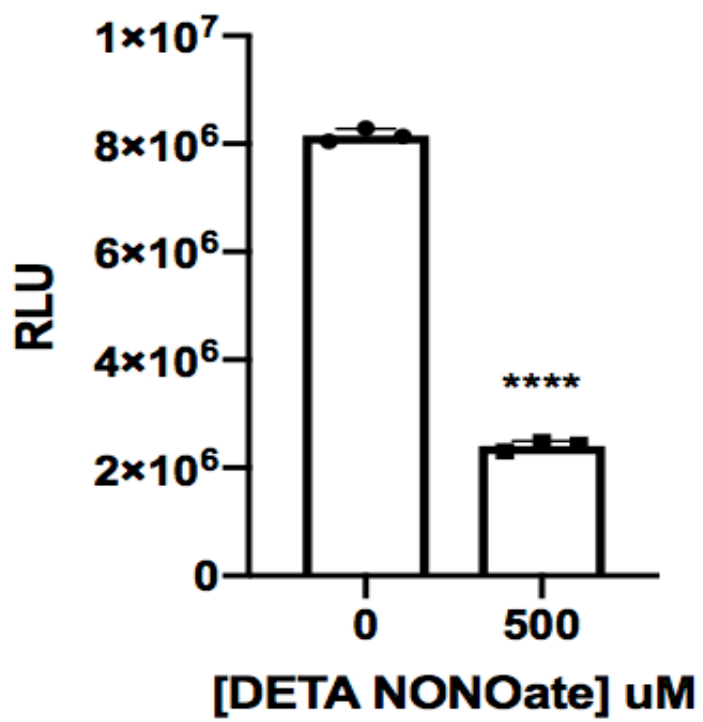


Figure 4.2: Nitric oxide reduces expression of the V1080 operon. Wildtype *V. cholerae* A1552 strains harboring the pBBR-pVC1080-87-lux operon reporter were grown aerobically, shaking, in LB + Cm (5 µg/mL) overnight. Cells were diluted 1:200 into LB containing 25mM TMAO in a white, flat-bottom 96-well plate in an anaerobic chamber. Half of the samples were treated with 500µM of DETANONOate, and the other half of samples were supplied with an equal volume of sterile water. Cells were grown statically under anaerobic conditions for 16 hours until they reached an OD₆₀₀ of approximately 0.5. Luminescence and optical density (600 nm) were measured using a Perkin Elmer Victor3 multilabel counter. Relative luminescence units (RLU) are expressed as luminescent counts · min⁻¹ · mL⁻¹ · OD₆₀₀⁻¹. Assays were performed in three independent biological replicates. Statistical analysis was performed using GraphPad Prism 7. **** p<= 0.0001.

VC1086 may be involved in a convergent TCS involving VCA0719, a NO-associated histidine kinase

Having established that VC1080 operon expression reduces c-di-GMP and modulates c-di-GMP-associated phenotypes, we next sought to examine potential signals affecting expression of the VC1080 operon. Studies from Plate and Marletta demonstrated that VCA0719 displayed rapid phosphotransfer to VC1086 (Plate and Marletta 2012). VCA0719 is an H-NOX responsive histidine kinase, which does not encode a traditional periplasmic sensing domain, and relies instead on the H-NOX protein VCA0720 to serve a sensory role (Plate and Marletta 2012). H-NOX is a heme-nitric oxide/oxygen binding domain that senses nitric oxide, and is found in both eukaryotes and bacteria (Plate and Marletta 2013). In bacteria, H-NOX proteins interact with bacterial signaling proteins in two-component signaling systems or in cyclic-di-GMP metabolism (Plate and Marletta 2013). Bacterial H-NOX proteins contain a heme cofactor, which is buried between N-terminal and C-terminal subdomains (Hossain, Heckler, and Boon 2018). In the inactive, ligand-free state, the heme is held in a distorted spring-loaded conformation through coordination with a histidine residue (Plate and Marletta 2013). NO binding and subsequent dissociation of the histidine releases the heme coordination, inducing a conformational change and activating the protein (Plate and Marletta 2013). This prompted us to investigate the relationship between VCA0719 and VC1086 *in vivo*. Overexpression of VCA0719 led to a loss of colony corrugation (Figure 4.3). We hypothesized if this loss of corrugation could be due to activation of VC1086 and found that the loss of

corrugation when VCA0719 is overexpressed is abolished when VCA0719 is overexpressed in the absence of VC1086 (Figure 4.3) suggesting that the phenotype may be the result of a reduction in c-di-GMP caused by activation of VC1086.

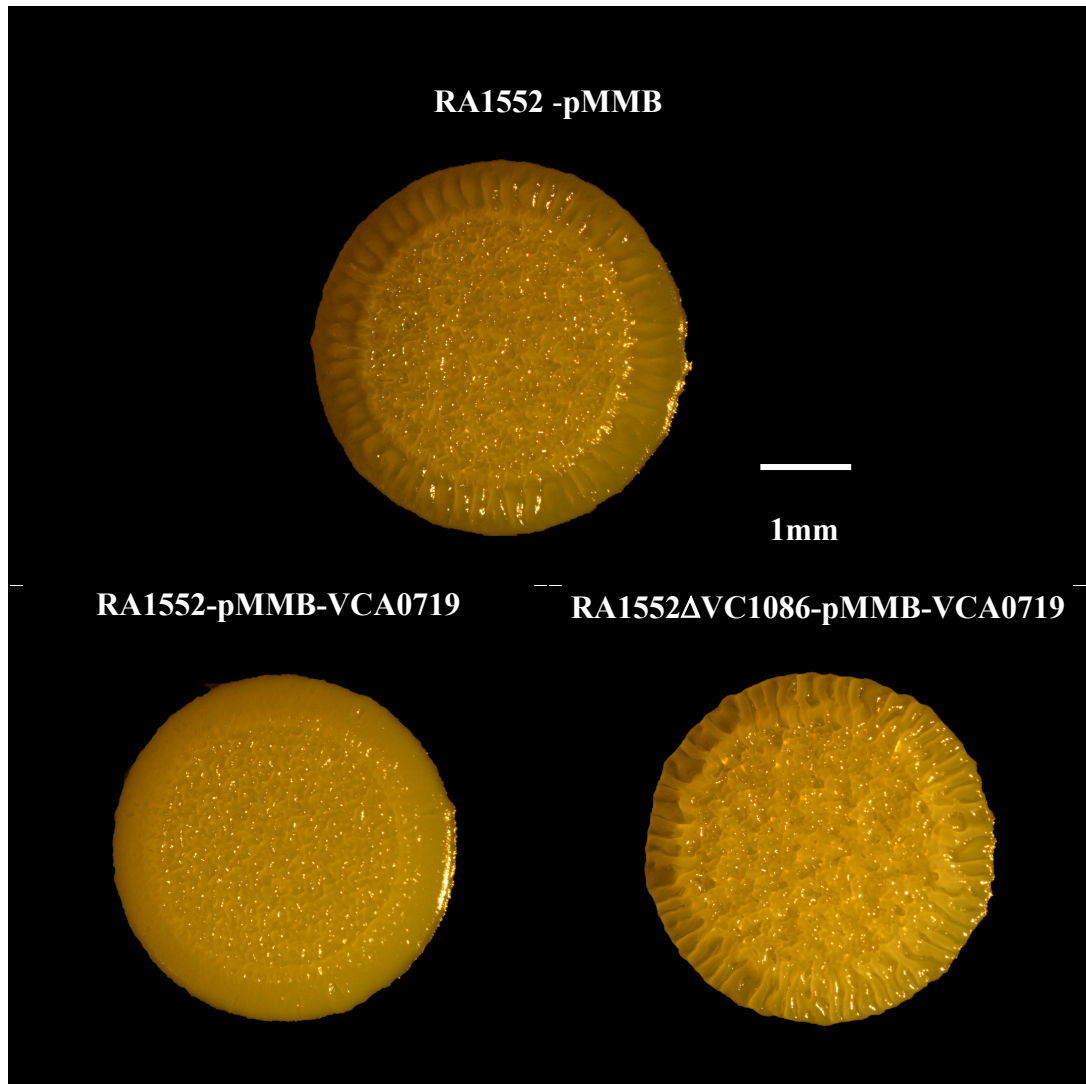


Figure 4.3: Genetic dependency of VCA0719 and VC1086. VCA0719 was overexpressed by replacing the native promoter with an IPTG inducible promoter. Overnight cultures of each strain (RA1552, RA1552/pMMB-VCA0719, RA1552 Δ VC1086/pMMMB-VCA0719) were diluted 1:200. 3 μ L were spotted onto standard LB agar plates containing 0.1 mM IPTG and 100 μ g/mL ampicillin and incubated at 30 °C for 48 hours. The experiment was repeated in three biological replicates, images presented are representative of isolated trials.

Conclusion

We conclude that the VC1080 operon influences *V. cholerae* biofilm formation. Specifically, overexpression of the entire operon, as well as individual overexpression of VC1086 and VC1084 lead to a reduction in spot biofilm corrugation. Overexpression of VC1086, VC1084, and VC1081 lead to a decrease in corrugation when grown as pellicle biofilms. We establish a dependency between VC1084 and VC1086, suggesting a cognate histidine-kinase-response-regulator interaction. We found that overexpression of both VC1084 and VC1086 lead to a decrease in levels of intracellular c-di-GMP, with VC1081 producing a reproducible, but not statistically significant decrease. We also described the effect of gene deletion and overexpression on c-di-GMP-regulated phenotypes. Overexpression of VC1086 lead to an increase in motility, while overexpression of VC1081 lead to a decrease in motility. We also investigated how deletion of genes affected levels of *vpsL* and found that deletion of VC1087 and VC1081 reduced *vpsL* gene expression in the wild-type background. Finally, we investigated the relationship between VCA0719, a nitric-oxide responsive histidine kinase, and VC1086, and showed that the reduction in corrugation observed when VCA0719 is overproduced, is dependent on the presence of VC1086. We interpreted this to suggest that VCA0719 may also phosphorylate VC1086. As a NO-responsive histidine kinase, we finally investigated the effect of nitric oxide on VC1080 operon expression and found that expression was decreased in the presence of NO. The data presented here suggest that nitric oxide may be a signal for the

VC1080 operon, and that the outcome of NO sensing is a repression in expression of genes in this region. Repression of the VC1080 operon would lead to a build-up of c-di-GMP levels, and ultimately an increase in biofilm formation. Based on genetic dependency experiments, VC1086, VCA0719, and VC1084 are likely involved in a convergent two component system in *V. cholerae* that responds to NO, as sensed by H-NOX (VCA0720). Sensing of NO by VCA0720 represses autophosphorylation of VCA0719, thus preventing phosphotransfer to VC1086 and decreasing its PDE activity (Figure 4.4). This model is homologous to that proposed in *Shewanella oneidensis* (Plate and Marletta 2012), suggesting that this NO signaling cascade is conserved across more than one bacterial species, and establishing the importance of NO as a signaling molecule that can affect biofilm formation.

V. cholerae also encodes a second NO-sensing module which indirectly controls *VC1080-87* gene expression through HapR. This NO-sensing module involves *vpsV* (VC1444), which is in the same putative operon as *vpsS* (VC1445). These genes are part of a complex signaling pathway which regulates biofilm formation and dispersal through quorum sensing processes (Hossain, Heckler, and Boon 2018). When NO is sensed by VpsV, VpsS is predicted to act as a phosphatase, drawing phosphate away from LuxO (Henares, Higgins, and Boon 2012). LuxO dephosphorylation allows translation of HapR (Henares, Higgins, and Boon 2012), which we predict will increase *VC1080-87* expression (Henares, Higgins, and Boon 2012). In this model, NO acts analogously to an autoinducer in *V. cholerae*, mimicking a high cell density

state and indirectly affecting expression of *VC1080-87* genes on the transcriptional level. (Henares, Higgins, and Boon 2012).

NO is likely encountered by *V. cholerae* during colonization of human hosts, or during interaction with amoeba. *V. cholerae* may directly encounter NO during colonization of the human gastrointestinal tract, as studies have found elevated levels of NO in the serum and stool of individuals with symptomatic cholera disease, demonstrating that acute cholera infection elicits NO production in humans (Janoff et al. 1997). NO may also be encountered by *V. cholerae* during passage through the stomach (Davies et al. 2011). Following ingestion, *V. cholerae* is exposed to the exceptionally antagonistic environment of the stomach, where the pH of gastric acid can reach as low as one (Smith 2003). Nitrite from food sources and the salivary nitrite cycle can enter the stomach creating acidified nitrite, which has potent antimicrobial effects on gut pathogens (Duncan et al. 1995). There is also evidence that *V. cholerae* encounters NO during protozoan grazing comes from a study that showed *V. cholerae* can survive and grow for several weeks inside the free-living amoeba *Acanthamoeba castellanii* (Abd, Weintraub, and Sandstrom 2005). This finding is significant because the bactericidal mechanisms used by amoeba and human immune cells, such as macrophages, are conserved, and include defensive burst from reactive oxygen and nitrogen species, including NO (Sun, Noorian, and McDougald 2018). Authors found that association with *A. castellanii* actually enhances the survival of *V. cholerae* (Abd, Weintraub, and Sandstrom 2005).

Overall, this study investigated a genomic region that we suspected was involved in regulation of *V. cholerae* biofilm formation in response to environmental signals. The genomic region is particularly enriched in two component system proteins with domains that are able to degrade c-di-GMP. This study investigated the influence of each gene encoded in the operon on two phenotypes that are regulated by c-di-GMP in *V. cholerae*. Biofilm formation and motility were both found to be influenced by overexpression of certain genes in the region, and the entire operon was repressed in the presence of nitric oxide, suggesting that the genes encoded in this region function to degrade c-di-GMP in response to environmental signals.

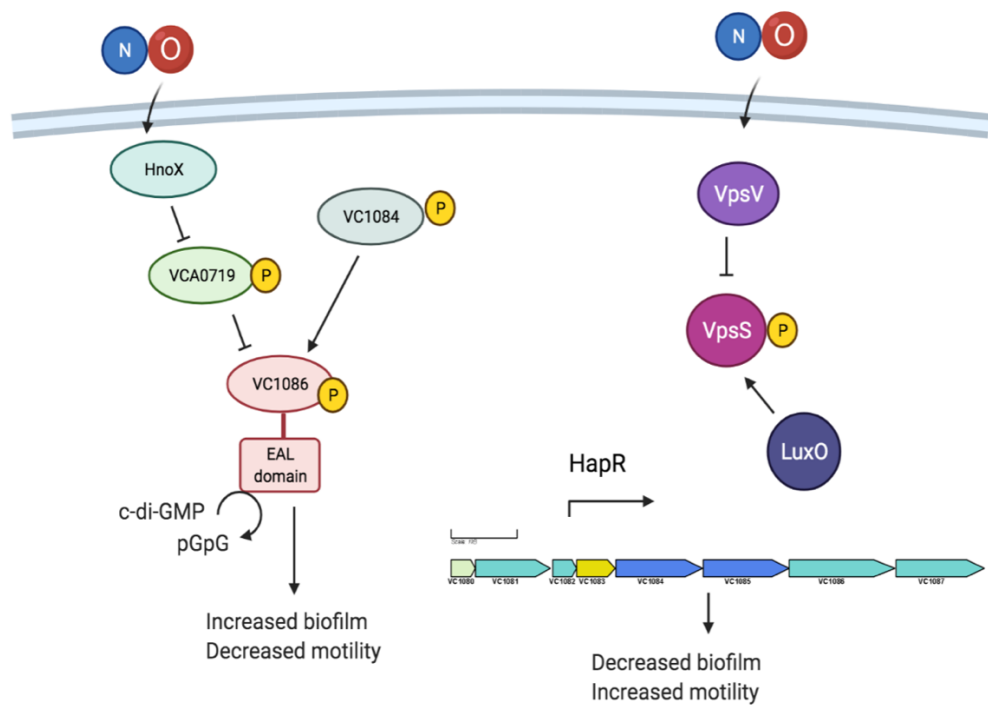


Figure 4.4: Model for NO signaling through VC1080 genes in *V. cholerae*.

VCA0719 and VC1084 are histidine kinases capable of completing phosphotransfer to VC1086. In the presence of NO, which is sensed by VCA0720 (H-NOX), autophosphorylation of VCA0719 is repressed, preventing phosphotransfer to VC1086 and reducing its PDE activity, ultimately decreasing the intracellular c-di-GMP pool and reducing biofilm formation. NO is also sensed by VpsV. When VpsV senses NO, VpsS is predicted to act as a phosphatase, drawing phosphate away from LuxO (Henares, Higgins, and Boon 2012). LuxO dephosphorylation allows translation of HapR (Henares, Higgins, and Boon 2012), which we predict will increase *VC1080-87* expression.

Materials and Methods

Bacterial strains, plasmids, and culture conditions

Bacterial strains and plasmids used in this study are listed in Table 2.1 and 2.2. *Escherichia coli* DH5 α pir was used for DNA and plasmid construction and manipulation. *E. coli* S17 λ pir was used for conjugation with *V. cholerae*. *E. coli* strains were grown aerobically at 37 °C, while *V. cholerae* strains were grown aerobically at 30 °C. Cultures were grown in Luria-Bertani (LB) broth (1% Tryptone, 0.5% Yeast Extract, 1% NaCl), pH 7.5. Colonies were grown on LB agar medium containing 1.5% (wt/vol) granulated agar. Antibiotics were used at the following concentrations: ampicillin 100 μ g/ml; rifampicin 100 μ g/ml; chloramphenicol 5 μ g/ml. For gene induction, IPTG was added at a concentration of 0.1 mM.

Recombinant DNA techniques and genetic manipulation

DNA manipulations were carried out by standard molecular techniques according to the manufacturers' instructions. Restriction and DNA modification enzymes were purchased from New England BioLabs (Ipswich, MA). PCRs were carried out using primers purchased from ELIM Biopharmaceuticals, Inc. (Hayward, CA) and the PfuUltra II Fusion HS DNA polymerase (Agilent Technologies, Santa Clara, CA). In-frame gene deletions were generated through allelic exchange of a native open reading frame (ORF) with the truncated ORF. For each gene deleted, a 5' (500bp) and

3' (500bp) region was amplified by PCR, including start and stop codons. Primers used for each deletion are listed in table 2.3. AB primers were used for the upstream region of the gene, while CD primers were used for the downstream region of the gene. These 503 -bp amplicons were cloned into pGP704-sacB28 via Gibson Assembly (NEB E2611L). Recombinant plasmids containing the upstream and downstream regions were transformed into *E. coli* DH5 DH5 α pir. Plasmids from successful transformants were purified and sequenced (UC Berkeley DNA Sequencing Facility, Berkeley CA). Successful constructs were transformed into *E. coli* S17 λ pir and used for conjugation with *V. cholerae*. Trans-conjugants were selected on LB agar medium containing ampicillin (100 μ g/ml) and rifampicin (100 μ g/ml). Sucrose based selection was used to select *V. cholerae* mutants that had undergone homologous recombination between the wild-type chromosomal copy of the gene and rejected the plasmid. Briefly, ampicillin and rifampicin-resistant colonies trans-conjugates were randomly selected from the sucrose plates, streaked on LB agar containing ampicillin (100 μ g/ml) and rifampicin (100 μ g/ml), and incubated at 30 °C. Single colonies were then inoculated into liquid LB and incubated for 8 hours at 37 °C, shaking (200 rpm). Approximately 10 μ l of these liquid cultures was streaked onto LB agar plates containing 6% (wt/vol) sucrose without NaCl. Sucrose plates were incubated at room temperature for 48 hours. Single colonies, where were not sensitive to sucrose, were patched onto LB and LB containing ampicillin (100 μ g/ml) plates to check for ampicillin sensitivity. These plates were incubated at 30 °C for 24 hours. Patches were screened by PCR to detect the presence of the deletion.

Deletion mutants were stored at -80 °C. Overexpression constructs were made by cloning the entire gene of interest into the plasmid backbone of pMMB67EH which contains the IPTG-inducible pTAC promoter. Plasmids in the yildiz lab collection generated by previously published methods were introduced into *V. cholerae* strains via conjugation (Zamorano-Sánchez et al. 2015).

Table 2.1 Bacterial Strains

<i>E. coli</i> strain	Genotype	Source
S17 λ pi	TprSmrrecAthipror-Km-KRP4 : : 2-Tc : :MuKm Tn7 λ pi	Herrero et al. (1990)
DH5 α	F'endA1 hsdR17 supE44 thi-1 recA1 gyrA96relA1 Δ (argF-lacZYA)U169(ϕ 80dlac Δ M15)	Promega
<i>V. cholerae</i> strain	Genotype	Source
FY_Vc_1	<i>Vibrio cholerae</i> O1 El Tor Strain A1552 Rif ^r (Smooth)	Yildiz & Schoolnik (1999)
FY_Vc_2	<i>Vibrio cholerae</i> O1 El Tor A1552, rugose wild-type variant, Rif ^r (Rugose)	Yildiz & Schoolnik (1999)
FY_Vc_2790	Rugose Δ VC1080, Rif ^r	Yildiz Lab Collection
FY_Vc_316	Rugose Δ VC1081, Rif ^r	Yildiz Lab Collection
	Rugose Δ VC1082, Rif ^r	This study, Megan Mouw, 2018
FY_Vc_4340	Rugose Δ VC1083, Rif ^r	Yildiz Lab Collection
	Rugose Δ VC1084, Rif ^r	Yildiz Lab Collection
FY_Vc_12192	Rugose Δ VC1085, Rif ^r	Yildiz Lab Collection
FY_Vc_864	Rugose Δ VC1086, Rif ^r	Yildiz Lab Collection
FY_Vc_14203	Rugose Δ VC1087, Rif ^r	This study, Megan Mouw, 2018
FY_Vc_2391	S Δ VC1080 4	Yildiz Lab Collection
FY_Vc_8329	SDVC1081 #111	Yildiz Lab Collection
FY_Vc_8180	SDVC1082 #111	Yildiz Lab Collection
FY_Vc_4337	S Δ VC1083 #111	Yildiz Lab Collection

FY_Vc_10861	SΔVC1084 A24	Yildiz Lab Collection
FY_Vc_10864	SΔVC1085 A21	Yildiz Lab Collection
FY_Vc_1936	SΔVC1086 3	Yildiz Lab Collection
FY_Vc_2760	SΔVC1087 2	Yildiz Lab Collection
FY_Vc_13542	Rugose / pMMB67EH -VC1080 Rif ^r , Amp ^r	Yildiz Lab Collection
FY_Vc_13543	Rugose / pMMB67EH -VC1081 Rif ^r , Amp ^r	Yildiz Lab Collection
FY_Vc_13544	Rugose / pMMB67EH -VC1082 Rif ^r , Amp ^r	Yildiz Lab Collection
FY_Vc_13545	Rugose / pMMB67EH -VC1083 Rif ^r , Amp ^r	Yildiz Lab Collection
FY_Vc_13546	Rugose / pMMB67EH -VC1084 Rif ^r , Amp ^r	Yildiz Lab Collection
FY_Vc_13547	Rugose / pMMB67EH -VC1085 Rif ^r , Amp ^r	Yildiz Lab Collection
FY_Vc_13548	Rugose / pMMB67EH -VC1086 Rif ^r , Amp ^r	Yildiz Lab Collection
FY_Vc_13549	Rugose / pMMB67EH -VC1087 Rif ^r , Amp ^r	Yildiz Lab Collection
FY_Vc_8902	Rugose/ pMMB67EH #1 Rif ^r , Amp ^r	Yildiz Lab Collection
FY_Vc_13582	Rugose ΔVC1086/ pMMB67EH -VC1084 Rif ^r , Amp ^r	Yildiz Lab Collection
FY_Vc_10368	Rugose :: pTac-VC1080-87	This study, Megan Mouw, 2020
FY_Vc_10369	Rugose ΔVC1084:: pTac-VC1080-87	This study, Megan Mouw, 2020
FY_Vc_16564	Rugose ΔVC1086:: pTac-VC1080-87	This study, Megan Mouw, 2020
FY_Vc_16556	Smooth ΔVC1080/ pBBR- <i>vpsL</i> -lux, Rif ^r , Cm ^r	This study, Megan Mouw, 2018

FY_Vc_16557	Smooth ΔVC1081/ pBBR- <i>vpsL</i> -lux, Rif ^r , Cm ^r	This study, Megan Mouw, 2018
FY_Vc_16558	Smooth ΔVC1082/ pBBR- <i>vpsL</i> -lux, Rif ^r , Cm ^r	This study, Megan Mouw, 2018
FY_Vc_16559	Smooth ΔVC1083/ pBBR- <i>vpsL</i> -lux, Rif ^r , Cm ^r	This study, Megan Mouw, 2018
FY_Vc_16560	Smooth ΔVC1084/ pBBR- <i>vpsL</i> -lux, Rif ^r , Cm ^r	This study, Megan Mouw, 2018
FY_Vc_16561	Smooth ΔVC1085/ pBBR- <i>vpsL</i> -lux, Rif ^r , Cm ^r	This study, Megan Mouw, 2018
FY_Vc_16562	Smooth ΔVC1086/ pBBR- <i>vpsL</i> -lux, Rif ^r , Cm ^r	This study, Megan Mouw, 2018
FY_Vc_16563	Smooth ΔVC1087/ pBBR- <i>vpsL</i> -lux, Rif ^r , Cm ^r	This study, Megan Mouw, 2018
Fy_Vc_10366	Smooth/pBBR-lux	
FY_Vc_10367	Smooth/pBBR-pVC1080-lux	This study, Megan Mouw 2018

Table 2.2. Plasmids

pGP704sacB28	pGP704 derivative,mob/oriT sacB, Ap ^r	G. Schoolnik
pGP704sacB28	pGP704SacB-ΔVC1080,Ap ^r	Yildiz Lab Collection
pGP704sacB28	pGP704SacB-ΔVC1081,Ap ^r	Yildiz Lab Collection
pGP704sacB28	pGP704SacB-ΔVC1082,Ap ^r	Yildiz Lab Collection
pGP704sacB28	pGP704SacB-ΔVC1083,Ap ^r	Yildiz Lab Collection
pGP704sacB28	pGP704SacB-ΔVC1084,Ap ^r	Yildiz Lab Collection
pGP704sacB28	pGP704SacB-ΔVC1085,Ap ^r	Yildiz Lab Collection
pGP704sacB28	pGP704SacB-ΔVC1086,Ap ^r	Yildiz Lab Collection
pGP704sacB28	pGP704SacB-ΔVC1087,Ap ^r	This study, Megan Mouw, 2018
pMMB67EH	pMMB67EH	Yildiz Lab Collection
pMMB67EH	pMMB67EH-VC1080, Amp ^r	Yildiz Lab Collection
pMMB67EH	pMMB67EH-VC1081, Amp ^r	Yildiz Lab Collection
pMMB67EH	pMMB67EH-VC1082, Amp ^r	Yildiz Lab Collection
pMMB67EH	pMMB67EH-VC1083, Amp ^r	Yildiz Lab Collection

pMMB67EH	pMMB67EH-VC1084, Amp ^r	Yildiz Lab Collection
pMMB67EH	pMMB67EH-VC1085, Amp ^r	Yildiz Lab Collection
pMMB67EH	pMMB67EH-VC1086, Amp ^r	Yildiz Lab Collection
pMMB67EH	pMMB67EH-VC1087, Amp ^r	Yildiz Lab Collection
pBBR-lux	pBBR- <i>lux</i> VpsL promoter, Cm ^r (-607, +158)	Zamorano, Sanchez, et all, 2015
pBBR-lux	pBBR- <i>lux</i> -VC1080-87 promoter, Cm ^r (+245)	Yildiz Lab Collection

Table 2.3 Primers

VC1080_del_A	gatcgagctcagatggacgatcaacgga
VC1080_del_D	gatcccatggatactgcaatttggcgaa
VC1081_del_A	ctgccatgggggtgtccggtgtttgaaggg
VC1081_del_D	ctggagctcgtcgggtgtaataataatcagcggc
VC1082_del_A	gatctctagaattctgctgctcgaagat
VC1082_del_D	gatcccatggtggagatatccaaaatgc
VC1083_del_A	gatctctagatcacgcaagtccgtgatt
VC1083_del_D	gatcccatggttcgaggtttgatacat
VC1084_del_A	catgccatggcatgttcccaacattc
VC1084_del_D	ctagtctagaactgcgttgatga
VC1085_del_A	gatcgagctccgaacgttgaaaatca
VC1085_del_D	catgccatggcagagataggggtggt
VC1086_del_A	atcgtctagatcgttcgagcctcaatg
VC1086_del_D	cgattctagactgattcgcaactccag
VC1087_del_A	gctctagaggaggagaagcaagcagaac
VC1087_del_D	ccgagctcgacagcacttgggtttctcc
VC1080_500up_fw d	ggccgctctagaactagtggGGTCGCCCATTCAGAGAG
VC1080_500up_rev	catttggccgcaactagaggCTGCTCCATCTCTTTTTCATTC
VC1080_245up_fwd	ggccgctctagaactagtggAACTTACTCGCATCATCC

VC1080_245up_rev	catttgccgcaactagaggCTGCTCCATCT CTTTTTC
VC1080- 87_AB_f wd	atccacgaagettcccatggGGTCGCCATT CAGAGAG
VC1080-87_AB_rev	tgtgtccttaCATCTCTTTTTTCATTCCAA TGTTAGG
VC1080- 87_CD_f wd	aaaagagatgTAAGGACACAGGATAA GGATTCGTCAG
VC1080-87_CD_rev	cctagagggtaccagagctcACCCGCGCTC CATGACAG
VC1080pTac_CD_fwd	ggtaccgggATGGAGCAGAGTGTCG CATTTAAC
VC1080pTac_CD_rev	cctagagggtaccagagctcATCCACCACC CAATGGTTAG
VC1080pTac_AB_rev	acaatagagtTACTAAGGTTTATCGTT CAAAGCATTC
pTac_fwd	aaccttagtaACTCTATTGTAAACAAG ACATTTTTATCTTTTATATTCAAT GGCTTATTTTCC
pTac_rev	tctgtccatCCCGGGTACCGAGCTCG A
VC1080pTac_AB_fwd	atccacgaagettcccatggCGAATGCCGAC CGATTCTAAAC

Spot Biofilm Morphology Analysis

For analysis of corrugated colony morphology development, cultures were grown overnight at 30°C shaking (200 rpm). 3 µl of diluted (1:200) culture were spotted onto LB agar medium (20 ml) that had been dried at room temperature for 48 hours. Samples were then incubated at 30°C for 48 hours before imaging. For overexpression strains, LB agar plates supplemented with ampicillin (100 µg/µL) and 0.1 mM IPTG was used. Experiments were completed in two biological replicates with three technical replicates each. Statistical analysis was performed using GraphPad Prism 7

Pellicle Morphology

For analysis of pellicle morphology development, cultures grown overnight at 30°C shaking (200 rpm), then diluted 1:200 into a sterile 24-well plate containing LB with ampicillin (100 µg/µL) and 0.1 mM IPTG. Plates were incubated at 30 °C. Images were taken after 48 hours of growth. Experiments were completed in two biological replicates with three technical replicates each. Statistical analysis was performed using GraphPad Prism 7.

Motility assay

Soft agar motility assays were carried out in 150x15mm petri plates filled with 100mL of LB containing 0.3% agar supplemented with ampicillin (100 µg/µL) and 0.1 mM IPTG. Motility plates were incubated at room temperature for 24 hours

before a single colony of each strain was inoculated into the agar with a sterile toothpick. Plates were incubated for 22 hours at 30°C. Experiments were performed in triplicate, with two technical replicates on each plate. Statistical analysis was performed using GraphPad Prism 7.

Analysis of c-di-GMP abundance

Colony biofilms of *V. cholerae* strains were grown for 24 h at 30°C on LB agar plates. Intracellular c-di-GMP quantification via mass spectroscopy was done for a given strain from 20 spot biofilms. All spots were scraped and pooled in 1 mL LB, containing sterile glass beads and vortexed thoroughly. After being spun down, decanted, and resuspended with 2.5 mL of 2% SDS, 250 µL was removed and used for BCA quantification. The remaining 750 µL of suspension was spun down, decanted, and resuspended in 1 mL of extraction buffer (40% acetonitrile, 40% methanol, 0.1% formic acid, 19.9% HPLC grade H₂O). Insoluble components were spun down, and 800 µL of the supernatant was collected and dried under vacuum. The dried sample was then resuspended in 50 µL HPLC grade H₂O containing 184 mM NaCl, and c-di-GMP was quantified via LC-MS/MS at the UCSC Chemistry and Biochemistry Mass Spectrometry facility. c-di-GMP standard curves were generated using c-di-GMP standards (SIGMA) of 25, 50, 100, 500, 2000, 3500, and 5000 nM dissolved in HPLC grade H₂O containing 184 mM NaCl. The abundance of c-di-GMP was extrapolated from the mass spectroscopy data and normalized to protein abundance per 1 mL of the spot suspension. Experiments were performed with three

technical replicates and two biological replicates. Statistical analysis was performed using GraphPad Prism 7.

Luminescence assay

V. cholerae strains harboring the *PvpsL-lux* construct were grown in LB containing chloramphenicol (5 µg/mL). Overnight grown cultures were diluted 1:200 into a white, flat-bottom 96-well plate for a total volume of 200 µL. Luminescence and optical density (600 nm) was measured using a Perkin Elmer Victor3 multilabel counter. Relative luminescence units (RLU) are expressed as luminescent counts · min⁻¹ · mL⁻¹ · OD₆₀₀⁻¹. Assays were performed in three independent biological replicates. Statistical analysis was performed using GraphPad Prism 7.

VC1080 operon expression in the presence of NO

A pBBR-pVC1080-87 lux reporter strain was created by fusing 245 bp and 500bp upstream of the VC1080 gene to lux reporter genes. These two constructs were tested for expression levels at exponential phase (supplemental Figure 1). Expression between the two constructs was not significantly different, and subsequent assays were performed with the construct containing 245 bp upstream of VC1080. Wildtype *V. cholerae* A1552 strains harboring the pBBR-pVC1080-87-lux operon reporter were grown aerobically, shaking (200rpm), in LB + Cm (5 µg/mL) overnight. Cells were diluted 1:200 into LB+25mM Trimethylamine N-oxide (TMAO) in a white, flat-bottom 96-well plate in an anaerobic chamber. Half of the samples were treated

with 500 μ M of DETANONOate (Cayman Chemicals item number 82120), and the other half of samples were supplied with an equal volume of sterile water. DETANONOate is a nitric oxide donor that spontaneously dissociates in a pH-dependent manner. The dissociation is a first-order process with a half-life of 20 hours and 56 hours at 37°C and 22-25°C, pH 7.4, respectively. A stock of the compound was prepared by dissolving in 10 mM NaOH and stored at -80 °C and protected from light. When the compound was included in assays it was diluted 100-fold into LB at pH of 7.4. Cells were grown statically under anaerobic conditions for 16 hours until they reached an OD₆₀₀ of approximately 0.5. Luminescence and optical density (600 nm) were measured using a Perkin Elmer Victor3 multilabel counter. Relative luminescence units (RLU) are expressed as luminescent counts \cdot min⁻¹ \cdot mL⁻¹ \cdot OD₆₀₀⁻¹. Assays were performed in three independent biological replicates.

References

- Abd, Hadi, Andrej Weintraub, and Gunnar Sandstrom. 2005. "Intracellular Survival and Replication of *Vibrio Cholerae* O139 in Aquatic Free-Living Amoebae." *Environmental Microbiology* 7 (7): 1003–8. <https://doi.org/10.1111/j.1462-2920.2005.00771.x>.
- Absalon, Cedric, Katrina Van Dellen, and Paula I. Watnick. 2011. "A Communal Bacterial Adhesin Anchors Biofilm and Bystander Cells to Surfaces." Edited by Ralph R. Isberg. *PLoS Pathogens* 7 (8): e1002210. <https://doi.org/10.1371/journal.ppat.1002210>.
- Amikam, Dorit, and Michael Y. Galperin. 2006. "PilZ Domain Is Part of the Bacterial C-Di-GMP Binding Protein." *Bioinformatics* 22 (1): 3–6. <https://doi.org/10.1093/bioinformatics/bti739>.
- Arora, Shiwani K., Bruce W. Ritchings, Ernesto C. Almira, Stephen Lory, and Reuben Ramphal. 1997. "A Transcriptional Activator, FleQ, Regulates Mucin Adhesion and Flagellar Gene Expression in *Pseudomonas Aeruginosa* in a Cascade Manner." *Journal of Bacteriology* 179 (17): 5574–81. <https://doi.org/10.1128/jb.179.17.5574-5581.1997>.
- Berk, Veysel, Jiunn C N Fong, Graham T Dempsey, Omer N Develioglu, Xiaowei Zhuang, Jan Liphardt, Fitnat H Yildiz, and Steven Chu. 2012. "Molecular Architecture and Assembly Principles of *Vibrio Cholerae* Biofilms." <https://doi.org/10.1126/science.1222981>.
- Beyhan, Sinem, Kivanc Bilecen, Sofie R. Salama, Catharina Casper-Lindley, and

- Fitnat H. Yildiz. 2007a. "Regulation of Rugosity and Biofilm Formation in *Vibrio Cholerae*: Comparison of VpsT and VpsR Regulons and Epistasis Analysis of VpsT, VpsR, and HapR." *Journal of Bacteriology* 189 (2): 388–402. <https://doi.org/10.1128/JB.00981-06>.
- . 2007b. "Regulation of Rugosity and Biofilm Formation in *Vibrio Cholerae*: Comparison of VpsT and VpsR Regulons and Epistasis Analysis of VpsT, VpsR, and HapR." *Journal of Bacteriology* 189 (2): 388–402. <https://doi.org/10.1128/JB.00981-06>.
- Beyhan, Sinem, Lindsay S. Odell, and Fitnat H. Yildiz. 2008. "Identification and Characterization of Cyclic Diguanylate Signaling Systems Controlling Rugosity in *Vibrio Cholerae*." *Journal of Bacteriology* 190 (22): 7392–7405. <https://doi.org/10.1128/JB.00564-08>.
- Beyhan, Sinem, and Fitnat H. Yildiz. 2007. "Smooth to Rugose Phase Variation in *Vibrio Cholerae* Can Be Mediated by a Single Nucleotide Change That Targets C-Di-GMP Signalling Pathway." *Molecular Microbiology* 63 (4): 995–1007. <https://doi.org/10.1111/j.1365-2958.2006.05568.x>.
- Bilecen, Kivanc, Jiunn C. Jiunn, Andrew Cheng, Christopher J. Jones, David Zamorano-Sánchez, and Fitnat H. Yildiz. 2015. "Polymyxin B Resistance and Biofilm Formation in *Vibrio Cholerae* Are Controlled by the Response Regulator CarR." *Infection and Immunity* 83 (3): 1199–1209. <https://doi.org/10.1128/IAI.02700-14>.
- Breugelmans, Philip, Kim Bundvig Barken, Tim Tolker-Nielsen, Johan Hofkens,

- Winnie Dejonghe, and Dirk Springael. 2008. "Architecture and Spatial Organization in a Triple-Species Bacterial Biofilm Synergistically Degrading the Phenylurea Herbicide Linuron." *FEMS Microbiology Ecology* 64 (2): 271–82. <https://doi.org/10.1111/j.1574-6941.2008.00470.x>.
- Bridges, Andrew A., Chenyi Fei, and Bonnie L. Bassler. 2020. "Identification of Signaling Pathways, Matrix-Digestion Enzymes, and Motility Components Controlling *Vibrio Cholerae* Biofilm Dispersal." *Proceedings of the National Academy of Sciences*, December, 202021166. <https://doi.org/10.1073/pnas.2021166117>.
- Camilli, Andrew, and John J. Mekalanos. 1995. "Use of Recombinase Gene Fusions to Identify *Vibrio Cholerae* Genes Induced during Infection." *Molecular Microbiology* 18 (4): 671–83. https://doi.org/10.1111/j.1365-2958.1995.mmi_18040671.x.
- Capra, Emily J., and Michael T. Laub. 2012. "Evolution of Two-Component Signal Transduction Systems." *Annual Review of Microbiology* 66 (1): 325–47. <https://doi.org/10.1146/annurev-micro-092611-150039>.
- Casper-Lindley, Catharina, and Fitnat H. Yildiz. 2004. "VpsT Is A Transcriptional Regulator Required for Expression of Vps Biosynthesis Genes and the Development of Rugose Colonial Morphology in *Vibrio Cholerae* O1 El Tor." *Journal of Bacteriology* 186 (5): 1574–78. <https://doi.org/10.1128/JB.186.5.1574-1578.2004>.
- Chan, C., R. Paul, D. Samoray, N. C. Amiot, B. Giese, U. Jenal, and T. Schirmer.

2004. “Structural Basis of Activity and Allosteric Control of Diguanilate Cyclase.” *Proceedings of the National Academy of Sciences* 101 (49): 17084–89. <https://doi.org/10.1073/pnas.0406134101>.
- Chang, Ya Wen, Alexandros A. Fragkopoulos, Samantha M. Marquez, Harold D. Kim, Thomas E. Angelini, and Alberto Fernández-Nieves. 2015. “Biofilm Formation in Geometries with Different Surface Curvature and Oxygen Availability.” *New Journal of Physics* 17 (3): 033017. <https://doi.org/10.1088/1367-2630/17/3/033017>.
- Charles, Richelle C., and Edward T. Ryan. 2011. “Cholera in the 21st Century.” *Current Opinion in Infectious Diseases*. *Curr Opin Infect Dis*. <https://doi.org/10.1097/QCO.0b013e32834a88af>.
- Chen, H. Deborah, and Eduardo A. Groisman. 2013. “The Biology of the PmrA/PmrB Two-Component System: The Major Regulator of Lipopolysaccharide Modifications.” *Annual Review of Microbiology* 67 (September): 83–112. <https://doi.org/10.1146/annurev-micro-092412-155751>.
- Cheng, Andrew T., David Zamorano-Sánchez, Jennifer K. Teschler, Daniel Wu, and Fitnat H. Yildiz. 2018. “NtrC Adds a New Node to the Complex Regulatory Network of Biofilm Formation and Vps Expression in *Vibrio Cholerae*.” *Journal of Bacteriology* 200 (15). <https://doi.org/10.1128/JB.00025-18>.
- Colvin, Kelly M., Vernita D. Gordon, Keiji Murakami, Bradley R. Borlee, Daniel J. Wozniak, Gerard C.L. Wong, and Matthew R. Parsek. 2011. “The Pel Polysaccharide Can Serve a Structural and Protective Role in the Biofilm Matrix

- of *Pseudomonas Aeruginosa*.” *PLoS Pathogens* 7 (1): 1001264.
<https://doi.org/10.1371/journal.ppat.1001264>.
- Daddi Oubekka, S, R Briandet, M.-P Fontaine-Aupart, and K Steenkeste. 2012.
“Correlative Time-Resolved Fluorescence Microscopy To Assess Antibiotic
Diffusion-Reaction in Biofilms.” <https://doi.org/10.1128/AAC.00216-12>.
- Dahlstrom, Kurt M., and George A. O’Toole. 2017. “A Symphony of Cyclases:
Specificity in Diguanylate Cyclase Signaling.” *Annual Review of Microbiology*
71 (September): 179–95. <https://doi.org/10.1146/annurev-micro-090816-093325>.
- Davies, Bryan W., Ryan W. Bogard, Nicole M. Dupes, Tyler A. I. Gerstenfeld, Lyle
A. Simmons, and John J. Mekalanos. 2011. “DNA Damage and Reactive
Nitrogen Species Are Barriers to *Vibrio Cholerae* Colonization of the Infant
Mouse Intestine.” Edited by Craig R. Roy. *PLoS Pathogens* 7 (2): e1001295.
<https://doi.org/10.1371/journal.ppat.1001295>.
- Díaz-Pascual, Francisco, Raimo Hartmann, Martin Lempp, Lucia Vidakovic, Boya
Song, Hannah Jeckel, Kai M. Thormann, et al. 2019. “Breakdown of *Vibrio*
Cholerae Biofilm Architecture Induced by Antibiotics Disrupts Community
Barrier Function.” *Nature Microbiology*. Nature Research.
<https://doi.org/10.1038/s41564-019-0579-2>.
- Duerig, Anna, Sören Abel, Marc Folcher, Micael Nicollier, Torsten Schwede, Nicolas
Amiot, Bernd Giese, and Urs Jenal. 2009. “Second Messenger-Mediated
Spatiotemporal Control of Protein Degradation Regulates Bacterial Cell Cycle
Progression.” *Genes and Development* 23 (1): 93–104.

<https://doi.org/10.1101/gad.502409>.

- Duncan, C, H Dougall, P Johnston, S Green, R Brogan, C Leifert, L Smith, M Golden, and N Benjamin. 1995. “Chemical Generation of Nitric Oxide in the Mouth from the Enterosalivary Circulation of Dietary Nitrate.” *Nature Medicine* 1 (6): 546–51. <http://www.ncbi.nlm.nih.gov/pubmed/7585121>.
- Faruque, Shah M., Kuntal Biswas, S. M. Nashir Udden, Qazi Shafi Ahmad, David A. Sack, and G. Balakrish Nair. 2006. “Transmissibility of Cholera: In Vivo-Formed Biofilms and Their Relationship to Infectivity and Persistence in the Environment.” *Proceedings of the National Academy of Sciences of the United States of America* 103 (16): 6350–55. <https://doi.org/10.1073/pnas.0601277103>.
- Flemming, Hans-Curt. 2008. “Why Microorganisms Live in Biofilms and the Problem of Biofouling.” In *Marine and Industrial Biofouling*, 3–12. Springer Berlin Heidelberg. https://doi.org/10.1007/978-3-540-69796-1_1.
- Flemming, Hans Curt, and Jost Wingender. 2010. “The Biofilm Matrix.” *Nature Reviews Microbiology*. *Nat Rev Microbiol*. <https://doi.org/10.1038/nrmicro2415>.
- Flemming, Hans Curt, Jost Wingender, Ulrich Szewzyk, Peter Steinberg, Scott A. Rice, and Staffan Kjelleberg. 2016. “Biofilms: An Emergent Form of Bacterial Life.” *Nature Reviews Microbiology*. Nature Publishing Group. <https://doi.org/10.1038/nrmicro.2016.94>.
- Flemming, Hans Curt, and Stefan Wuertz. 2019. “Bacteria and Archaea on Earth and Their Abundance in Biofilms.” *Nature Reviews Microbiology* 17 (4): 247–60. <https://doi.org/10.1038/s41579-019-0158-9>.

Floyd, Kyle A, Calvin K Lee, Wujing Xian, Mahmoud Nametalla, Aneesa Valentine, Benjamin Crair, Shiwei Zhu, et al. 2020. “C-Di-GMP Modulates Type IV MSHA Pilus Retraction and Surface Attachment in *Vibrio Cholerae*.”
<https://doi.org/10.1038/s41467-020-15331-8>.

Fong, Jiunn C.N., Kevin Karplus, Gary K. Schoolnik, and Fitnat H. Yildiz. 2006a. “Identification and Characterization of RbmA, a Novel Protein Required for the Development of Rugose Colony Morphology and Biofilm Structure in *Vibrio Cholerae*.” *Journal of Bacteriology* 188 (3): 1049–59.
<https://doi.org/10.1128/JB.188.3.1049-1059.2006>.

———. 2006b. “Identification and Characterization of RbmA, a Novel Protein Required for the Development of Rugose Colony Morphology and Biofilm Structure in *Vibrio Cholerae*.” *Journal of Bacteriology* 188 (3): 1049–59.
<https://doi.org/10.1128/JB.188.3.1049-1059.2006>.

Fong, Jiunn C.N., Khalid A. Syed, Karl E. Klose, and Fitnat H. Yildiz. 2010. “Role of *Vibrio* Polysaccharide (Vps) Genes in VPS Production, Biofilm Formation and *Vibrio Cholerae* Pathogenesis.” *Microbiology* 156 (9): 2757–69.
<https://doi.org/10.1099/mic.0.040196-0>.

Fong, Jiunn C.N., and Fitnat H. Yildiz. 2007. “The RbmBCDEF Gene Cluster Modulates Development of Rugose Colony Morphology and Biofilm Formation in *Vibrio Cholerae*.” *Journal of Bacteriology* 189 (6): 2319–30.
<https://doi.org/10.1128/JB.01569-06>.

Fong, Jiunn Cn, Andrew Rogers, Alicia K. Michael, Nicole C. Parsley, William Cole

- Cornell, Yu Cheng Lin, Praveen K. Singh, et al. 2017. “Structural Dynamics of RbmA Governs Plasticity of *Vibrio Cholerae* Biofilms.” *ELife* 6 (August).
<https://doi.org/10.7554/eLife.26163>.
- Gallego-Hernandez, A L, W H Depas, J H Park, J K Teschler, R Hartmann, H Jeckel, K Drescher, et al. 2020. “Upregulation of Virulence Genes Promotes *Vibrio Cholerae* Biofilm Hyperinfectivity” 117 (20): 11010–17.
<https://doi.org/10.1073/pnas.1916571117/-/DCSupplemental>.
- Galperin, M Y, D A Natale, L Aravind, and E V Koonin. 1999. “A Specialized Version of the HD Hydrolase Domain Implicated in Signal Transduction.” *Journal of Molecular Microbiology and Biotechnology* 1 (2): 303–5.
<http://www.ncbi.nlm.nih.gov/pubmed/10943560>.
- Giglio, Krista M., Jiunn C. Fong, Fitnat H. Yildiz, and Holger Sondermann. 2013. “Structural Basis for Biofilm Formation via the *Vibrio Cholerae* Matrix Protein RbmA.” *Journal of Bacteriology* 195 (14): 3277–86.
<https://doi.org/10.1128/JB.00374-13>.
- Groisman, Eduardo A. 2016. “Feedback Control of Two-Component Regulatory Systems.” *Annu. Rev. Microbiol* 70: 103–24. <https://doi.org/10.1146/annurev-micro-102215-095331>.
- Hammer, Brian K., and Bonnie L. Bassler. 2003a. “Quorum Sensing Controls Biofilm Formation in *Vibrio Cholerae*.” *Molecular Microbiology* 50 (1): 101–4.
<https://doi.org/10.1046/j.1365-2958.2003.03688.x>.
- . 2003b. “Quorum Sensing Controls Biofilm Formation in *Vibrio Cholerae*.”

- Molecular Microbiology* 50 (1): 101–4. <https://doi.org/10.1046/j.1365-2958.2003.03688.x>.
- Harris, Jason B., Regina C. LaRocque, Firdausi Qadri, Edward T. Ryan, and Stephen B. Calderwood. 2012. “Cholera.” In *The Lancet*, 379:2466–76. Lancet Publishing Group. [https://doi.org/10.1016/S0140-6736\(12\)60436-X](https://doi.org/10.1016/S0140-6736(12)60436-X).
- Hay, Amanda J., and Jun Zhu. 2015. “Host Intestinal Signal-Promoted Biofilm Dispersal Induces *Vibrio Cholerae* Colonization.” *Infection and Immunity* 83 (1): 317–23. <https://doi.org/10.1128/IAI.02617-14>.
- Henares, Bernadette M., Kate E. Higgins, and Elizabeth M. Boon. 2012. “Discovery of a Nitric Oxide Responsive Quorum Sensing Circuit in *Vibrio Harveyi*.” *ACS Chemical Biology* 7 (8): 1331–36. <https://doi.org/10.1021/cb300215t>.
- Hengge, Regine. 2009. “Principles of C-Di-GMP Signalling in Bacteria.” *Nature Reviews Microbiology* 7 (4): 263–73. <https://doi.org/10.1038/nrmicro2109>.
- Hengge, Regine, Angelika Gründling, Urs Jenal, Robert Ryan, and Fitnat Yildiz. 2016. “Bacterial Signal Transduction by Cyclic Di-GMP and Other Nucleotide Second Messengers.” *Journal of Bacteriology*. American Society for Microbiology. <https://doi.org/10.1128/JB.00331-15>.
- Hollenbeck, Emily C., Jiunn C.N. Fong, Ji Youn Lim, Fitnat H. Yildiz, Gerald G. Fuller, and Lynette Cegelski. 2014. “Molecular Determinants of Mechanical Properties of *V. Cholerae* Biofilms at the Air-Liquid Interface.” *Biophysical Journal* 107 (10): 2245–52. <https://doi.org/10.1016/j.bpj.2014.10.015>.
- Hossain, Sajjad, Ilana Heckler, and Elizabeth M Boon. 2018. “Discovery of a Nitric

- Oxide Responsive Quorum Sensing Circuit in *Vibrio Cholerae*.” *ACS Chemical Biology* 13 (8): 1964–69. <https://doi.org/10.1021/acscchembio.8b00360>.
- Hsieh, Meng Lun, Deborah M. Hinton, and Christopher M. Waters. 2018. “VpsR and Cyclic Di-GMP Together Drive Transcription Initiation to Activate Biofilm Formation in *Vibrio Cholerae*.” *Nucleic Acids Research* 46 (17): 8876–87. <https://doi.org/10.1093/nar/gky606>.
- Hsieh, Meng Lun, Christopher M. Waters, and Deborah M. Hinton. 2020. “VpsR Directly Activates Transcription of Multiple Biofilm Genes in *Vibrio Cholerae*.” *Journal of Bacteriology* 202 (18). <https://doi.org/10.1128/JB.00234-20>.
- Jang, Jeyoun, Kyung Tae Jung, Jungchan Park, Cheon Kwon Yoo, and Gi Eun Rhie. 2011. “The *Vibrio Cholerae* VarS/VarA Two-Component System Controls the Expression of Virulence Proteins through ToxT Regulation.” *Microbiology* 157 (5): 1466–73. <https://doi.org/10.1099/mic.0.043737-0>.
- Janoff, Edward N., Hiroshi Hayakawa, David N. Taylor, Claudine E. Fasching, Julie R. Kenner, Edgar Jaimes, and Leopoldo Rajj. 1997. “Nitric Oxide Production during *Vibrio Cholerae* Infection.” *American Journal of Physiology-Gastrointestinal and Liver Physiology* 273 (5): G1160–67. <https://doi.org/10.1152/ajpgi.1997.273.5.G1160>.
- Jenal, Urs, Alberto Reinders, and Christian Lori. 2017. “Cyclic Di-GMP: Second Messenger Extraordinaire.” *Nature Reviews Microbiology*. Nature Publishing Group. <https://doi.org/10.1038/nrmicro.2016.190>.
- Jones, Christopher J., Andrew Utada, Kimberly R. Davis, Wiriya Thongsomboon,

- David Zamorano Sanchez, Vinita Banakar, Lynette Cegelski, Gerard C. L. Wong, and Fitnat H. Yildiz. 2015. “C-Di-GMP Regulates Motile to Sessile Transition by Modulating MshA Pili Biogenesis and Near-Surface Motility Behavior in *Vibrio Cholerae*.” Edited by Matthew R. Parsek. *PLOS Pathogens* 11 (10): e1005068. <https://doi.org/10.1371/journal.ppat.1005068>.
- Khatoon, Zohra, Christopher D McTiernan, Erik J Suuronen, Thien-Fah Mah, and Emilio I Alarcon. 2018. “Bacterial Biofilm Formation on Implantable Devices and Approaches to Its Treatment and Prevention.” *Heliyon* 4 (12): e01067. <https://doi.org/10.1016/j.heliyon.2018.e01067>.
- Kitts, Giordan, Krista M. Giglio, David Zamorano-Sánchez, Jin Hwan Park, Loni Townsley, Richard B. Cooley, Benjamin R. Wucher, et al. 2019. “A Conserved Regulatory Circuit Controls Large Adhesins in *Vibrio Cholerae*.” *MBio* 10 (6). <https://doi.org/10.1128/mBio.02822-19>.
- Koch, Hanna, Sebastian Lücker, Mads Albertsen, Katharina Kitzinger, Craig Herbold, Eva Spieck, Per Halkjaer Nielsen, Michael Wagner, and Holger Daims. 2015. “Expanded Metabolic Versatility of Ubiquitous Nitrite-Oxidizing Bacteria from the Genus *Nitrospira*.” *Proceedings of the National Academy of Sciences of the United States of America* 112 (36): 11371–76. <https://doi.org/10.1073/pnas.1506533112>.
- Król, Jaroslaw E., Andrzej J. Wojtowicz, Linda M. Rogers, Holger Heuer, Kornelia Smalla, Stephen M. Krone, and Eva M. Top. 2013. “Invasion of *E. Coli* Biofilms by Antibiotic Resistance Plasmids.” *Plasmid* 70 (1): 110–19.

<https://doi.org/10.1016/j.plasmid.2013.03.003>.

- Lee, Kai Wei Kelvin, Saravanan Periasamy, Manisha Mukherjee, Chao Xie, Staffan Kjelleberg, and Scott A. Rice. 2014. "Biofilm Development and Enhanced Stress Resistance of a Model, Mixed-Species Community Biofilm." *ISME Journal* 8 (4): 894–907. <https://doi.org/10.1038/ismej.2013.194>.
- Lee, S H, M J Angelichio, J J Mekalanos, and A Camilli. 1998. "Nucleotide Sequence and Spatiotemporal Expression of the *Vibrio Cholerae* VieSAB Genes during Infection." *Journal of Bacteriology* 180 (9): 2298–2305.
<http://www.ncbi.nlm.nih.gov/pubmed/9573178>.
- Lenz, Derrick H., Kenny C. Mok, Brendan N. Lilley, Rahul V. Kulkarni, Ned S. Wingreen, and Bonnie L. Bassler. 2004. "The Small RNA Chaperone Hfq and Multiple Small RNAs Control Quorum Sensing in *Vibrio Harveyi* and *Vibrio Cholerae*." *Cell* 118 (1): 69–82. <https://doi.org/10.1016/j.cell.2004.06.009>.
- Liu, Cong, Di Sun, Jingrong Zhu, Jiawen Liu, and Weijie Liu. 2020. "The Regulation of Bacterial Biofilm Formation by CAMP-CRP: A Mini-Review." *Frontiers in Microbiology* 11 (May): 802. <https://doi.org/10.3389/fmicb.2020.00802>.
- Liu, Xianxian, Sinem Beyhan, Bentley Lim, Roger G. Linington, and Fitnat H. Yildiz. 2010. "Identification and Characterization of a Phosphodiesterase That Inversely Regulates Motility and Biofilm Formation in *Vibrio Cholerae*." *Journal of Bacteriology* 192 (18): 4541–52. <https://doi.org/10.1128/JB.00209-10>.
- Liu, Zhi, Fiona R. Stirling, and Jun Zhu. 2007. "Temporal Quorum-Sensing Induction

- Regulates *Vibrio Cholerae* Biofilm Architecture.” *Infection and Immunity* 75 (1): 122–26. <https://doi.org/10.1128/IAI.01190-06>.
- López, Daniel, Hera Vlamakis, Richard Losick, and Roberto Kolter. 2009. “Cannibalism Enhances Biofilm Development in *Bacillus Subtilis* Mi_6882 609..618.” <https://doi.org/10.1111/j.1365-2958.2009.06882.x>.
- Lories, Bram, Stefanie Roberfroid, Lise Dieltjens, David De Coster, Kevin R. Foster, and Hans P. Steenackers. 2020. “Biofilm Bacteria Use Stress Responses to Detect and Respond to Competitors.” *Current Biology* 30 (7): 1231-1244.e4. <https://doi.org/10.1016/j.cub.2020.01.065>.
- Martinez-Wilson, Hector F, Rita Tamayo, Anna D Tischler, David W Lazinski, and Andrew Camilli. 2008. “The *Vibrio Cholerae* Hybrid Sensor Kinase VieS Contributes to Motility and Biofilm Regulation by Altering the Cyclic Diguanylate Level.” *JOURNAL OF BACTERIOLOGY* 190 (19): 6439–47. <https://doi.org/10.1128/JB.00541-08>.
- McKee, Robert W., Ankunda Kariisa, Benjamin Mudrak, Courtney Whitaker, and Rita Tamayo. 2014a. “A Systematic Analysis of the in Vitro and in Vivo Functions of the HD-GYP Domain Proteins of *Vibrio Cholerae*.” *BMC Microbiology* 14 (1). <https://doi.org/10.1186/s12866-014-0272-9>.
- McKee, Robert W, Ankunda Kariisa, Benjamin Mudrak, Courtney Whitaker, and Rita Tamayo. 2014b. “A Systematic Analysis of the in Vitro and in Vivo Functions of the HD-GYP Domain Proteins of *Vibrio Cholerae*.” *BMC Microbiology* 14 (October): 272. <https://doi.org/10.1186/s12866-014-0272-9>.

- Merighi, Massimo, Vincent T. Lee, Mamoru Hyodo, Yoshihiro Hayakawa, and Stephen Lory. 2007. "The Second Messenger Bis-(3'-5')-Cyclic-GMP and Its PilZ Domain-Containing Receptor Alg44 Are Required for Alginate Biosynthesis in *Pseudomonas Aeruginosa*." *Molecular Microbiology* 65 (4): 876–95. <https://doi.org/10.1111/j.1365-2958.2007.05817.x>.
- Mitchell, Stephanie L, Ayman M Ismail, Sophia A Kenrick, and Andrew Camilli. 2015. "The VieB Auxiliary Protein Negatively Regulates the VieSA Signal Transduction System in *Vibrio Cholerae*." *BMC Microbiology* 15 (March): 59. <https://doi.org/10.1186/s12866-015-0387-7>.
- Mulcahy, Heidi, Laetitia Charron-Mazenod, and Shawn Lewenza. 2010. "Pseudomonas Aeruginosa Produces an Extracellular Deoxyribonuclease That Is Required for Utilization of DNA as a Nutrient Source." *Environmental Microbiology* 12 (6): 1621–29. <https://doi.org/10.1111/j.1462-2920.2010.02208.x>.
- Orr, Mona W., Gregory P. Donaldson, Geoffrey B. Severin, Jingxin Wang, Herman O. Sintim, Christopher M. Waters, and Vincent T. Lee. 2015. "Oligoribonuclease Is the Primary Degradative Enzyme for PGpG in *Pseudomonas Aeruginosa* That Is Required for Cyclic-Di-GMP Turnover." *Proceedings of the National Academy of Sciences of the United States of America* 112 (36): E5048–57. <https://doi.org/10.1073/pnas.1507245112>.
- Papenfort, Kai, and Bonnie L Bassler. 2016. "Quorum Sensing Signal-Response Systems in Gram-Negative Bacteria." *Nature Reviews. Microbiology* 14 (9):

576–88. <https://doi.org/10.1038/nrmicro.2016.89>.

Paul, R., Stefan Weiser, Nicholas C Amiot, Carmen Chan, Tilman Schirmer, Bernd Giese, and Urs Jenal. 2004. “Cell Cycle-Dependent Dynamic Localization of a Bacterial Response Regulator with a Novel Di-Guanylate Cyclase Output Domain.” *Genes & Development* 18 (6): 715–27.

<https://doi.org/10.1101/gad.289504>.

Pickering, Bradley S., Daniel R. Smith, and Paula I. Watnick. 2012. “Glucose-Specific Enzyme IIA Has Unique Binding Partners in the *Vibrio Cholerae* Biofilm.” *MBio* 3 (6). <https://doi.org/10.1128/mBio.00228-12>.

Plate, Lars, and Michael A. A Marletta. 2012. “Nitric Oxide Modulates Bacterial Biofilm Formation through a Multicomponent Cyclic-Di-GMP Signaling Network.” *Molecular Cell* 46 (4): 449–60.

<https://doi.org/10.1016/J.MOLCEL.2012.03.023>.

Plate, Lars, and Michael A Marletta. 2013. “Nitric Oxide-Sensing H-NOX Proteins Govern Bacterial Communal Behavior.” *Trends Biochem Sci* 38 (11): 566–75.

<https://doi.org/10.1016/j.tibs.2013.08.008>.

Pontes, Mauricio Henriques, Kari Lyn Smith, Linda De Vooght, Jan Van Den Abbeele, and Colin Dale. 2011. “Attenuation of the Sensing Capabilities of PhoQ in Transition to Obligate Insect–Bacterial Association.” Edited by Nancy A. Moran. *PLoS Genetics* 7 (11): e1002349.

<https://doi.org/10.1371/journal.pgen.1002349>.

Pratt, J. T., E. McDonough, and A. Camilli. 2009. “PhoB Regulates Motility,

- Biofilms, and Cyclic Di-GMP in *Vibrio Cholerae*.” *Journal of Bacteriology* 191 (21): 6632–42. <https://doi.org/10.1128/JB.00708-09>.
- Pratt, Jason T., Rita Tamayo, Anna D. Tischler, and Andrew Camilli. 2007. “PilZ Domain Proteins Bind Cyclic Diguanylate and Regulate Diverse Processes in *Vibrio Cholerae*.” *Journal of Biological Chemistry* 282 (17): 12860–70. <https://doi.org/10.1074/jbc.M611593200>.
- Prouty, M. G., N. E. Correa, and K. E. Klose. 2001. “The Novel $\Sigma 54$ - and $\Sigma 28$ -Dependent Flagellar Gene Transcription Hierarchy of *Vibrio Cholerae*.” *Molecular Microbiology* 39 (6): 1595–1609. <https://doi.org/10.1046/j.1365-2958.2001.02348.x>.
- Rendueles, Olaya, and Jean-Marc Ghigo. 2015. “Mechanisms of Competition in Biofilm Communities.” *Microbiology Spectrum* 3 (3). <https://doi.org/10.1128/microbiolspec.mb-0009-2014>.
- Roelofs, Kevin G., Christopher J. Jones, Sarah R. Helman, Xiaoran Shang, Mona W. Orr, Jonathan R. Goodson, Michael Y. Galperin, Fitnat H. Yildiz, and Vincent T. Lee. 2015. “Systematic Identification of Cyclic-Di-GMP Binding Proteins in *Vibrio Cholerae* Reveals a Novel Class of Cyclic-Di-GMP-Binding ATPases Associated with Type II Secretion Systems.” *PLoS Pathogens* 11 (10). <https://doi.org/10.1371/journal.ppat.1005232>.
- Römling, Ute, Michael Y Galperin, and Mark Gomelsky. 2013. “Cyclic Di-GMP: The First 25 Years of a Universal Bacterial Second Messenger.” *Microbiology and Molecular Biology Reviews : MMBR* 77 (1): 1–52.

<https://doi.org/10.1128/MMBR.00043-12>.

Sack, David A., R. Bradley Sack, G. Balakrish Nair, and A. K. Siddique. 2004.

“Cholera.” In *Lancet*, 363:223–33. Elsevier Limited.

[https://doi.org/10.1016/S0140-6736\(03\)15328-7](https://doi.org/10.1016/S0140-6736(03)15328-7).

Samanta, Prosenjit, Rahul Shubhra Mandal, Rudra Narayan Saha, Sreeja Shaw,

Priyanka Ghosh, Shanta Dutta, Amit Ghosh, et al. 2020. “A Point Mutation in

Carr Is Involved in the Emergence of Polymyxin B-Sensitive *Vibrio Cholerae*

O1 El Tor Biotype by Influencing Gene Transcription.” *Infection and Immunity*

88 (5). <https://doi.org/10.1128/IAI.00080-20>.

Savage, Victoria J., Ian Chopra, and Alex J. O’Neill. 2013. “Staphylococcus Aureus

Biofilms Promote Horizontal Transfer of Antibiotic Resistance.” *Antimicrobial*

Agents and Chemotherapy 57 (4): 1968–70. [https://doi.org/10.1128/AAC.02008-](https://doi.org/10.1128/AAC.02008-12)

12.

Schmidt, Andrew J., Dmitri A. Ryjenkov, and Mark Gomelsky. 2005. “The

Ubiquitous Protein Domain EAL Is a Cyclic Diguanylate-Specific

Phosphodiesterase: Enzymatically Active and Inactive EAL Domains.” *Journal*

of Bacteriology 187 (14): 4774–81. [https://doi.org/10.1128/JB.187.14.4774-](https://doi.org/10.1128/JB.187.14.4774-4781.2005)

4781.2005.

Shikuma, Nicholas J., Jiunn C.N. Fong, Lindsay S. Odell, Barrett S. Perchuk, Michael

T. Laub, and Fitnat H. Yildiz. 2009. “Overexpression of VpsS, a Hybrid Sensor

Kinase, Enhances Biofilm Formation in *Vibrio Cholerae*.” *Journal of*

Bacteriology 191 (16): 5147–58. <https://doi.org/10.1128/JB.00401-09>.

- Singh, Praveen K., Sabina Bartalomej, Raimo Hartmann, Hannah Jeckel, Lucia Vidakovic, Carey D. Nadell, and Knut Drescher. 2017. "Vibrio Cholerae Combines Individual and Collective Sensing to Trigger Biofilm Dispersal." *Current Biology* 27 (21): 3359-3366.e7.
<https://doi.org/10.1016/j.cub.2017.09.041>.
- Smith, James L. 2003. "The Role of Gastric Acid in Preventing Foodborne Disease and How Bacteria Overcome Acid Conditions." *Journal of Food Protection* 66 (7): 1292–1303. <http://www.ncbi.nlm.nih.gov/pubmed/12870767>.
- Srivastava, Disha, Meng Lun Hsieh, Atul Khataokar, Matthew B. Neiditch, and Christopher M. Waters. 2013. "Cyclic Di-GMP Inhibits Vibrio Cholerae Motility by Repressing Induction of Transcription and Inducing Extracellular Polysaccharide Production." *Molecular Microbiology* 90 (6): 1262–76.
<https://doi.org/10.1111/mmi.12432>.
- Sun, Shuyang, Parisa Noorian, and Diane McDougald. 2018. "Dual Role of Mechanisms Involved in Resistance to Predation by Protozoa and Virulence to Humans." *Frontiers in Microbiology* 9 (May): 1017.
<https://doi.org/10.3389/fmicb.2018.01017>.
- Tamayo, Rita, Bharathi Patimalla, and Andrew Camilli. 2010. "Growth in a Biofilm Induces a Hyperinfectious Phenotype in Vibrio Cholerae." *Infection and Immunity* 78 (8): 3560–69. <https://doi.org/10.1128/IAI.00048-10>.
- Tamayo, Rita, Anna D Tischler, and Andrew Camilli. 2005. "The EAL Domain Protein VieA Is a Cyclic Diguanylate Phosphodiesterase." *The Journal of*

Biological Chemistry 280 (39): 33324–30.

<https://doi.org/10.1074/jbc.M506500200>.

Teschler, Jennifer K., Andrew T. Cheng, and Fitnat H. Yildiz. 2017. “The Two-Component Signal Transduction System VxrAB Positively Regulates *Vibrio Cholerae* Biofilm Formation.” *Journal of Bacteriology* 199 (18).

<https://doi.org/10.1128/JB.00139-17>.

Teschler, Jennifer K., David Zamorano-Sánchez, Andrew S. Utada, Christopher J. A.

Warner, Gerard C. L. Wong, Roger G. Linington, and Fitnat H. Yildiz. 2015.

“Living in the Matrix: Assembly and Control of *Vibrio Cholerae* Biofilms.”

Nature Reviews Microbiology 13 (5): 255–68.

<https://doi.org/10.1038/nrmicro3433>.

Tischler, Anna D, and Andrew Camilli. 2004. “Cyclic Diguanylate (c-Di-GMP)

Regulates *Vibrio Cholerae* Biofilm Formation.” *Molecular Microbiology* 53 (3):

857–69. <https://doi.org/10.1111/j.1365-2958.2004.04155.x>.

Tischler, Anna D, Sang Ho Lee, and Andrew Camilli. 2002. “The *Vibrio Cholerae*

VieSAB Locus Encodes a Pathway Contributing to Cholera Toxin Production.”

Journal of Bacteriology 184 (15): 4104–13.

<https://doi.org/10.1128/jb.184.15.4104-4113.2002>.

Tschowri, N., S. Busse, and R. Hengge. 2009. “The BLUF-EAL Protein YcgF Acts

as a Direct Anti-Repressor in a Blue-Light Response of *Escherichia Coli*.” *Genes*

& Development 23 (4): 522–34. <https://doi.org/10.1101/gad.499409>.

Tsou, Amy M., Zhi Liu, Tao Cai, and Jun Zhu. 2011. “The VarS/VarA Two-

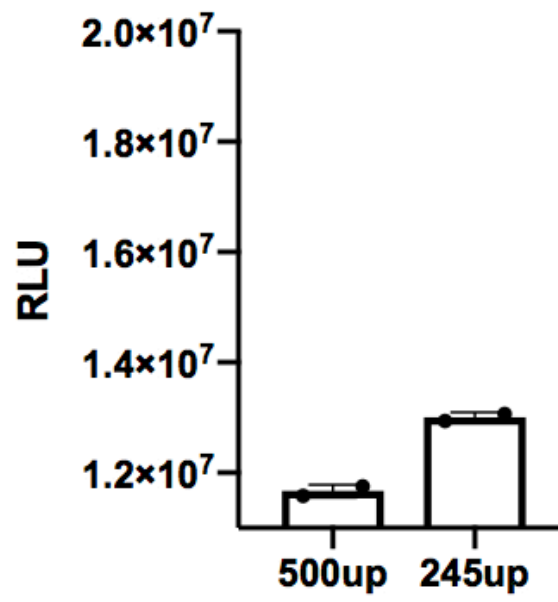
- Component System Modulates the Activity of the *Vibrio Cholerae* Quorum-Sensing Transcriptional Regulator HapR.” *Microbiology* 157 (6): 1620–28. <https://doi.org/10.1099/mic.0.046235-0>.
- Utada, Andrew S, Rachel R Bennett, Jiunn C N Fong, Maxsim L Gibiansky, Fitnat H Yildiz, Ramin Golestanian, and Gerard C L Wong. 2014. “ARTICLE *Vibrio Cholerae* Use Pili and Flagella Synergistically to Effect Motility Switching and Conditional Surface Attachment.” <https://doi.org/10.1038/ncomms5913>.
- Vance, Russell E., Jun Zhu, and John J. Mekalanos. 2003. “A Constitutively Active Variant of the Quorum-Sensing Regulator LuxO Affects Protease Production and Biofilm Formation in *Vibrio Cholerae*.” *Infection and Immunity* 71 (5): 2571–76. <https://doi.org/10.1128/IAI.71.5.2571-2576.2003>.
- Vos, Willem M. De. 2015. “Microbial Biofilms and the Human Intestinal Microbiome.” *Npj Biofilms and Microbiomes*. Nature Publishing Group. <https://doi.org/10.1038/npjbiofilms.2015.5>.
- Wang, Xin, Ashok K. Dubey, Kazushi Suzuki, Carol S. Baker, Paul Babitzke, and Tony Romeo. 2005. “CsrA Post-Transcriptionally Represses *PgaABCD*, Responsible for Synthesis of a Biofilm Polysaccharide Adhesin of *Escherichia Coli*.” *Molecular Microbiology* 56 (6): 1648–63. <https://doi.org/10.1111/j.1365-2958.2005.04648.x>.
- Wassmann, Paul, Carmen Chan, Ralf Paul, Andreas Beck, Heiko Heerklotz, Urs Jenal, and Tilman Schirmer. 2007. “Structure of BeF₃-Modified Response Regulator PleD: Implications for Diguanylate Cyclase Activation, Catalysis, and

- Feedback Inhibition.” *Structure* 15 (8): 915–27.
<https://doi.org/10.1016/j.str.2007.06.016>.
- Waters, C. M., W. Lu, J. D. Rabinowitz, and B. L. Bassler. 2008. “Quorum Sensing Controls Biofilm Formation in *Vibrio Cholerae* through Modulation of Cyclic Di-GMP Levels and Repression of VpsT.” *Journal of Bacteriology* 190 (7): 2527–36. <https://doi.org/10.1128/JB.01756-07>.
- Waters, Christopher M., Wenyun Lu, Joshua D. Rabinowitz, and Bonnie L. Bassler. 2008a. “Quorum Sensing Controls Biofilm Formation in *Vibrio Cholerae* through Modulation of Cyclic Di-GMP Levels and Repression of VpsT.” *Journal of Bacteriology* 190 (7): 2527–36. <https://doi.org/10.1128/JB.01756-07>.
- . 2008b. “Quorum Sensing Controls Biofilm Formation in *Vibrio Cholerae* through Modulation of Cyclic Di-GMP Levels and Repression of VpsT.” *Journal of Bacteriology* 190 (7): 2527–36. <https://doi.org/10.1128/JB.01756-07>.
- Watnick, Paula I., and Roberto Kolter. 1999. “Steps in the Development of a *Vibrio Cholerae* El Tor Biofilm.” *Molecular Microbiology* 34 (3): 586–95.
<https://doi.org/10.1046/j.1365-2958.1999.01624.x>.
- West, Stuart A., Ashleigh S. Griffin, Andy Gardner, and Stephen P. Diggle. 2006. “Social Evolution Theory for Microorganisms.” *Nature Reviews Microbiology*. *Nat Rev Microbiol*. <https://doi.org/10.1038/nrmicro1461>.
- Wu, Daniel C., David Zamorano-Sánchez, Fernando A. Pagliai, Jin Hwan Park, Kyle A. Floyd, Calvin K. Lee, Giordan Kitts, et al. 2020. “Reciprocal C-Di-GMP Signaling: Incomplete Flagellum Biogenesis Triggers c-Di-GMP Signaling

- Pathways That Promote Biofilm Formation.” Edited by Josep Casadesús. *PLOS Genetics* 16 (3): e1008703. <https://doi.org/10.1371/journal.pgen.1008703>.
- Yildiz, Fitnat, Jiunn Fong, Irina Sadovskaya, Thierry Grard, and Evgeny Vinogradov. 2014. “Structural Characterization of the Extracellular Polysaccharide from *Vibrio Cholerae* O1 El-Tor.” Edited by Christiane Forestier. *PLoS ONE* 9 (1): e86751. <https://doi.org/10.1371/journal.pone.0086751>.
- Zamorano-Sánchez, David, Jiunn C.N. Fong, Sefa Kilic, Ivan Erill, and Fitnat H. Yildiz. 2015. “Identification and Characterization of VpsR and VpsT Binding Sites in *Vibrio Cholerae*.” *Journal of Bacteriology* 197 (7): 1221–35. <https://doi.org/10.1128/JB.02439-14>.
- Zamorano-Sánchez, David, Wujing Xian, Calvin K. Lee, Mauro Salinas, Wiriya Thongsomboon, Lynette Cegelski, Gerard C.L. Wong, and Fitnat H. Yildiza. 2019. “Functional Specialization in *Vibrio Cholerae* Diguanylate Cyclases: Distinct Modes of Motility Suppression and c-Di-Gmp Production.” *MBio* 10 (2). <https://doi.org/10.1128/mBio.00670-19>.
- Zelezniak, Aleksej, Sergej Andrejev, Olga Ponomarova, Daniel R. Mende, Peer Bork, and Kiran Raosaheb Patil. 2015. “Metabolic Dependencies Drive Species Co-Occurrence in Diverse Microbial Communities.” *Proceedings of the National Academy of Sciences of the United States of America* 112 (20): 6449–54. <https://doi.org/10.1073/pnas.1421834112>.
- Zhu, Jun, and John J. Mekalanos. 2003. “Quorum Sensing-Dependent Biofilms Enhance Colonization in *Vibrio Cholerae*.” *Developmental Cell* 5 (4): 647–56.

[https://doi.org/10.1016/S1534-5807\(03\)00295-8](https://doi.org/10.1016/S1534-5807(03)00295-8).

Appendices



Appendix Figure 1: Expression of the VC1080 operon reporter with either 245 or 500 base pairs upstream of the VC1080 gene fused to lux reporter genes.